

University of Windsor

Scholarship at UWindor

Electronic Theses and Dissertations

Theses, Dissertations, and Major Papers

2005

Magnetic susceptibility mapping of Point Pelee National Park beaches.

Blessing A. Igbokwe
University of Windsor

Follow this and additional works at: <https://scholar.uwindsor.ca/etd>

Recommended Citation

Igbokwe, Blessing A., "Magnetic susceptibility mapping of Point Pelee National Park beaches." (2005).
Electronic Theses and Dissertations. 2658.
<https://scholar.uwindsor.ca/etd/2658>

This online database contains the full-text of PhD dissertations and Masters' theses of University of Windsor students from 1954 forward. These documents are made available for personal study and research purposes only, in accordance with the Canadian Copyright Act and the Creative Commons license—CC BY-NC-ND (Attribution, Non-Commercial, No Derivative Works). Under this license, works must always be attributed to the copyright holder (original author), cannot be used for any commercial purposes, and may not be altered. Any other use would require the permission of the copyright holder. Students may inquire about withdrawing their dissertation and/or thesis from this database. For additional inquiries, please contact the repository administrator via email (scholarship@uwindsor.ca) or by telephone at 519-253-3000ext. 3208.

Magnetic Susceptibility Mapping of Point Pelee National Park Beaches

By
Blessing A. Igbokwe

A Thesis
Submitted to the Faculty of Graduate Studies and Research
through Earth Sciences
in Partial Fulfillment of the Requirements for
the Degree of Master of Science at the
University of Windsor

Windsor, Ontario, Canada
2005

© 2005 Blessing Igbokwe



Library and
Archives Canada

Bibliothèque et
Archives Canada

Published Heritage
Branch

Direction du
Patrimoine de l'édition

395 Wellington Street
Ottawa ON K1A 0N4
Canada

395, rue Wellington
Ottawa ON K1A 0N4
Canada

Your file *Votre référence*

ISBN: 0-494-09768-X

Our file *Notre référence*

ISBN: 0-494-09768-X

NOTICE:

The author has granted a non-exclusive license allowing Library and Archives Canada to reproduce, publish, archive, preserve, conserve, communicate to the public by telecommunication or on the Internet, loan, distribute and sell theses worldwide, for commercial or non-commercial purposes, in microform, paper, electronic and/or any other formats.

The author retains copyright ownership and moral rights in this thesis. Neither the thesis nor substantial extracts from it may be printed or otherwise reproduced without the author's permission.

AVIS:

L'auteur a accordé une licence non exclusive permettant à la Bibliothèque et Archives Canada de reproduire, publier, archiver, sauvegarder, conserver, transmettre au public par télécommunication ou par l'Internet, prêter, distribuer et vendre des thèses partout dans le monde, à des fins commerciales ou autres, sur support microforme, papier, électronique et/ou autres formats.

L'auteur conserve la propriété du droit d'auteur et des droits moraux qui protègent cette thèse. Ni la thèse ni des extraits substantiels de celle-ci ne doivent être imprimés ou autrement reproduits sans son autorisation.

In compliance with the Canadian Privacy Act some supporting forms may have been removed from this thesis.

Conformément à la loi canadienne sur la protection de la vie privée, quelques formulaires secondaires ont été enlevés de cette thèse.

While these forms may be included in the document page count, their removal does not represent any loss of content from the thesis.

Bien que ces formulaires aient inclus dans la pagination, il n'y aura aucun contenu manquant.


Canada

Abstract

In the preliminary studies, the western and the Eastern shores of Point Pelee National Park (PPNP) showed a distinct spatial variation in their sediment magnetic properties (magnetic susceptibility). In order to determine the degree of spatial variability of field magnetic susceptibility and potential causes, the magnetic susceptibility of the beach sands were mapped in transects perpendicular to the shoreline of Lake Erie with a Bartington susceptibility meter. The West beaches showed no significant variation in susceptibility measurements, the East beaches showed highly variable susceptibility values which tended to increase towards the vegetation line. The East beaches magnetic susceptibility varied from 68×10^{-6} to 9000×10^{-6} (SI units), the West beaches were in the low range of 14×10^{-6} to 243.5×10^{-6} . Magnetic susceptibility values were analysed and displayed with ARCGIS. Mineral magnetic analysis (anhysteretic remanence and saturation isothermal remanence measurements as well as temperature dependence of susceptibility measurements) indicated that the primary magnetic mineral throughout the Point Pelee beaches is pseudo single domain to single domain magnetite. Some variation in composition is apparent. Similar compositions and grain size were observed to the north east of PPNP, on the Rondeau Provincial Park beaches and Wheatley beaches, suggesting either the same source or a similar sediment source. The temporal variations in susceptibility distribution, as well as high surface magnetic susceptibility due to the presence of magnetite-rich lamina suggest that sediment sorting and other beach processes is likely to cause the high magnetite concentration on the East beaches.

Acknowledgments

The completion of this thesis was made possible by the contribution of so many people. My sincere gratitude goes to my thesis supervisor, Dr. Maria Cioppa, who gave me the opportunity to work with her on this project and introduced me to the unique field of environmental magnetism; her suggestions, advice, instructions, detailed proof reading and corrections are greatly appreciated. My thanks also go to Dr. A. Trenhaile for his valuable suggestions on the beach processes and sediment transport aspect of the thesis. I would also like to thank my external supervisor Dr. J. Lovett-Doust for his time, corrections, and suggestions.

My thanks also go to Shanmugan Johari Pannalal for his assistance and guide in using the paleomagnetic equipment and his help in taking magnetic measurements in the freezing cold. Also, my thanks go to Erica Szabo for her assistance and instructions on how to use Corel Draw for my analysis. I also wish to say a big thank you to Nicoli Garner for being a wonderful class/office mate. To my field assistants; Janice Kenney, Nadia Al-Aasm and Michael Bishara, I owe you a lot! To you three I say thank you for helping me take those magnetic measurements and cross the creeks even in rough weather.

My appreciation also goes to the scientific staffs of Point Pelee National Park (Mr. Tom Linke and Geordon Harvey) for all their assistance. Finally, to my husband I say thank you for understanding; and to my three little angels Victor, Emmanuel and Tee, I say way to go!

Table of Contents	page
Abstract	iii
Acknowledgments	iv
List of Tables	viii
List of Illustrations	ix
List of Appendices	xii

CHAPTER ONE: INTRODUCTION

1.1. Background of study	1
1.2. Statement of problem	5
1.3. Objectives of study	5
1.4. Significance of study	6
1.5. Scope of study	6

CHAPTER TWO: LITERATURE REVIEW

2.1. Area of study: Point Pelee National Park beaches	8
2.2. Previous studies on environmental magnetic properties of sediments	11

CHAPTER THREE: METHODOLOGY

3.1. Data sets	14
3.2. Instrumentation	14
3.3. Field magnetic susceptibility measurements and sediment data collection	15
3.4. Sample preparation and laboratory magnetic measurements	17
3.4.1. pARM and ARM measurements	
3.4.2. SIRM and S-ratios	
3.4.3. Susceptibility-Temperature dependence measurements	
3.5. Magnetic data analysis	18
3.5.1. pARM	
3.5.2. SIRM	
3.5.3. Magnetic susceptibility	

3.5.4.	Susceptibility/temperature variation	
3.5.5.	Magnetic ratios and parameter table	
3.6.	Geographic Information System (GIS) exploration and display of field data	20
3.6.1.	GIS Geostatistical data exploration	
3.6.2.	Data representation	
3.6.3.	Geostatistical analyst surface fitting methodology	
3.7.	Statistical analysis and test of hypothesis	26

CHAPTER FOUR: ANALYSIS AND RESULTS PRESENTATION OF MAGNETIC MEASUREMENTS

4.1.	Field magnetic susceptibility	29
4.2.	pARM	33
4.3.	SIRM analysis and results	42
4.4.	Susceptibility variation with temperature measurements	49
4.5.	Magnetic ratios	51

CHAPTER FIVE: ANALYSIS AND PRESENTATION OF GEOSTATISTICAL SURFACE MODELS

5.1.	Field magnetic susceptibility	55
5.2.	Data exploration	55
5.2.1.	Histograms	
5.2.2.	Normal QQ plots	
5.2.3.	Trend analysis	
5.3.	Model fitting process	60
5.3.1.	Log transformation	
5.3.2.	Detrending	
5.4.	Display of model result	60
5.5.	Models performance and prediction error table	61

CHAPTER SIX: TEST OF HYPOTHESES AND PRESENTATION OF STATISTICAL RESULTS

6.1.	Hypothesis 1: Spatial variation	69
6.2.	Hypothesis 2: Individual beach seasonal variability	70
6.3.	Hypothesis 3: Intrabeach variability	70

CHAPTER 7: DISCUSSION OF RESULTS, FINDINGS AND CONCLUSIONS

7.1.	Objectives	72
7.2.	GIS model, display and results implication	73
7.3.	Magnetic mineralogy and granulometry	74
	7.3.1. Magnetic mineralogy	
	7.3.2. Magnetic granulometry	
7.4.	Seasonal variation of magnetic susceptibility in PPNP	81
7.5.	Spatial variation and comparison of beaches	82
	7.5.1. Comparison of magnetic mineralogy and granulometry – spatial variation	
	7.5.2. Magnetic susceptibility (χ)-spatial variation	
	7.5.3. Magnetic ratios - spatial variation	
7.6.	Sediment transport and beach processes: an explanation for the high magnetite concentration on beaches	88
7.7.	Sediment source/origin of magnetic sediment on PPNP beaches	90
7.8.	Summary and conclusion	92
	References	94
	Vita auctoris	143

List of Tables	page
Table 1.1: A list of magnetic parameters that are commonly used in environmental magnetism to classify mineralogy, grain size and concentration of magnetic minerals	3
Table 1.2: Magnetic class and typical susceptibility values for a number of common mineral	4
Table 1.3: Typical values for the field at which SIRM is achieved, for some common magnetic minerals	4
Table 1.4: Unblocking temperature of some magnetic minerals	5
Table 3.1: Average values of magnetic parameters and ratios used for comparison	23
Table 4.1: Field Magnetic susceptibility summary for Eastern beaches	29
Table 4.2: Field Magnetic susceptibility summary for Western beaches	30
Table 4.3: Summary of $S_{0.1T}$ and $S_{0.3T}$	51
Table 4.4: Sample parameter ratios and summary	52
Table 5.1: Model comparison and error report for all beaches	62
Table 6.1: Test statistic summary for hypothesis 1	69
Table 6.2: Test statistics summary for hypothesis 2	70
Table 6.3: Test statistics summary for hypothesis 3	71
Table 7.1: HIRM values obtained from SIRM and IRM values	78

List of Illustrations	page
Figure 2.1: Location map of the Study area (Point Pelee and the Southern Coast of Essex and Kent Countries, South Western Ontario)	8
Figure 2.2: Location of Wheatley, and Rondeau Provincial Park. [Scanned map sheet of Windsor-Toronto Area (Department of Mines and Resources) at a scale of 1:500000]	11
Figure 3.1: Schematic representation of field magnetic susceptibility data collection with Bartington MS2 susceptibility meter	16
Figure 3.2: pARM curves for synthetic samples containing magnetic with discrete grain size	19
Figure 3.3A: Plot for identification of SD magnetite and pyrrhotite grains	20
Figure 3.3B: SIRM acquisition and crossover plot for magnetite	20
Figure 3.3C: Combined magnetite and hematite plot	20
Figure 3.4: Surface fitting methodology flowchart	26
Figure 4.1: Average magnetic susceptibility at each transect 1meter interval points for all ten beaches (2003)	31
Figure 4.2: Average magnetic susceptibility at transect 1meter interval points for all beaches (2004)	31
Figure 4.3: Average magnetic susceptibility for transect 1meter interval points for EB beach(2004)	32
Figure 4.4: Average magnetic susceptibility for transect 1meter interval points for Rondeau beach(2004)	32
Figure 4.5: Average magnetic susceptibility at each data point	33
Figure 4.6: pARM for EB	34
Figure 4.7: pARM for EB Top and Lower sediments	34
Figure 4.8: pARM for NEB sediment samples	35
Figure 4.9: pARM for NEB sieved sediment samples	35
Figure 4.10: pARM for NEB sieved sediment samples	36
Figure 4.11: pARM for MEB sediment samples	36
Figure 4.12: pARM for MEB sieved sediment samples	37
Figure 4.13: pARM for MEB sieved sediment samples	37

Figure 4.14: pARM for MEB sieved sediment samples	38
Figure 4.15: pARM spectra for SB sediments	38
Figure 4.16: pARM spectra for other Western beaches	39
Figure 4.17: pARM spectra for sediments from other Western beaches	39
Figure 4.18: pARM spectra for sediments from other EB, MEB, WB (2004)	40
Figure 4.19: pARM spectra for Wheatley sediments, Transect 1	41
Figure 4.20: pARM spectra for Wheatley sediments, Transect 2	41
Figure 4.21: pARM spectra for Wheatley sediments, Transect 3	42
Figure 4.22: pARM spectra for sediment from Rondeau	42
Figure 4.23: SIRM spectra for sediment samples from the Western beaches	43
Figure 4.24: SIRM spectra for sediment samples from the EB	44
Figure 4.25: SIRM spectra for sediment from top and lower cores (EB)	44
Figure 4.26: SIRM spectra for sieved sediments MEB	45
Figure 4.27: SIRM spectra for MEB sediment	45
Figure 4.28: SIRM spectra for sediment from core samples NEB: (A: Top, B: Middle, and C: Lowest)	46
Figure 4.29: SIRM spectra for sieved sediment (NEB)	46
Figure 4.30: SIRM spectra for NEB sediment samples	47
Figure 4.31: SIRM spectra for Wheatley sediment samples	48
Figure 4.32: SIRM spectra for Wheatley sediment samples	48
Figure 4.33: SIRM spectra for Rondeau, EB, WB and MEB (2004)	49
Figure 4.34A-J: Selected magnetic susceptibility vs. temperature curves for PPNP, Rondeau and Wheatley beaches and bluffs	61
Figure 5.1: Histogram exploration for East beach dataset (no transformation)	56
Figure 5.2: Histogram exploration for East beach dataset (log transformation)	56
Figure 5.3: Histogram exploration for West beach dataset (no transformation)	57
Figure 5.4: Histogram exploration for West beach dataset (log transformation)	57
Figure 5.5: Normal QQ plot for EBR	58
Figure 5.6: Normal QQ plot for EBR with log transformation	58
Figure 5.7: Normal QQ plot for SB (no transformation)	58
Figure 5.8: Normal QQ plot for SB (Log transformation)	59

Figure 5.9: Trend analysis for East beach at different angles of rotation	59
Figure 5.10: Kriging and IDW surface model for MEB	63
Figure 5.11: Kriging and IDW surface model for EB	64
Figure 5.12: Kriging and IDW surface Model for NEB	65
Figure 5.13: Kriging and IDW surface Model for SB	66
Figure 5.14: Kriging and IDW surface model for WB	67
Figure 5.15: Kriging and IDW surface model for EBR	68
Figure 7.1: Susceptibility versus temperature heating and cooling curves for A. Wheatley (bluff sample), B. West beach samples, and C. East beach samples	76
Figure 7.2: Magnetic domain sizes for samples from the various beaches plotted on the Symons and Cioppa (2000) templates	81
Figure 7.3: Spatial distribution of magnetic mineralogy from SIRM analysis	84
Figure 7.4: Spatial distribution of magnetic grain size from PARM analysis	85
Figure 7.5: Spatial distribution of T- type curves	86
Figure 7.6: Spatial distribution of field magnetic susceptibility (volume specific) at PPNP and surrounding areas	87

List of Appendices	page
Appendix A: Location of PPNP beaches	99
Appendix B: Points where sediment samples were collected in PPNP	100
Appendix C: Parameters used for calculating magnetic ratios	101
Appendix D: Test of hypotheses	102
Appendix E: Magnetic susceptibility data used for mapping and statistics	117
Appendix F: East beach random data used for mapping	137
Appendix G: Rondeau field magnetic susceptibility data points	140

CHAPTER ONE

INTRODUCTION

1.1 Background of study

Environmental magnetism is a fairly recent field in which the properties and characteristics of magnetic minerals are used as proxies for environmental processes (Thompson and Oldfield, 1986, Dekkers, 1997, and Van Oorschot, 2001). Examples include provenance studies of sediment, studies of anthropogenically induced pollution, archaeological investigations, paleoceanographic studies, and paleoclimate analysis (Dekkers, 1997). Magnetic properties have also been used for erosion and sediment transport studies to facilitate sediment tracing and sediment source location in catchment areas. Natural materials have various types of magnetic behaviour. These behaviours can be identified from relatively simple experiments which involve recording the response of the specimens to the changes in variables such as magnetic field and temperature. Many of the changes can be related to the properties of the crystal structure and to the effects of crystal size and shape (Thompson and Oldfield, 1986). These properties along with others related to concentration of magnetic minerals (e.g. magnetic susceptibility), form the basis for the magnetic differentiation of soils, sediment, peat and dust.

As magnetic properties of minerals tend to be conservative within a system (e.g. erosion and sediment transport system), the magnetic properties of the sediment can be used for erosion and sediment transport studies; where the unique magnetic characteristics of sediment can facilitate sediment tracing and source location for sediment in the catchment's area. Of particular interest to this study is the use of magnetic parameters as sediment tracers. The magnetic techniques are fairly easy, fast and non-destructive, grain size indicative, and little sample preparation is required (Dekkers, 1997, Thompson and Oldfield, 1986). The magnetic properties of samples allow the characterisation of magnetic mineralogy, concentration and grain size. A comparison of magnetic characteristics from various catchment areas will be prognostic in determining if the sediments have a common source.

The magnetic minerals all contains iron, this gives them their specific magnetic characteristics. Some common and significant magnetic minerals in natural rocks and sediments include:

- ❖ The Fe_3O_4 - FeTiO_4 series which is the solid solution between magnetite (Fe_3O_4) and ulvospinel (Fe_2TiO_4) i.e. titanomagnetite;
- ❖ The Fe_2O_3 - FeTiO_3 series which is the solid solution between hematite ($\alpha\text{Fe}_2\text{O}_3$) and ilmenite (FeTiO_3);
- ❖ Maghemite and the titanomaghemite ($\gamma\text{Fe}_2\text{O}_3$ - FeTiO_3 having a spinel structure); and
- ❖ Pyrrhotite (FeS_{1+x})

Other minor magnetic minerals include iron hydroxides (e.g. goethite) and oxyhydroxides. The magnetic properties of these minerals allow the mineral to be distinguished from one another. These intrinsic magnetic properties are: Curie temperature (the temperature at which interatomic distances have increased to the point at which exchange coupling is destroyed and resultant magnetization J_s reduced to zero), coercive force (the magnetic field h_c required to force magnetisation over the energy barrier of an individual single domain grain), the temperature of certain phase transitions, magnetic susceptibility (the ease with which a material can be magnetised; it is normally synonymous with magnetite concentration since it has the highest measurable values out of all the other magnetic minerals), hysteresis properties and remanent magnetisation intensities. Artificially imparted remanence and magnetisations can be used to distinguish between various types of magnetic minerals and their grain sizes. Hysteresis and thermomagnetic properties can provide further information about the type of magnetic minerals and magnetic mixtures in natural materials (Thompson and Oldfield, 1986).

The magnetic susceptibility, saturation remanence, isothermal or anhysteretic remanence, saturation magnetisation and Curie temperature, are some of the main magnetic parameters that are used for characterising the magnetic mineralogy and granulometry of natural samples (Thompson and Oldfield, 1986). In order to understand the influence of environment on magnetic minerals, a method to describe the mineralogy, grain size and concentration of magnetic mineral in natural samples has to be developed (Van Oorschot, 2001). A list of common parameters and ratios used in environmental magnetism is given in Table 1.1.

Symbol	Parameter Description	Dependent on/indicative of
χ	Mass specific susceptibility (m^3/kg)	Concentration of ferromagnetic grains, and grain size
SIRM	Saturation isothermal remanent magnetisation ($=M_{rs}$)[$\text{Am}^2\text{kg}^{-1}$] or [Am^{-1}]	Concentration, grain size
IRM-0.3T/SIRM 1.2T	S-value [-]	Mineralogy (ferromagnetic vs. antiferromagnetic)
T_c	Curie Temperature [$^{\circ}\text{C}$]	Mineralogy
ARM	Anhysteretic remanent magnetisation [$\text{Am}^2\text{kg}^{-1}$] or [Am^{-1}]	Concentration of SD ferromagnetic minerals
ARM/SIRM	Magnetic ratio [-]	Grain size, concentration, of SD remanence carrying particles
SIRM/ χ	Ratio of IRM to susceptibility [10^3Am^{-1}]	Concentration, gain size, mineralogy

Table 1.1: A list of magnetic parameters that are commonly used in environmental magnetism to classify mineralogy, grain size and concentration of magnetic minerals. Adapted from Van Oorschot (2001).

The first parameter, susceptibility, usually reflects the content of magnetic minerals of the sample; a high susceptibility indicates a high content of magnetic minerals (Van Oorschot, 2001). Table 1.2 list the formula, magnetic class and susceptibility values for (at room temperature) a number of common minerals.

The SIRM is the maximum remanent magnetisation that can be induced in a sample; it is an expression of domain state of remanence-carrying minerals (Van Oorschot, 2001). The grain size of magnetic mineral will also influence the remanent magnetisation. Using the SIRM parameter magnetic minerals can be categorized into high or low coercivity, and single domain (SD), pseudo-single domain (PSD) or Multidomain (MD) grain sizes. Particles of SD grains have the strongest SIRM for a given mineral. Ratios of isothermal remanent magnetisation (IRM) at different field values are often used to estimate the contribution of ferromagnetic and antiferromagnetic minerals. Ferrimagnetic mineral are more easily magnetised than antiferromagnetic mineral, therefore, the ferrimagnetic minerals will reach their SIRM at lower field than the latter (see Table 1.3). A widely used ratio is the S-values (or ratios), which ranges between 0 and 1. A ratio close to one indicates dominant magnetic minerals to be ferrimagnetic, and this value will decrease with increasing contribution from

antiferromagnetic minerals. A full discussion on how to derive the S-ratio is given in the methodology.

Mineral	Formula	Magnetism	χ [$10^{-8} \text{m}^3 \text{kg}^{-1}$]
Magnetite	Fe_3O_4	ferrimagnetic	57000
Maghemite	$\gamma\text{Fe}_2\text{O}_3$	ferrimagnetic	57000
Hematite	$\alpha\text{-Fe}_2\text{O}_3$	antiferromagnetic	60-600
Goethite	$\alpha\text{-FeOOH}$	antiferromagnetic	70
Pyrite	FeS_2	paramagnetic	30
Quartz	SiO_2	diamagnetic	-0.6
Clay Minerals	e.g. illite, kaolinite	Dia-/paramagnetic	-2-100
Calcium Carbonate	CaCO_3	diamagnetic	-0.5

Table 1.2: Magnetic class and typical susceptibility values for a number of common mineral. Adapted from Van Oorschot (2001).

Mineral	Saturation field [mT]
Magnetite and maghemite	~100mT (MD), 150-300mT (SD)
Hematite	400-500mT (MD) 800-2500mT (SD)
Goethite	>3000mT

Table 1.3: Typical values for the field at which SIRM is achieved, for some common magnetic minerals, Thompson and Oldfield (1986).

Some sediment magnetic parameters are subject to change on heating or cooling. This behaviour is mineral specific and such measurement as susceptibility response to temperature change can yield information on the unblocking temperature; defined as the temperature at which all magnetic susceptibility is lost. This temperature is very similar to the Curie temperature (T_C).

Mineral	Unblocking Temperature
Magnetite	~575-580°C
Pyrrhotite	~320°C
Hematite	680°C
Goethite	~120°C

Table 1.4: Unblocking temperature of some magnetic minerals.
 Values compiled from Thompson and Oldfield (1986).

1.2 Statement of problem

The field magnetic susceptibility values measured on the Eastern coast of Point Pelee National Park (PPNP) were high compared to the beaches on the western coast which had fairly low and uniform magnetic susceptibility values. This variation could be due to a number of factors. In an attempt to provide plausible explanations for these observed variations, this thesis will use environment magnetic methods in characterising beach sediments and determining sediment magnetic mineralogy of the western and Eastern coasts of PPNP.

Therefore, the basic magnetic mineralogy of the sediments on PPNP beaches needs to be characterised; in order to identify major magnetic minerals causing the high magnetic susceptibility; and to make a reasonable comparison between the East and West beach sediment magnetic characteristics. In order to understand potential sediment source and to provide an explanation for the concentration of magnetic minerals on the Eastern beaches, both field and laboratory sediment magnetic measurements had to be taken.

1.3 Objectives of study

The objectives of this study are:

1. To use a Geographic Information System (GIS) to map and display the magnetic susceptibility of Point Pelee beaches and their attributes in order to show the spatial variation at a glance and produce a map that can be easily updated with new data.
2. To determine the magnetic mineralogy at each beach and to delineate the effective grain size of the major magnetic minerals present in the beach sediment that caused the observed susceptibility variation.

3. To determine if the source of the sediments on the various beaches are the same through comparison of the sediments' magnetic characteristics.
4. To ascertain if the varying susceptibility on the beach is temporal.
5. To characterize and compare sediments from potential source/areas suggested by Trenhaile et al., (2000) i.e. PPNP and bluffs of Wheatley and the beach sediment.
6. To examine physical processes like erosion, sediment transport, deposition and beach nourishment as potential causes of the magnetic susceptibility variation observed on the west and the East beaches.

1.4 Significance of study

Thompson and Oldfield (1986) noted that magnetic mineral in lake sediments can be formed after deposition by chemical and biogenic processes; the result of the transformation of existing magnetic or non-magnetic minerals into new magnetic types; or brought into the lake from an outside source. These three possibilities are referred to as authigenesis, diagenetic alteration and allogeneses respectively. If the source is determined to be allogenic, this study will provide information on the erosional patterns, sediment transport/movement and depositional activities on the beaches of Point Pelee National Park and how they affect magnetic susceptibility variation. Potential sources of the mineral causing the high susceptibility will be examined and if anthropogenic, serve as a background to further studies in pollution.

Finally, this study will use Geographic Information System (GIS) for mapping and for attribute data management. The map will provide a database where additional georeferenced data can be easily added and updated for future purposes; this map with updates will show the pattern of magnetic susceptibility on the beaches and the direction of change.

1.5 Scope of study

The primary focus of this study is to use sediment magnetic methods and characterise the magnetic mineralogy on PPNP beaches; and to use these magnetic characteristics in explaining the variations observed on the western and Eastern coast.

In achieving the above, this study will also map the magnetic susceptibility of beach sediments on Point Pelee beaches using the Bartington susceptibility meter. This mapping

forms the basis for a GIS database that could be used for display. The major beaches considered were East beach (EB), North East beach (NEB), Middle East beach (MEB), Sleepy Hollow (SH), Dunes (D), Black Willow (BW), White Pine (WP) and West beach (WB). Magnetic susceptibility maps of the beaches will be produced using ESRI Arc-Info Geographic Information System (GIS). This study also attempted to determine if there was a temporal variation in the observed susceptibility on the Eastern beaches, through the collection of a second set of field susceptibility data in January and May, 2004 from all the beaches. Statistical analysis was used to formulate hypotheses and test them for significance. In addition to the field susceptibility measurements and field observations, sediment samples were collected from these ten beaches in order to characterize the magnetic mineralogy of these beach sediments.

Characterization of sediments from probable sources and comparison of magnetic mineralogy with those observed on the beaches allowed examination of some physical/environmental processes (erosion/accretion processes, sediment transport, and human activities) and their effects or contributions to the observed variation on the Eastern beaches. Finally, this study examined Rondeau Provincial Park, another cusped foreland in order to determine if the high concentration of magnetic mineral on the coast is a process common to cusped forelands in Lake Erie.

CHAPTER TWO

LITERATURE REVIEW

2.1 Areas of study: Point Pelee National Park beaches

The area of study is Point Pelee National Park (PPNP), a triangular-shaped cusped foreland (Trenhaile et al., 2000). The park is located at $41^{\circ} 58' 00'' \text{ N} / 82^{\circ} 31' 58'' \text{ W}$, with an elevation of 580m above sea level. The Park extends about 15 kilometres into the shallow western basin of Lake Erie, which is as far south as the northern border of California. It is situated on the northern shore of Lake Erie at the southernmost point in Canada. Point Pelee is a 20 kilometre long landscape with the unique blend of vegetation in the marshes, forest, savannah grasslands and beachfronts supporting a complexity of wild life (www.canadianparks.com).

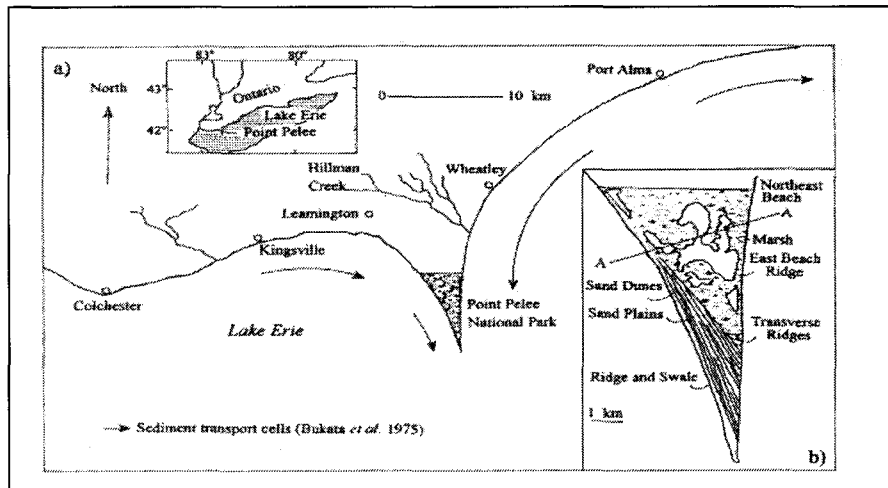


Figure 2.1: Location map of the Study area (Point Pelee and the Southern Coast of Essex and Kent Counties, South Western Ontario) Trenhaile et al., (2000).

PPNP contains a large marsh, and is flanked by beach systems, with the Northeast beach being characterised by periodic episodes of erosion (LaValle et al., 2001). Various studies have been done on some of these beaches; including modelling a space time series of beach and shoreline data in PPNP (LaValle et al. 2001). A semi-annual topographic and bathymetric data collected by LaValle (1978-1994) over a predetermined grid established at the Northeast beach. These data provided the measurements necessary to calculate beach net sediment flux (the volume of net sediment change occurring over a

six-month period for one meter wide area extending from the back- beach limit to the lowest water-line observed in the six month period) and net shoreline positional change (the difference in shoreline position along the survey transect measured in the six-month period). The model was used to produce a space-time metemap of net shoreline positional changes. The result shows that there is a pattern of initial shoreline advances giving way to retreat, followed by a pattern of reduced shoreline advances through time. These initial shoreline advances in the first eighteen months of the monitoring period were attributed to a relatively low lake level. Between 1982 and 1991 shoreline retreat dominated the Northeast beach. This retreat the authors associated with the combined effects of armor stone breakwater, tetra pod failure and unusually high lake levels.

PPNP also experiences the erosive effect of storm wave, seiches and surges (Lavalle et al., 2001). A Seiche is a variation in lake surface somewhat resembling a tide and is usually caused by changes in atmospheric pressure, and the wind. Seiches usually take place in the direction of the longest diameter of a lake (Moore, 1978). The waves are most frequently generated from the southwest and northwest, but can develop over fairly short fetches. A fetch is defined as the length of open water across which the wind is blowing which largely determines the height of waves (Moore, 1978). It is also reported that Lake Erie water levels has been rising since 1977 at a rate of 0.06m per annum and has exceeded record levels by 0.06 to 0.37m from June through October 1986 (LaValle et al., 2001). Typically, the level of Lake Erie fluctuates about 14 inches during a given year. During 2002, the Lake level actually fluctuated quite a bit more than this amount, about 20 inches. Since its steep decline from near record-high levels in 1997, the level of Lake Erie has generally remained below average since early 1999. However, a combination of favourable hydrologic conditions in late 2001 and early 2002 resulted in a marked recovery of lake levels, which hovered around average through the first half of the year. The recovery was short lived as a rather hot and dry summer negated these earlier improvements in lake levels. By the end of the year, Lake Erie's level had fallen back to about 8 inches below average, and more than 2 inches lower than the December 2001 level (Ohio Department of Natural Resources website: <http://www.dnr.state.oh.us/>).

Natural processes in the Great Lakes are spatially and temporally variable. These processes include hydrological cycle, wind systems, human induced processes like

eutrophication, beach nourishment, pollution, sediment movement, and erosion and deposition. All these processes intertwine to produce a unique and dynamic environment which is constantly evolving and changing in order to achieve a balance with the prevailing environmental conditions.

PPNP is a cusate foreland formed by accretion processes, and that the erosion taking place probably represents an abnormal reversal of this trend (Coakley, 1977). Coakley recognised shoreline recession as one of the fundamental physical processes at large in PPNP. PPNP is bounded in the NE, E, SW, W and NW by Lake Erie. Lake Erie experiences a mean seasonal fluctuation of 0.5m in lake level, and at times it could be as high as 1m. A lake level fluctuation of 2-3m can occur over a period of 5-15years (Coakley, 1976). With these variations in lake levels coupled with erosion and accretion rates, it is not surprising to observe variation in beach sediment magnetic susceptibility in PPNP.

One magnetic susceptibility mapping study has been done at PPNP. Morgan (2002) mapped the magnetic susceptibility of Camp Henry in PPNP. She used the Bartington susceptibility meter to take a radial transect measurement of some part of the area and a linear transect across a small cabin. A GIS map showing susceptibility with continuous contour interpolation was produced and the study showed a correlation between areas with heavy concentrations of anthropogenic material and high susceptibility values.

Finally, in order to study potential sediment source site and physical processes, study area was enlarged to include the following areas around PPNP; Wheatley and Rondeau Provincial Park. The areas are highlighted in the map on figure 2.2.

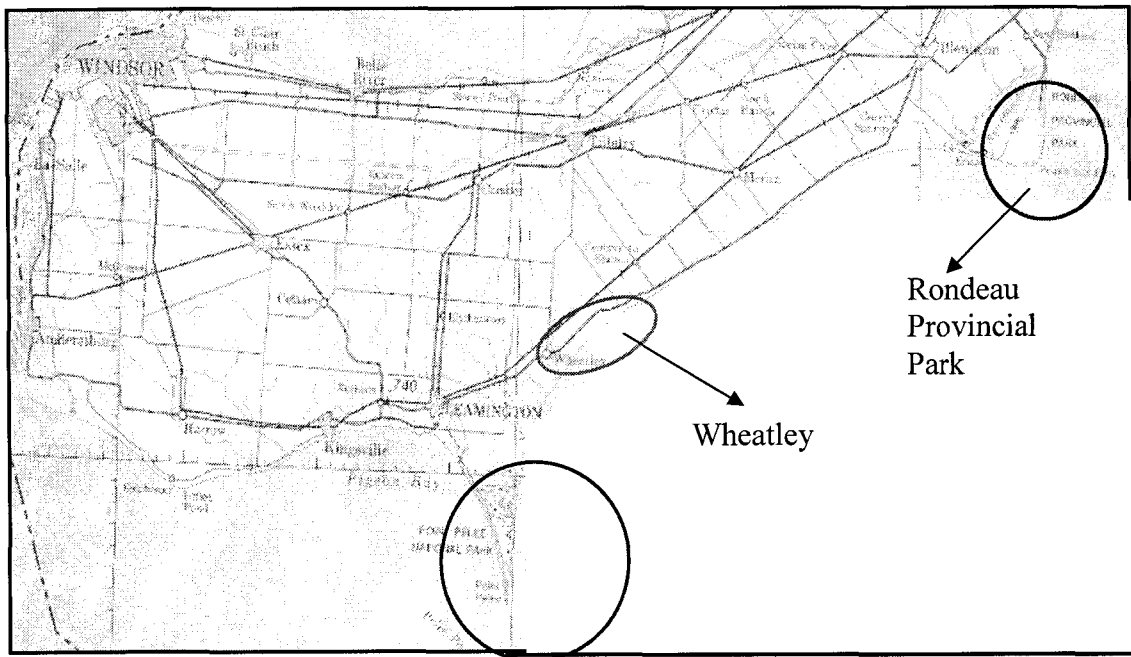


Figure 2.2: Location of Wheatley, and Rondeau Provincial Park. [Scanned map sheet of Windsor-Toronto Area (Department Mines and Resources) at a scale of 1:500000]

2.2 Previous studies on environmental magnetic properties of sediments

Sediment magnetic characteristics have been used in studies to trace sediment source (Thompson and Oldfield, 1986, Caitcheon, 1998, Ventura et al., 2001 and Royall, 2001). These studies range from using natural sediments to determine the relative contributions of sediment and associated substances at stream junctions especially where two magnetically homogeneous sources are mixed, to using artificial magnetic tracers for determining source of sediment erosion, and provenance sediment studies (Caitcheon, 1998). Sediment source determination is an important issue in erosion monitoring, pollution control and management, and catchments area contribution to sediment characteristics

Several studies have shown that sediment magnetic properties can be used to trace sediment source, especially for a magnetically homogeneous sediment source (Thompson & Oldfield, 1986; Caitcheon, 1998). These studies include tributary sediment contribution to a stream junction, tracing the source of eroded sediments, provenance sediment studies, to using synthetically constructed magnetic materials in determining erosion pathways (Ventura et al., 2001).

A fundamental condition that must be met by any tracing method is that the tracer substance(s) must remain unaltered within the spatial and temporal limits in which the tracing method is being applied (Caitcheon, 1998). Empirical studies have demonstrated that the spatial and temporal stability of magnetic components of fluvially transported sediments and the relationship between representative magnetic parameters were found to be constant in sediments sampled along river reaches, and in sediment cores representing several decades of deposition (Caitcheon, 1998). Results from the studies have shown that using magnetic minerals as tracers can help determine sediment redistribution in a catchment, source of eroded sediment, and a river channel sediment contribution to basin network (Caitcheon, 1998, Duck et al. 2001, Gruszowski et al., 2003).

A number of studies have mapped surface magnetic susceptibility of soil or sediments. Some of these have used magnetic susceptibility as a proxy for determining polluted areas, to show the patterns of pollution distribution and to detect polluted sites by identifying areas with high magnetic intensity. Magnetic susceptibility mapping has been done on both large and small scale levels. Boyko et al., (2001) investigated 298 locations in north and west Austria at 10x10km grid to create a magnetic susceptibility map of the forest top soil. Their results showed that the water content logged in the moss cover; nonhomogeneities with the investigated places and forest cover were all factors having significant impact on the susceptibility reading. The regression coefficient R^2 between the magnetic susceptibility values from the two data sets was 0.906, with an average difference of 2.3×10^{-5} SI indicating a high degree of agreement between the results of two mapping campaigns.

Hoffman et al., (1999) also mapped the magnetic susceptibility of surface soil. They acquired measurements of soil magnetic susceptibility obtained over large areas, comprising regions in Germany, Austria, Czech Republic and Poland. Susceptibility was measured at 1100 sites with over 21,000 individual susceptibility measurements acquired and processed. Areas of high susceptibility were linked to highly industrialized zones.

Magnetic susceptibility maps have also been used to detect road side pollution. Hoffman et al., (1999) used magnetic susceptibility mapping to trace the distribution of concentrations of contaminants in soils along roads and highways carrying appreciable traffic. The study noticed that the distribution of susceptibility represents polluted areas

and the measurements were strongly influenced by traffic frequency, roadside topography and meteorological conditions (wind direction).

Hanesch and Schoger (2002) assessed the potentials of pollution monitoring and mapping by means of susceptibility measurements at a large scale and at a regional scale. Susceptibility measurements at the soil surface, combined with geochemical analysis yielded a detailed picture of the spatial distribution of pollutants. Areas with high metal concentration (mercury, cadmium, and zinc) had the highest correlation with susceptibility, and it was possible to estimate their content in the soil from the magnetic susceptibility values. Boyce et al., (2001) evaluated the use of magnetic property measurements (magnetic susceptibility and other magnetic parameters) made by a towed Overhauser magnetometer for mapping contaminated harbour and waterways in Western Lake Ontario, and concluded that high resolution mapping has a good potential as a reconnaissance method for assessing the distribution of urban source magnetic sediments.

CHAPTER THREE

METHODOLOGY

Three primary methods were used for data analysis in this thesis; they were basic magnetic techniques, GIS Geostatistical Analyst for display and presentation of field data and statistical tests on the field magnetic susceptibility data. Field magnetic susceptibility data were collected in summer 2003, 2004 and also winter 2004 for East beach alone. A second set of magnetic susceptibility data was collected for East beach using random method as oppose to the usual transect methods used for all data collection. This was to ensure that data collection method did not have any effect on surface map creation.

3.1 Data sets

The data sets used for analysis are grouped into four main categories:

- i. Field data: Georeferenced field magnetic susceptibility measurements from the ten beaches collected in summer 2003, winter 2004, and summer 2004, Wheatley and Rondeau.
- ii. Lab data (sediments): Georeferenced sediment samples/specimens from PPNP beaches, and sediment samples from Wheatley and Rondeau beaches.
- iii. GIS data: Georeferenced aerial photograph of PPNP (Department of Earth Sciences, University of Windsor), and a map sheet of Windsor-Toronto Area (Department Mines and Resources) at a scale of 1:500000 for scanned display.
- iv. Literature from previous studies.

3.2 Instrumentation

In order to obtain all the necessary magnetic data needed for analysis and comparison, field magnetic susceptibility and sand sediments collected from the field were measured using the following instruments:

- a. 2G Cryogenic Magnetometer.
- b. Sapphire Instruments Impulse Magnetizer.

- c. Sapphire Instruments AF demagnetizer with DC coil for ARM measurements.
- d. Bartington field susceptibility suite and dual-frequency sensor.
- e. AGICO Kappa bridge KLY-3 susceptibility meter with furnace and low temperature attachment.

The magnetic data collected were partial anhysteretic remanent magnetisation (pARM), high and low coercivity ARM and ARM data, saturation isothermal remanent magnetization (SIRM) and S-ratio data, susceptibility dependence on temperature data, and hysteresis data. The pARM and ARM were imparted with the Sapphire AF demagnetizer with the DC coil bias. The acquired magnetization was measured with the 2G Cryogenic Magnetometer. The IRM was imparted with the Sapphire Instruments Impulse Magnetizer in a steady field and the acquired IRM was also measured with the 2G Cryogenic Magnetometer. The Bartington Field Susceptibility Meter (MS2 probe) was used for acquiring all the field magnetic susceptibility measurements from the beach sediments. The main part of the MS2 probe measurement kit is a coil, an alternating magnetic field produced by the coil when it is connected to the source alternating voltage. The frequency of this field changes as material is placed within reach of the magnetic field produced by the coil. The magnetic response will reflect the contribution from top 60-100mm of the land surface of any ferromagnetic material placed within the effective range of the coil. The susceptibility values will depend on the homogeneity of material measured (Schibler et al., 2002 and Dearing, 1999). The AGICO Kappa Bridge KLY-3 susceptibility meter with furnace attachment and argon gas was used for determining the susceptibility temperature dependence.

3.3 Field magnetic susceptibility measurements and sediment data collection

Magnetic susceptibility field data were collected from the ten beaches under study. Point measurements were collected with a Bartington Susceptibility Meter Probe, and location was measured using a hand held GPS. Point measurements were done in parallel transects perpendicular to the shoreline, along the beaches, as shown below. Surface beach sediment samples were also collected randomly from each beach. Each sample was georeferenced and bagged. Sediment samples were also collected vertically

downward at a depth of about 10cm in EB and NEB to determine if processes were occurring only at the surface level.

From preliminary analysis, it was observed that there was a high modelling error for the surface map creation. Therefore, another field work was undertaken, and field magnetic susceptibility data were collected from East beach in a random order as oppose to the initial transect method of data collection. This was to determine if sampling method had a significant contribution in surface magnetic susceptibility map creation.

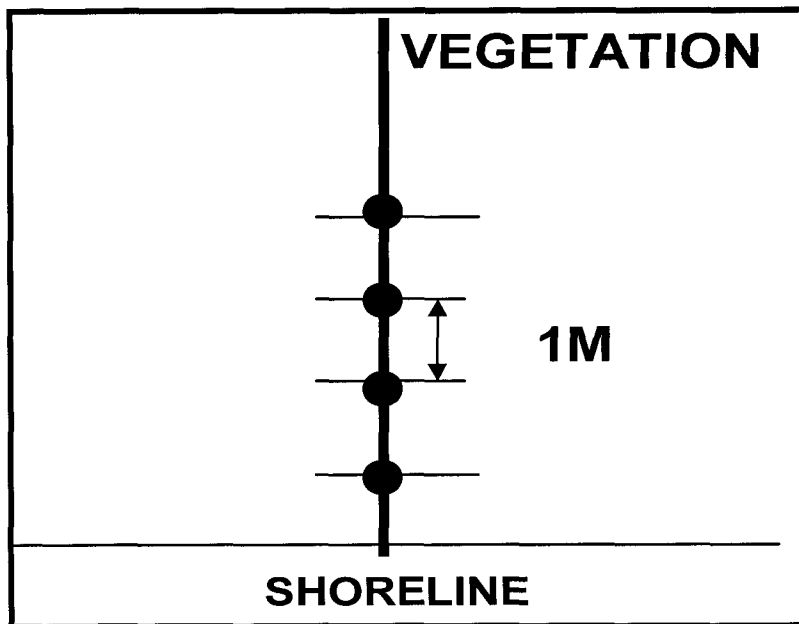


Figure 3.1: Schematic representation of field magnetic susceptibility data collection with Bartington MS2 susceptibility meter.

Sediment samples were also collected from Wheatley bluff and Wheatley beaches northeast of PPNP (see figure 2.2 on study area). These were used to determine if high magnetic susceptibility materials were sourced from the northeast. Also, some part of Rondeau Provincial Park (RPP) also a cusplate foreland was also mapped to determine if forelands in the Lake Erie catchments area were experiencing similar physical processes. Field magnetic susceptibility data as well as sample sediments were collected from RPP.

3.4 Sample preparation and laboratory magnetic measurements

Sediment samples were air dried and weighed. Plastic cubes and cylinders were used for sample containers. The magnetisations of the containers were measured to determine strength; containers with significant magnetisation ($<10^{-7}$) were discarded or demagnetised. Plaster was used to stabilize sediment samples to prevent movement during measurement in the magnetometer.

In other to characterize and determine the magnetic mineralogy of the beach sediments, the following suites of laboratory magnetic measurements were done on the sediment samples:

- ❖ pARM and ARM
- ❖ SIRM
- ❖ S-ratios
- ❖ Susceptibility- temperature dependence measurements

3.4.1. pARM and ARM measurements

Partial ARM's are imparted by switching on a DC field between two specified values of alternating field (AF). Grains with coercivity (H_{cr}) within that window acquire an ARM, while the rest of the assemblage is demagnetized. Moving the window over a range of AF's, a pARM curve is obtained, representing the spectrum of coercivity in the sample. pARM procedures affect low coercivity grains, and since coercivity is related to grain size.

The pARM and the ARM were acquired under a set alternating field (AF) of 110mT, and a DC bias field of 0.05mT. The sediment samples were treated with a step sequence of AF fields (windows) of 1-10mT, 10-20mT, 20-30mT... 90- 100mT using the AF demagnetizer with a DC bias field. The following steps were also done; 1-50mT (for low coercivity ARM) 50-100mT (for high coercivity ARM) and 1-100mT (ARM). The acquired pARM and ARM are measured using the magnetometer. Magnetization values obtained at each of these steps served as the pARM data.

3.4.2. SIRM and S-ratios

Isothermal remanent magnetisation as defined by Thompson and Oldfield, (1986) is the remanent magnetisation acquired by deliberate exposure of material to a steady field at a given steady temperature (most commonly room temperature). The maximum remanence that can be produced is called the saturation isothermal remanent magnetization (SIRM). In characterising sediment mineralogy, SIRM has been used to recognise high coercivity and low coercivity minerals.

In order to see how the SIRM was acquired, the sediment samples were subjected to increasing fields, and the acquired magnetization were measured between each steps with the 2G Cryogenic Magnetometer: The step sequence of saturation used were; 5, 10, 20, 30, 60, 100, 150, 200, 250, 300, 400, 550, 700, 900 and 1200mT. Following IRM acquisition, the specimens were step demagnetized with the AF demagnetizer in steps of 5, 10, 20, 30, 40, 60, 80, 100 and 120mT. The samples were also subjected to a back field step of 100 and 300mT (after maximum saturation, 1200mT) in order to determine the estimate of low or high coercivity minerals in the sample.

3.4.3. Susceptibility variation with temperature measurement

The AGICO Kappa Bridge KLY-3S furnace equipped with argon gas was used for measuring the susceptibility versus temperature of samples. The argon gas was used to keep a non-oxygenated environment and prevent chemical alteration and reaction at high temperature. The maximum temperature for temperature analysis was 700°C. the values of susceptibility against varying temperatures were acquired at several heating and cooling temperature steps.

3.5 Magnetic data analysis

The magnetic data obtained from pARM, SIRM, and susceptibility versus temperature measurements were analysed. The basic method of analysis is discussed below.

3.5.1. pARM

The acquired pARM values were normalized with pARM maximum value. A graph of pARM/pARM MAX versus magnetising field was plotted. The magnetic grain sizes were determined using a pARM spectra curve. The graph template of normalized

magnetization against field in Jackson et al., (1988) was used for comparing the acquired pARM spectra of the beach sediments to that of standard grain size magnetite in Jackson et al., (1988) (see figure 3.1). The maximum field for the pARM was 100mT.

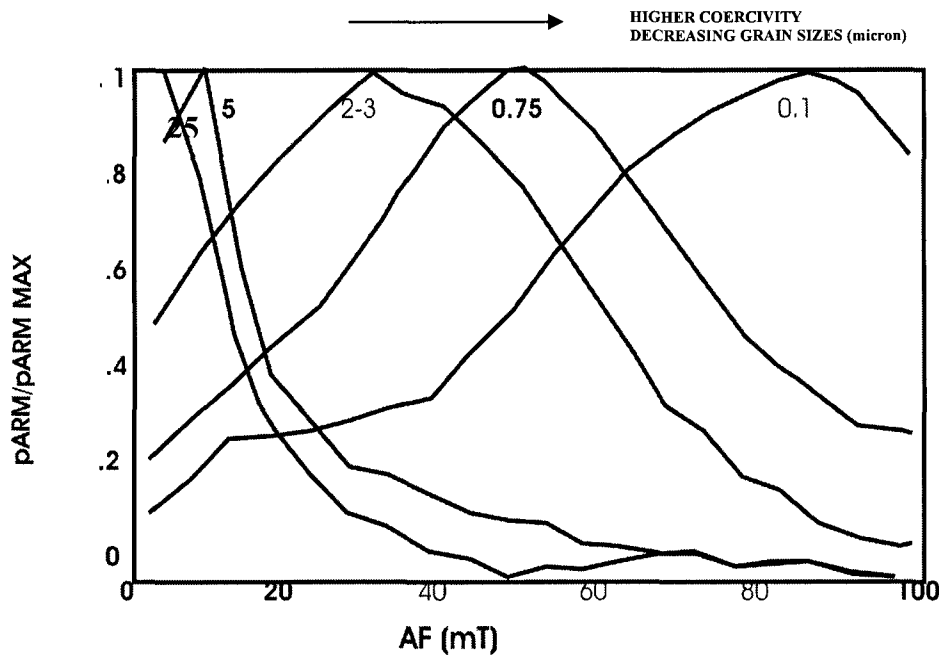


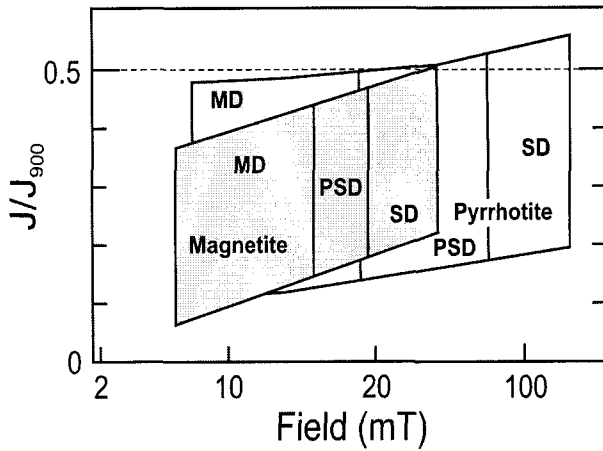
Figure 3.2: pARM curves for synthetic samples containing magnetite with discrete grain size. Adapted from Jackson et al., (1988).

3.5.2. SIRM

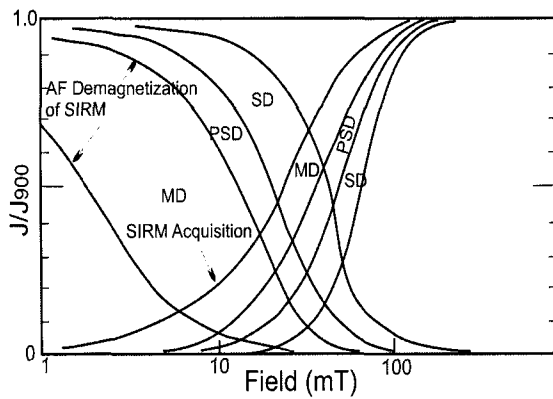
SIRM values depend on concentration, if it is high; then the amount of ferromagnetic material present is also high and vice versa (Thompson and Oldfield, 1986). The SIRM and the back-field values yielded useful parameter for estimating the enrichment of low coercivity or high coercivity minerals in the samples. The SIRM and back field IRM were used to calculate the S-ratios and HIRM. The data were used to determine if the sediments were of high or low coercivity (Akram et al., 1998). A plot of J/J_{max} (J =magnetisation) versus \log of H (H = field) distinguishes magnetic minerals with high coercivity and low coercivity with the shape of their curve.

Symons and Cioppa (2000) provided some useful templates for comparing and categorising SIRM acquisition data for some major magnetic minerals like magnetite, hematite, pyrrhotite and goethite. The templates were also used to characterise multi-domain (MD), pseudo-single domain (PSD), and single domain grain sizes (SD). The

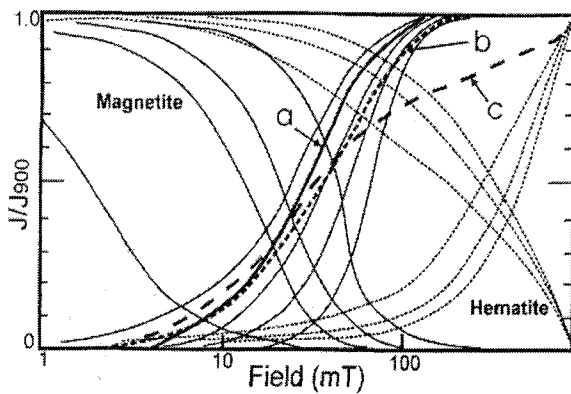
SIRM data were analysed by plotting J/J_{MAX} versus Log of magnetizing field (H). The resulting spectra were compared to the SIRM templates provided by Symons and Cioppa, (2000).



A



B



C

Figure 3.3 A, B and C: A- Plot for identification of SD magnetite and pyrrhotite grains, B- SIRM acquisition and crossover plot for magnetite, and C- combined magnetite and hematite plot (Symons and Cioppa, 2002).

3.5.3. Magnetic susceptibility

Magnetic susceptibility is mainly affected by the concentration of magnetic minerals and can be affected by grain size as well (Solheid et al., 1997). Mass specific susceptibility was obtained from bulk susceptibility measurements; in order to have an effective susceptibility comparison between the beaches. Mass specific susceptibility was obtained as specified below.

Volume of sample container = 8 cc

δ = density

Susceptibility = bulk k

Weight of sample = w

K SI = calculated susceptibility in SI units.

% of sediment = weight/ (density *8)

Calc. k = (bulk k * total mass)/% of sediment

kSI = calc. k/10

χ (Mass specific susceptibility) = kSI/ δ

3.5.4. Susceptibility temperature variation

Susceptibility varies with temperature; as temperature increases, the thermal energy increases the interatomic distance between couplings. Eventually, at a certain temperature, thermal energy overcomes the exchange coupling and produces a randomising effect. Each magnetic mineral has a unique Curie temperature which is defined as temperature at which thermal energy overcomes the exchange electronic force thereby causing magnetic coupling to disappear. Each minerals reacts differently with increasing temperature upon heating (Thompson and Oldfield, 1986). A plot of the resultant susceptibility against heating a cooling temperature produced a graph from which the Curie temperature of magnetic materials was fairly determined (Solheid et al., 1997).

3.5.5. Magnetic ratios

In order to classify the various magnetic components into their mineralogy, domain state, and concentration, some ratio parameters were calculated and compared

with standard calculated values (Peters and Dekkers, 2003) in Table 3.2). Several ratios were calculated from a combination of different magnetic measurements. These included:

- ❖ Remanent ratios: S-ratio at 0.1 and 0.3T.
- ❖ Hard isothermal remanent magnetization - HIRM
- ❖ Normalized ARM = ARM/SIRM
- ❖ Anhyseretic remanent magnetization/susceptibility- ARM/ χ
- ❖ Saturation remanent to susceptibility (χ) ratio.

A. S- ratios

$S_{-0.3T}$: this ratio parameter is a measure that indicates the relative abundance of low coercivity magnetic minerals it measures the ratio of remanent carrying ferromagnetic to antiferromagnetic mineral and it increases with low field susceptibility (Guo et al., 2001). It is calculated using the expression below.

$$S_{-0.1T} = [IRM_{-0.1T}/IRM_{(1.2T)}]$$

B. HIRM

SIRM and back field IRM values (0.3T) were used for estimating the enrichment of low coercivity or high coercivity minerals in the sample. The “hard IRM” (HIRM) is a parameter defined as follows:

$$HIRM = (IRM_{-0.3T} + SIRM) / 2$$

The HIRM is a measure of the concentration of high coercivity minerals, where HIRM values become large if high coercivity of minerals is relatively abundant. $IRM_{0.3T}$ denotes 0.3T back-field IRM values (Akram et al., 1997).

C. Normalised ARM = ARM/SIRM

Akram et al., (1997), noted that the intensity values of SIRM and ARM are concentration dependent parameters. They depend on the grain-size and amount of magnetic materials present. Therefore, to remove the effect of concentration and obtain only the intrinsic changes in the grain-

size (domain state) and or mineralogy of the magnetic carrier, the ARM intensity is normalized by SIRM. This gives the maximum remanence achievable.

Parameter or ratio	Mineral						
	Magnetite	Titano-magnetite	Maghemite	Hematite	Goethite	Pyrrhotite	Greigite
	Av. (no.)						
	[min → max]						
χ (10^{-6} m ³ kg ⁻¹)	674 (98) [285 → 1233]	422 (86) [46 → 806]	632 (17) [283 → 845]	0.97 (63) [0.13 → 3.83]	1.17 (59) [0.46 → 5.92]	32.1 (54) [5.7 → 67.5]	108 (13) [26 → 194]
χ_{FD} (%)	2.4 (23) [0.4 → 11]	No data	No data	No data	No data	No data	No data
σ_{RS} (A m ² kg ⁻¹)	5.3 (82) [0.3 → 33.1]	5.2 (43) [0.5 → 19.9]	6.8 (17) [3.6 → 10.2]	0.18 (95) [0.003 → 0.35]	0.052 (60) [0.015 → 0.12]	5.0 (54) [1.6 → 9.3]	5.4 (11) [0.8 → 12.3]
σ_S (A m ² kg ⁻¹)	62.2 (12) [50.3 → 89.5]	16.0 (10) [11.2 → 21.9]	63.6 (11) [61.5 → 65.6]	0.28 (18) [0.093 → 0.47]	0.22 (58) [0.02 → 0.59]	13.3 (54) [3.5 → 21.0]	14.1 (12) [3.1 → 29.2]
χ_{ARM} (10^{-6} m ³ kg ⁻¹)	1673 (72) [73 → 10510]	362 (19) [151 → 623]	376 (6) [324 → 408]	No data	No data	No data	608 (12) [242 → 916]
σ_{RS}/χ (10^3 A m ⁻¹)	11.3 (97) [0.3 → 80.8]	21.0 (53) [1.1 → 120]	11.0 (17) [9.2 → 16.1]	261 (63) [1.2 → 783]	57.4 (59) [5.9 → 212]	209 (64) [4.5 → 997]	70.7 (41) [11.2 → 174]
σ_{RS}/χ_{ARM} (10^3 A m ⁻¹)	7.7 (67) [0.5 → 23.1]	5.02 (19) [2.15 → 11.0]	10.4 (6) [9.2 → 11.8]	No data	No data	No data	8.6 (11) [2.6 → 15.7]
χ_{ARM}/χ	2.37 (72) [0.11 → 13.7]	1.64 (19) [0.35 → 3.92]	1.12 (6) [1.02 → 1.37]	No data	No data	No data	5.6 (27) [1.8 → 9.8]
$(B_0)_C$ (10^{-3} T)	9.8 (101) [0.1 → 34.3]	20.8 (87) [2.0 → 158]	7.2 (11) [6.4 → 9.0]	268 (18) [4 → 520]	217 (60) [25 → 890]	36.9 (64) [9.8 → 97.2]	42.6 (67) [10.0 → 71.3]
$(B_0)_{CR}$ (10^{-3} T)	24.4 (185) [8.0 → 69.5]	41.4 (96) [8.5 → 213]	20.8 (17) [16.9 → 31.0]	318 (96) [30 → 821]	1972 (60) [500 → 4100]	45.3 (64) [10.0 → 124.5]	67.1 (78) [37.0 → 94.8]
$(B_0)_{CR'}$ (10^{-3} T)	30.8 (58) [10 → 63]	30.3 (25) [8.5 → 138]	30.7 (15) [25.0 → 46.5]	270 (82) [28 → 769]	3386 (60) [1200 → 6999]	52.6 (45) [16.4 → 134.0]	75.0 (12) [41.4 → 96.8]
$(B_0)_{CR}/(B_0)_C$	9.1 (96) [1.4 → 65]	3.2 (87) [1.2 → 6.9]	2.62 (11) [2.54 → 2.67]	1.76 (13) [1.28 → 2.19]	19.1 (60) [2.5 → 66.7]	1.27 (63) [0.55 → 2.29]	1.74 (62) [1.21 → 5.09]
$(B_0)_{CR}/(B_0)_{CR'}$	0.68 (58) [0.44 → 0.95]	0.77 (25) [0.54 → 1.0]	0.66 (15) [0.65 → 0.68]	1.05 (82) [0.79 → 1.24]	0.65 (60) [0.25 → 1.65]	0.80 (45) [0.54 → 1.22]	0.79 (12) [0.73 → 0.89]
M_{RS}/M_S	0.12 (89) [0.0005 → 0.4]	0.19 (63) [0.01 → 0.53]	0.13 (11) [0.12 → 0.16]	0.58 (18) [0.43 → 0.85]	0.32 (58) [0.06 → 1.0]	0.36 (64) [0.02 → 0.58]	0.45 (67) [0.18 → 0.69]

Table 3.2: Average values of magnetic parameters and ratios used for comparison (Peters & Dekkers, 2003).

3.6 Geographic Information System (GIS) exploration and display of field data

A GIS is an organised collection of computer hardware, software, geographic data and personnel designed to efficiently capture, store, update, manipulate, analyze and display all forms of geographically referenced data (ESRI 1997). GIS and conventional maps differ. While the later aims at using graphics to represent geographic settings, the former is not just for making maps, but an analytical tool.

The georeferenced beach magnetic susceptibility measurements were inputted into a database file. Field magnetic susceptibility data collected from summer 2003, 2004 and winter 2004 were entered into a geodatabase, and merged with PPNP aerial photo. The database file layer was merged with the aerial photo of PPNP using ESRI ARC GIS

8.1. The Geostatistical Analyst extension was used for exploring and interpolating the magnetic susceptibility point data.

The Geostatistical Analyst is an advanced surface modeling tool that uses deterministic and geostatistical methods. It uses exploratory and interpolation methods that utilizes information on the spatial coordinates of data to formulate models used for estimation and prediction. Its main assumption in surface creation is based on the fact that: *“thing that are closer are more alike than those that are further apart”* (ESRI Inc, 2001).

Two main surface fitting techniques were chosen for the analysis;

1. Inverse Distance Weighted (IDW).
2. Kriging

The IDW creates surfaces from measured points based on extent of similarity between data point, while the Kriging is an interpolation method that uses single data type to predict (interpolate) values of the same data type at unsampled location.

I. GIS Geostatistical data exploration

The interpolation method that was used for surface generation produces a more accurate result when data are normally distributed. Therefore, in order to check for data distribution pattern, the susceptibility data were explored using the following geostatistical capabilities;

- ❖ Histogram Analysis
- ❖ Normal QQ Plot

Histogram

This displays the frequency histogram for the attributes in the dataset enabling the examination of the univariate distribution of the datasets for each attribute of interest. The dataset was highly skewed to the left. To make predictions more accurate, each data set was transformed in order to produce a more normal distribution. The log transformation was used since it produced a histogram that was closest to a normal distribution curve.

Normal QQ Plot

In this method of data exploration, the distribution of the dataset is compared with a standard normal distribution. The dataset was not identical to a normal distribution. When the log transformation was added, it produced a better fit.

II. Data representation

Arc Catalogue, ARCGIS/ARCMAP were used for the data organization, input and exploration respectively. The Aerial Photograph and the attribute database for all the beaches were integrated using Arcmap. The first data exploration was done by taking all the beaches into consideration. The results were inconsistent due to the following:

1. The areas the beaches covered were small in comparison to the whole Point Pelee area,
2. Data points were only on the beaches leaving a vast majority of the area in the middle empty, hence, an attempt to fit a model for the entire area would have made nonsense of the whole process.

Hence, it was necessary to analyze the data on an individual beach basis based on the above reasons. Using the aerial photo, the entire West beach area was divided into two main sections (Sanctuary beach and West beach), since data was relatively more uniform in the West beaches than on the East beaches. The East beaches were digitized individually. The attribute data sets were also separated to match with the area of interest.

III. Geostatistical Analyst surface model fitting process

The data exploration showed that the distribution of magnetic susceptibility was not random. Log transformation was used on data sets from East beach, Middle-East beach, Northeast beach and Sanctuary beach in the surface model fitting process (Kriging). This was done in order to have a data set that bore a closer resemblance to normal distribution. The data sets from West beach was not log transformed during analysis, as it showed a relatively more normal distribution without the transformation than it did with the log transformation. Magnetic susceptibility distribution maps for all the beaches at various seasons were produced. A display of the localities for the collected georeferenced magnetic sediments was also done in the GIS.

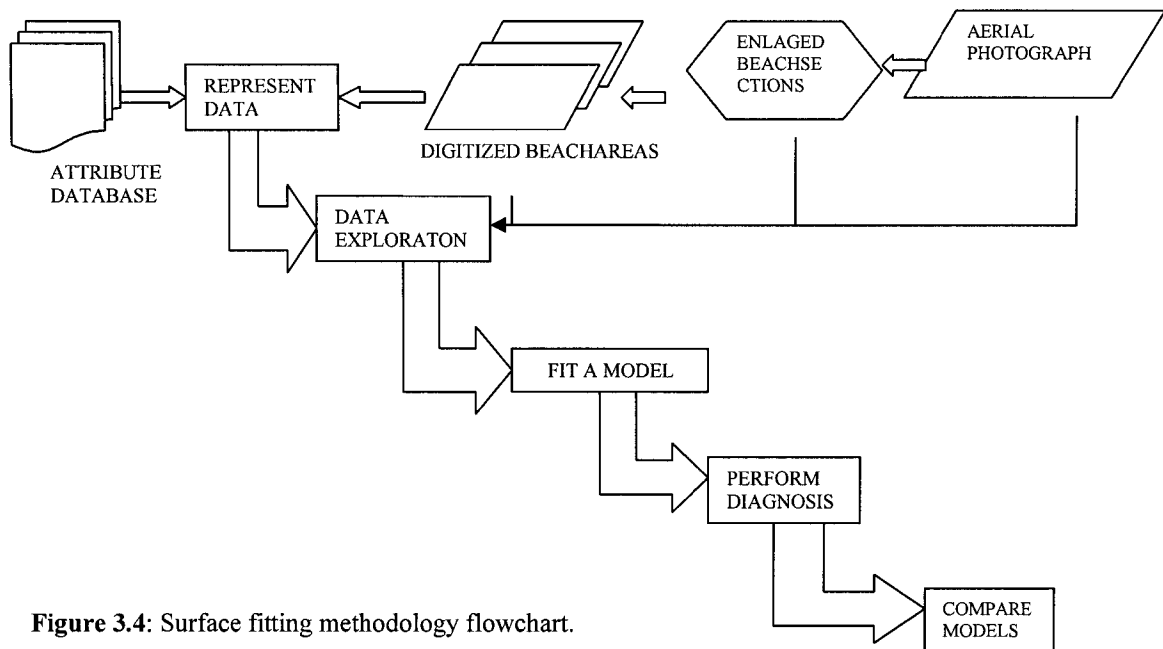


Figure 3.4: Surface fitting methodology flowchart.

3.7 Statistical analysis and test of hypotheses

As a guide to achieving some of the objectives set out for this study, various hypotheses were formulated, and each was tested statistically.

I. Hypotheses

Based on field magnetic susceptibility data collected from the beaches at various seasons, and the issues being studied, the following hypotheses have been formulated as an effective guide. Simple statistics would be applied at 5% level of significance.

1. There is no significant difference in the susceptibility (χ) observed on the Eastern beaches and those observed on the Western beaches.

Hypothesis (1)

$$H_0: 0\chi_{EB}=0\chi_{MED}=0\chi_{NEB}=0\chi_{SB}=0\chi_{SH}=0\chi_{WP}=0\chi_D=0\chi_{WB}=0\chi_{SH}=0\chi_{BW}$$

$$H_0: 0\chi_{EB} \square 0\chi_{MED} \square 0\chi_{NEB} \square 0\chi_{SB} \square 0\chi_{SH} \square 0\chi_{WP} \square 0\chi_D \square 0\chi_{WB} \square 0\chi_{SH} \square 0\chi_{BW}$$

2. There is no significant seasonal variation in susceptibility (χ) on the beaches.

Hypothesis (2)

$$H_0: 0\chi_{(Bi)} \text{ May03} = 0\chi_{(Bi)} \text{ May04}$$

$$H_1: 0\chi_{(Bi)} \text{ May03} \square 0\chi_{(Bi)} \text{ May04}$$

(Where Bi = EB, MEB ... WB)

3. There is no significant difference in susceptibility (χ) within the individual beaches i.e. from transect to transect.

From the preliminary ANOVA test of data from summer 2003 field work, it was observed that the sample variances are significantly different. This implies that the basic assumption of normality in the population distribution (distribution of magnetic susceptibility in Point Pelee beaches as a whole) is not met. Therefore, to compare the central tendency (we now use median) of the magnetic susceptibility of the beaches, a non parametric test must be employed. Generally, non parametric tests make no assumption about a specific shape of the population from which the samples are drawn. Unlike parametric tests which assume that the population distribution is normally distributed and therefore have uniform variance, non parametric tests can still compare statistics from different samples without making any specific assumptions about the shape of the population from which the samples are drawn (Freund, 1960).

The Kruskal-Wallis, test which is a non parametric alternative of the one way ANOVA, will be used to compare the central tendencies of the magnetic susceptibility data of the beaches. This test compares more than two independent samples. In this test, the null hypothesis is that the median of the k populations (beaches) are the same:

$$H_0: m_1 = m_2 = \dots = m_k, \text{ for } j = 1 \text{ through } k \text{ populations.}$$

$$H_1: m_1 \neq m_2 \neq \dots \neq m_k, \text{ [at least one median (m) differs from the others].}$$

The test is a one tailed test.

II. Test Statistic, H.

1. Rank the combined data value as if they were from a single group. The smallest data value gets the rank of 1, the next smallest, 2, and so on. In the event of a tie, each of the tied values gets their average rank.
2. Add the ranks for data values for each of the k groups, obtaining $\sum R_1$, $\sum R_2$, through $\sum R_k$.
3. The calculated value of the test statistics is;

$$H = \frac{12}{n(n+1)} \left[\frac{(\sum R_1)^2}{n_1} + \frac{(\sum R_2)^2}{n_2} + \dots + \frac{(\sum R_k)^2}{n_k} \right] - 3(n+1)$$

Where $n_1, n_2 \dots n_k$ = the respective sample sizes for the k samples

$$n = n_1 + n_2 + \dots + n_k$$

III. Critical Value of H

The distribution of H is closely approximated by the chi square distribution whenever each sample size is at least 5 and, α = the level of significance for the test, the critical H is the chi square value for which the degrees of freedom (df) = $k-1$ and the upper tail area is alpha (α).

IV. Decision rule

If the calculated H exceeds the critical value (theoretical H), the null hypothesis is rejected. Otherwise it cannot be rejected.

Given the volume of data with which we are working in this thesis, we shall use MINITAB computer software programme to perform the computations. For significant variation between seasons, a test of means was used.

CHAPTER FOUR

ANALYSIS AND RESULTS PRESENTATION OF MAGNETIC MEASUREMENTS

In order to determine magnetic mineralogy, the sediment samples were subjected to various magnetic measurements. This chapter deals with results from laboratory measurements and magnetic analysis of the beach sediments. Sieved sediments were used for the pARM and the SIRM analysis. In the display of pARM and SIRM results for the sieved sediment, the letter A, B and C were used to denote sediments with grain sizes greater than 0.6mm, B sediments greater than 0.3 but less than 0.6mm and C were samples with grain sizes less than 0.3mm.

4.1. Field magnetic susceptibility

The average magnetic susceptibility across transect for the beaches in PPNP at various seasons are summarized below. Values are from direct field measurements with the Bartington MS2D susceptibility meter in the summers of 2003 and 2004 respectively.

Beaches	Total Number of χ Points	Min χ	Min χ	Max χ	Max χ	Average	Average	No of Transects	Samples 03/04
		2003 (*10 ⁻⁶ SI units)	2004 (*10 ⁻⁶ SI units)	2003 (*10 ⁻⁶ SI units)	2004 (*10 ⁻⁶ SI units)	χ 2003 (*10 ⁻⁶ SI units)	χ 2004 (*10 ⁻⁶ SI units)		
EB	363	52	7	8888	6329	760	695.2	13	16/1
MEB	211	50	20	8882	6573	1995	941	8	4/1
NEB	254	32	17.5	3660	4005	275	137	20	8/0

Table 4.1: Field Magnetic susceptibility summary for Eastern beaches. Sixteen sediment samples were taken in 2003 for the EB, and one in 2004 for the EB and MEB. For NEB, 8 samples were taken in 2003.

Beaches	Total Number of χ Points	Min χ 2003 (*10 ⁻⁶ SI units)	Min χ 2004 (*10 ⁻⁶ SI units)	Max χ 2003 (*10 ⁻⁶ SI units)	Max χ 2004 (*10 ⁻⁶ SI units)	Average χ 2003 (*10 ⁻⁶ SI units)	Average χ 2004 (*10 ⁻⁶ SI units)	No of Transects	Samples 03/04
SB	202	14	15	243.5	221	88	72.6	11	4/0
NW	146	17	23	127.5	289.5	65	64.3	8	2/0
SH	54	47	22	245	119	92	64.2	3	1/0
DUNES	43	55	25	142	217	81	60	3	1/0
BW	31	52	37	160	147	84	72	3	1/0
WP	59	25	13	105	135	56.9	45.5	4	0/0
WB	151	37	23	132	114	79.99	65.2	9	2/1

Table 4.2: Field Magnetic susceptibility summary for Western beaches. A total of twelve sediment samples was taken from the Western beaches in 2003 and 2004.

The magnetic susceptibility measurements were collected at 1m intervals starting from the shoreline (section 3.3). A graph of average magnetic susceptibility across transect plotted against distance from the shoreline (Figures 4.1 - 4.5) showed the pattern observed across transects on the beaches. The magnitudes of magnetic susceptibility at the Eastern beaches were generally higher than those observed for the west beaches. The western beaches (SB, WH, BW, DUNES, SH, NW, AND WB) also showed a more uniform distribution than the Eastern beaches (EB, MEB and NEB). In 2004, the distributions of magnetic susceptibility on the western beaches were similar to the 2003 summer observations (Figure 4.2). The Eastern beaches also showed a generally higher magnetic susceptibility. In winter 2004 (Figure 4.3), EB had lower magnetic susceptibility than that observed for the summers of 2003 and 2004. This could be due to the extreme winter condition when the measurements were taken.

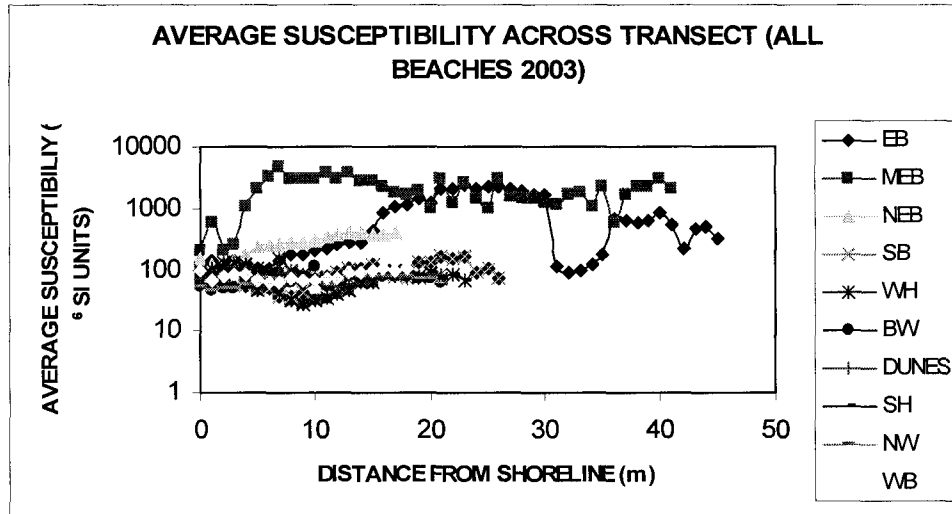


Figure 4.1: Average magnetic susceptibility at each transect 1meter interval points for all ten beaches (2003).

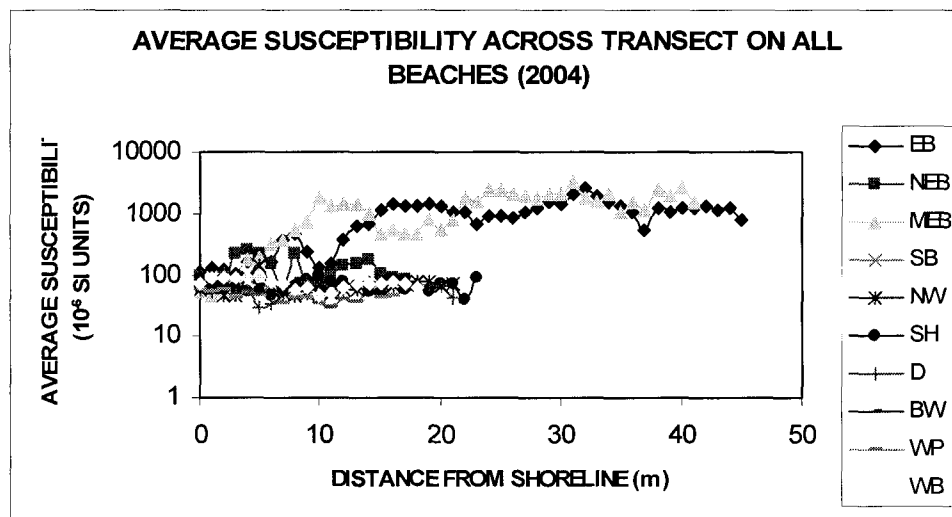


Figure 4.2: Average magnetic susceptibility at transect 1meter interval points for all beaches (2004).

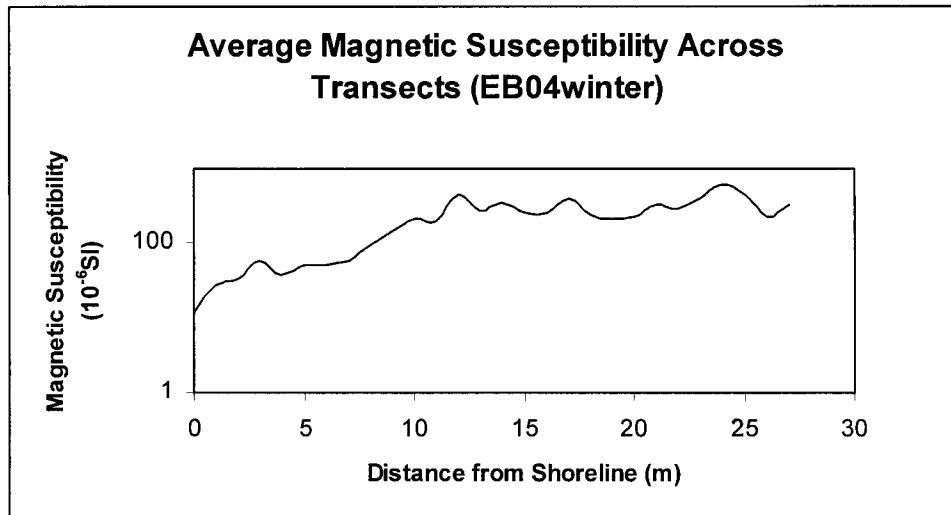


Figure 4.3: Average magnetic susceptibility for transect 1meter interval points for EB beach during the winter month- January (2004).

In Rondeau Provincial Park, the magnetic susceptibility pattern observed was similar to those observed in summer 2003 and 2004 at PPNP East beach although the magnitude was generally lower. The magnetic susceptibility gradually increased as one moved away from the shoreline.

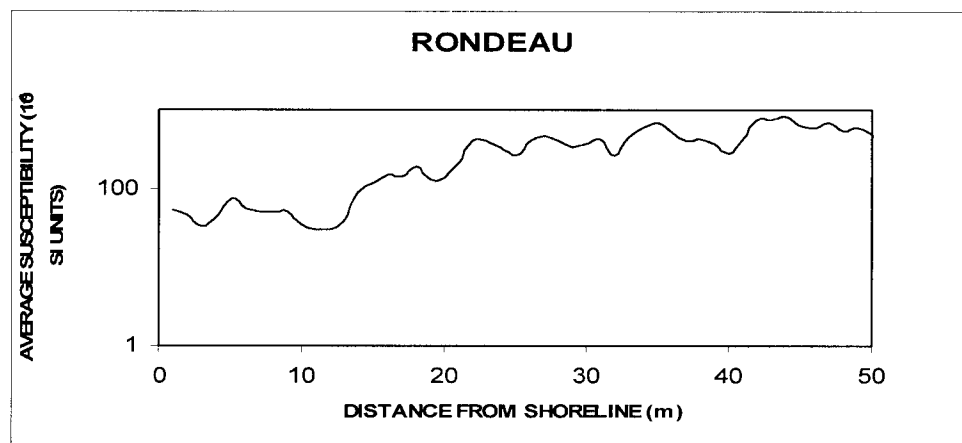


Figure 4.4: Average magnetic susceptibility at transect 1meter interval points for Rondeau beach(2004).

For Wheatley, the method of susceptibility data collection was slightly different from those of the PPNP beaches. Data points were not at one meter intervals, but they were still perpendicular to the shoreline. Only three transects were used for the magnetic

susceptibility data collection. There was an average of 5 points at each of the three transects where data were collected. Magnetic susceptibility was generally very low with an average of 122×10^{-6} (SI units). Only one data point was extremely high, this point was very close to the shoreline. Without this data point, the average magnetic susceptibility at Wheatley was at a low of 43.5×10^{-6} (SI units).

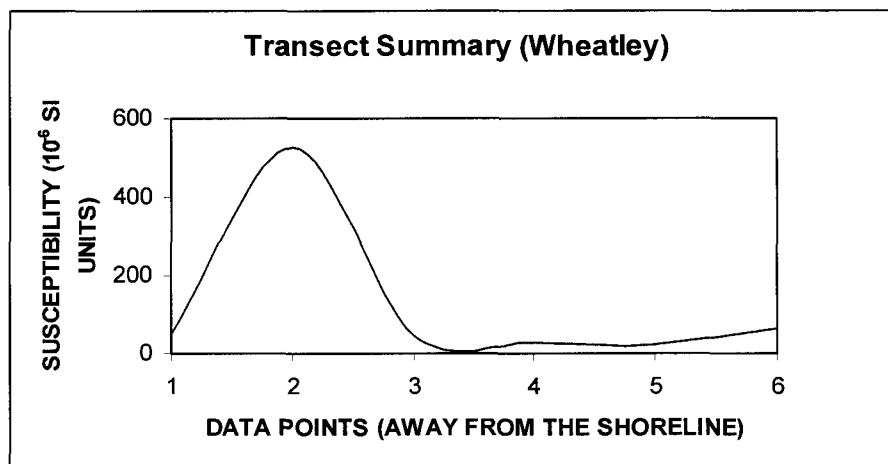


Figure 4.5: Average magnetic susceptibility at each data point

4.2. pARM

The effective magnetic grain sizes for sediments from each beach were determined using pARM spectra and Jackson et al. (1998)'s calibration. The pARM values were normalized and plotted against the inducing field. (Figures 4.22). For display of pARM for sieved samples, samples A were the sediments with grain sizes greater than 0.06cm, samples B with grain sizes greater than 0.03 but less than 0.06cm and samples C were samples with grain sizes less than 0.03cm.

A. East beach

The effective magnetic grain sizes of most EB sediments fell approximately in the 5-25 microns range. One sample (see S5 in Figure 4.6) showed a grain size smaller than 5 microns. For the top and lower sediments (L and T- sediments from top surface and underneath the top surface) from a point in EB (see Figure 4.7), there was no variation in the magnetic grain size. All samples peaked approximately at 5 microns grain size.

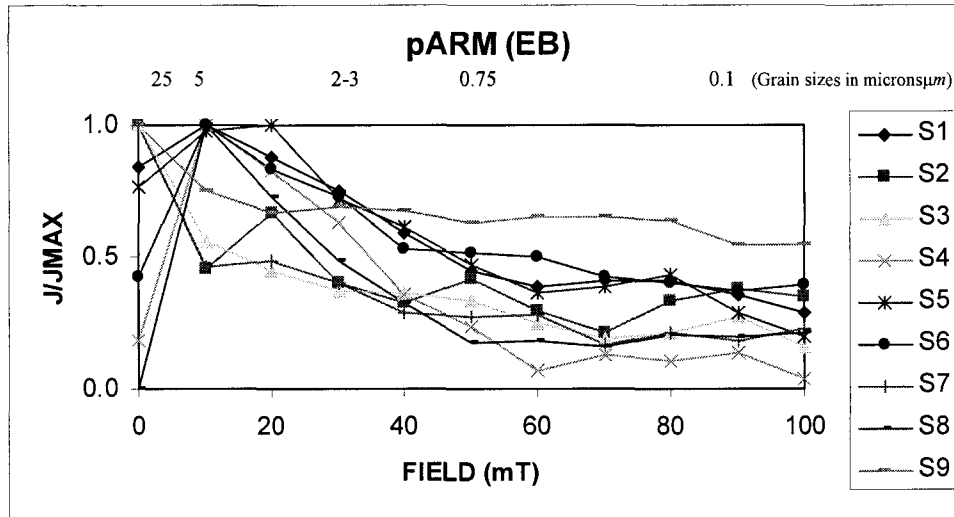


Figure 4.6: pARM for EB

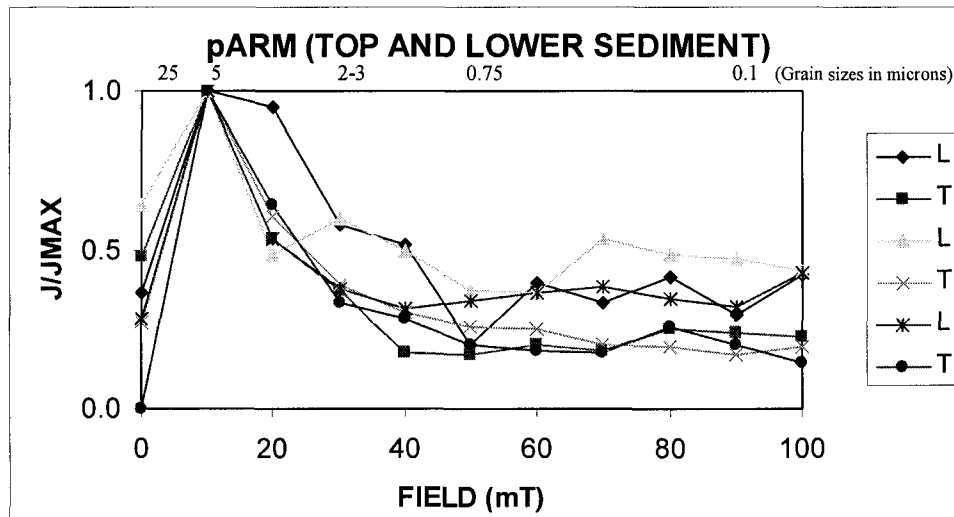


Figure 4.7: pARM for EB Top (T) and Lower (L) sediments: The T sediments are the surface sediments, while the L sediments were dug out beneath the top sediments.

B. Northeast beach

The effective magnetic grain sizes in these NEB sediments ranged from about 5 to grain sizes greater than 25 microns. Grain sizes for sieved samples and upper and lower sample did not vary much. The samples A are the larger grains while the samples C were the smallest grains of the seized samples. Some of the samples A and B had evidence of high coercivity minerals (see Figures. 4.8 and

4.10) or very few magnetic minerals present in them. This is consistent with the results of the pARM analysis; that is the grain sizes are very small.

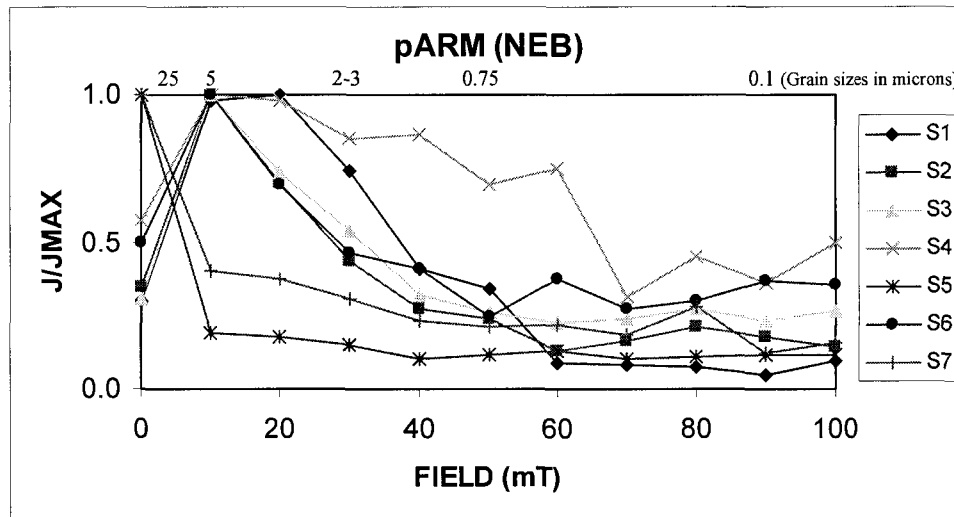


Figure 4.8: pARM for NEB sediment samples

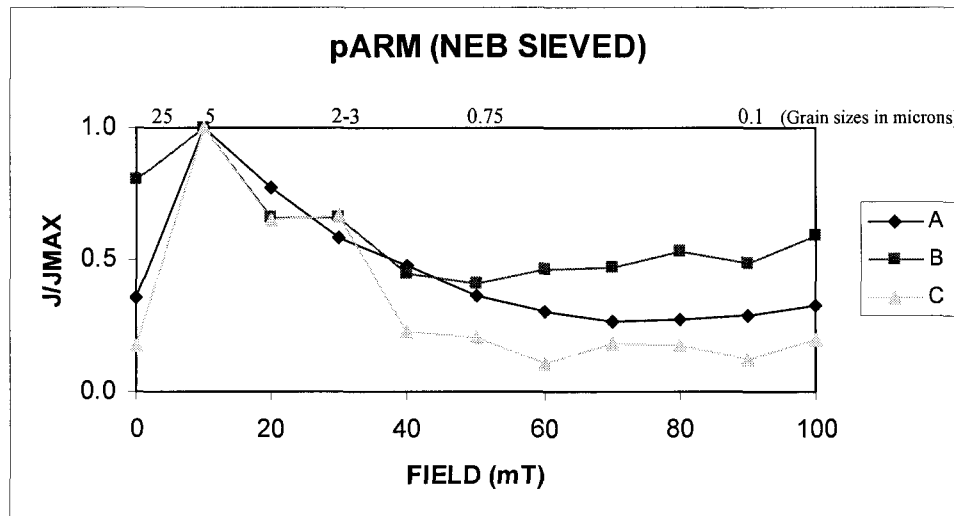


Figure 4.9: pARM for NEB sieved sediment samples

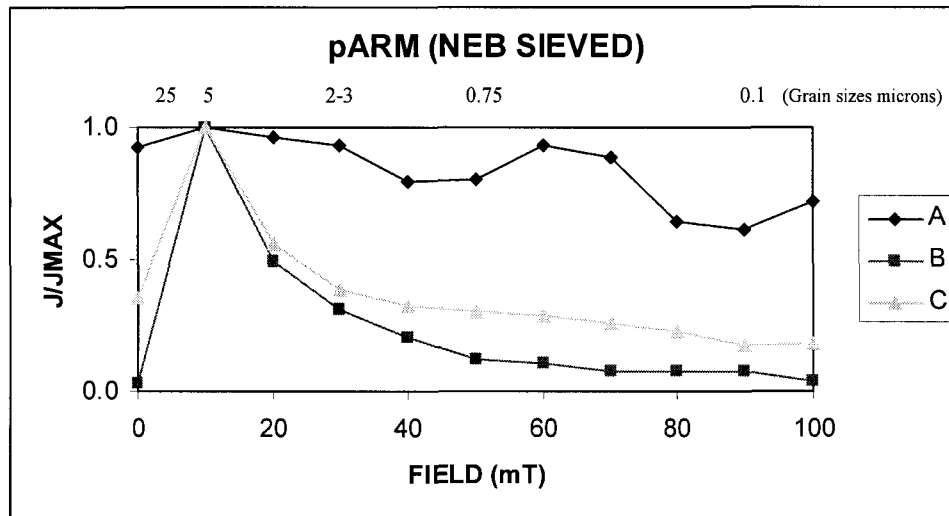


Figure 4.10: pARM for NEB sieved sediment samples

C. Middle-east beach

In the MEB sediments; all the magnetic grain sizes from sediments (see Figures. 4.11, 4.12, 4.13, and 4.14) were in the same range of about 5 microns. The larger grains (B) showed evidence of high coercivity materials. Some samples (for example S1) also showed evidence of a high coercivity material.

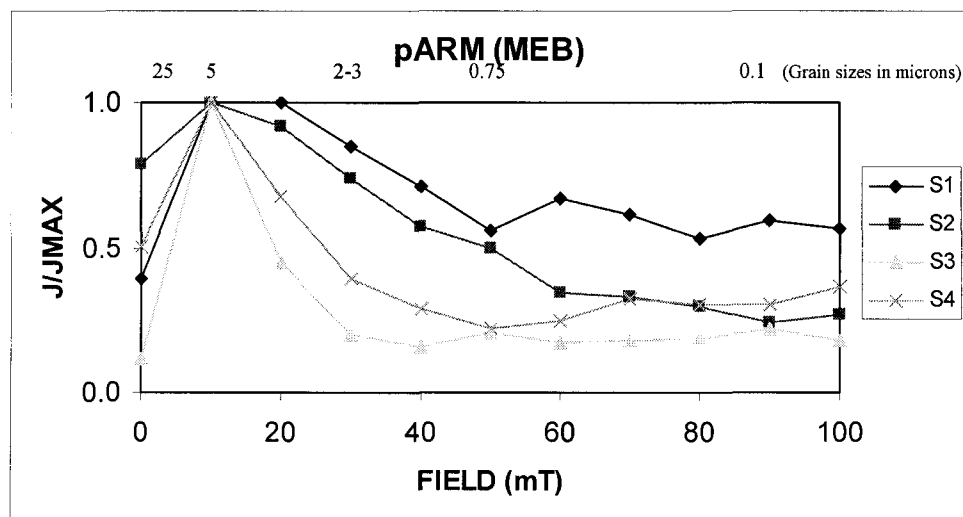


Figure 4.11: pARM for MEB sediment samples.

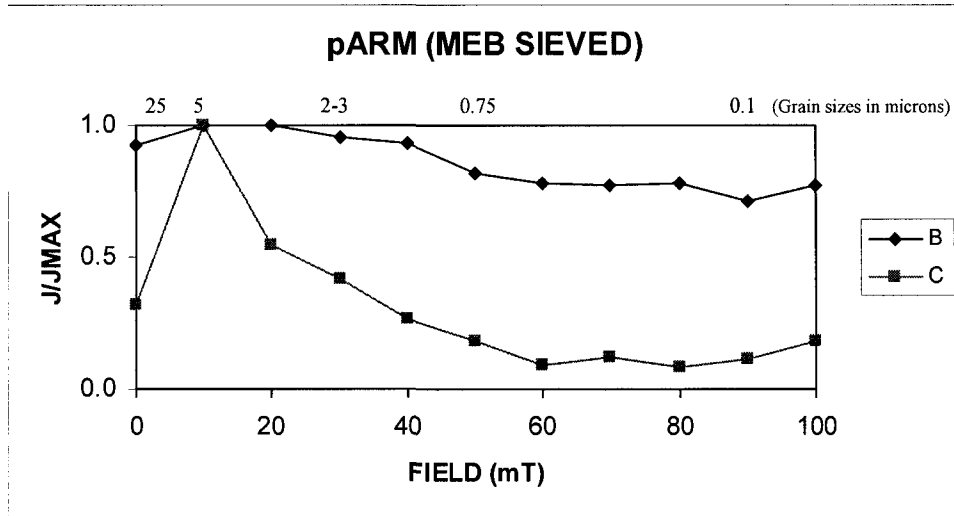


Figure 4.12: pARM for MEB sieved sediment samples.

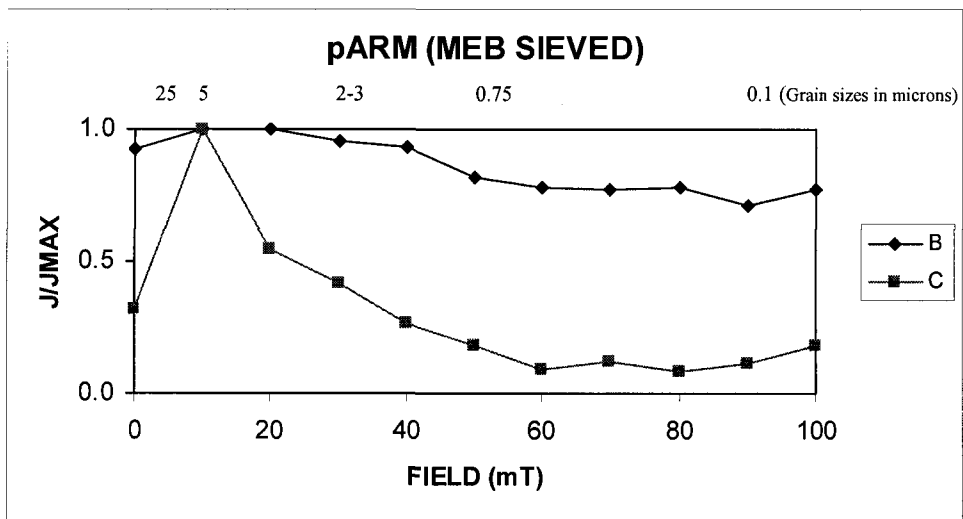


Figure 4.13: pARM for MEB sieved sediment samples

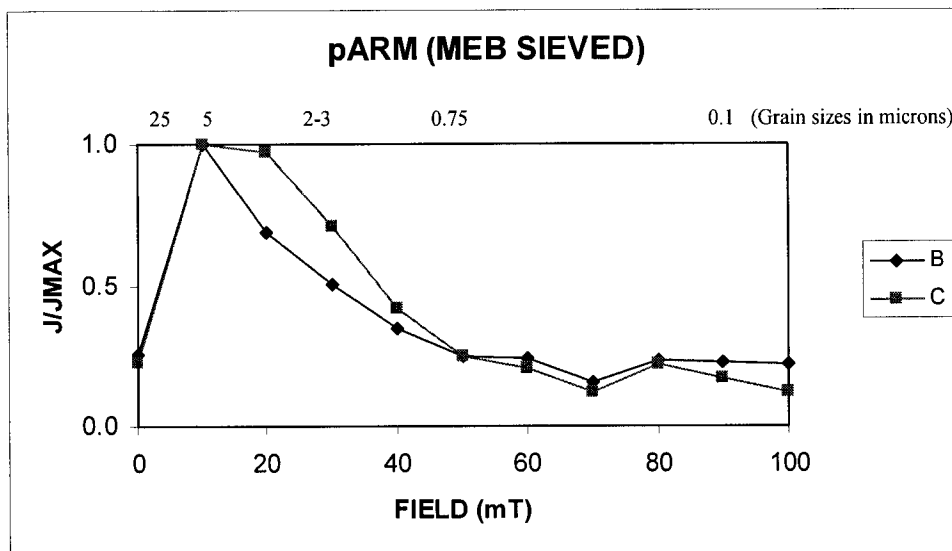


Figure 4.14: pARM for MEB sieved sediment samples

D. Sanctuary Beach

Sediment from SB peaked at grain sizes greater than 25 microns. All samples from this beach had large magnetic grain sizes.

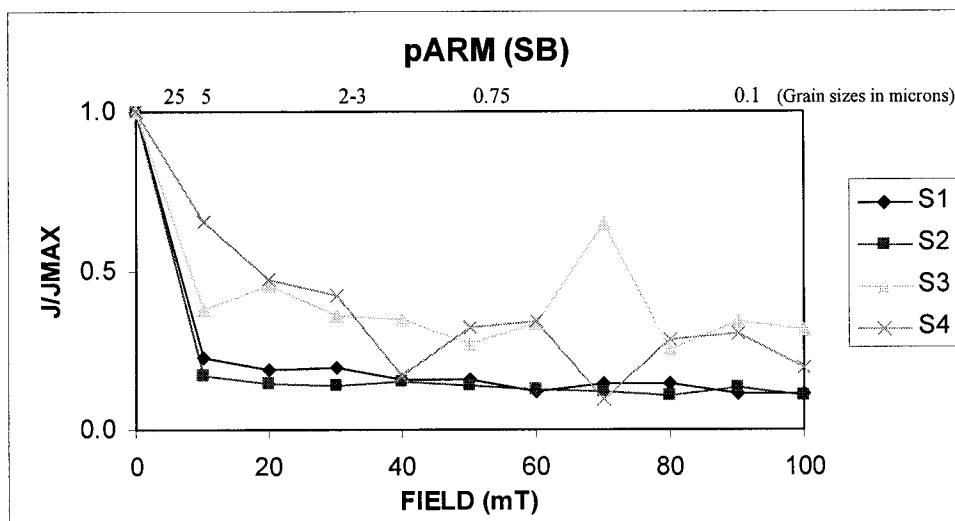


Figure 4.15: pARM spectra for SB sediments.

E. Other West Beaches (NWB, SH, D, BW, and WB)

The effective magnetic grain sizes of sediments within these beaches were approximately between 5 microns and greater than 25 microns.

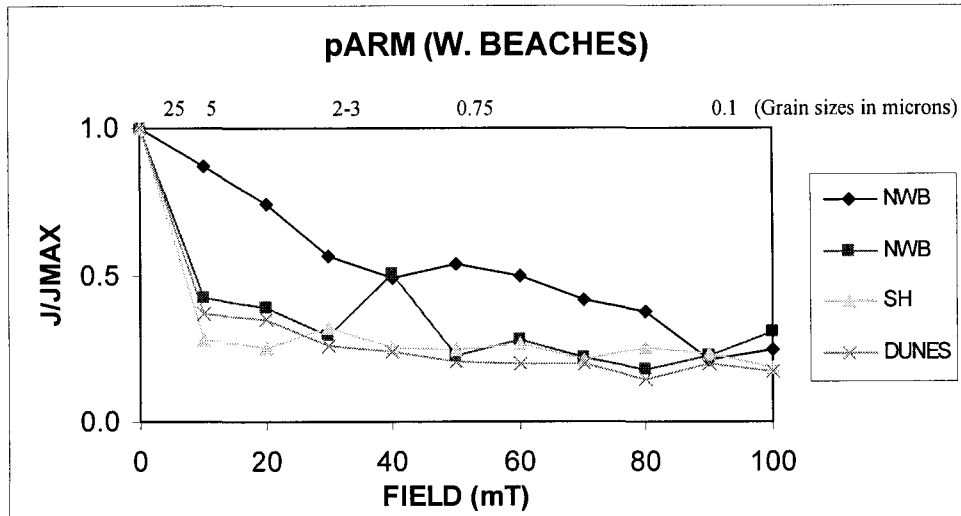


Figure 4.16: pARM spectra for other Western beaches.

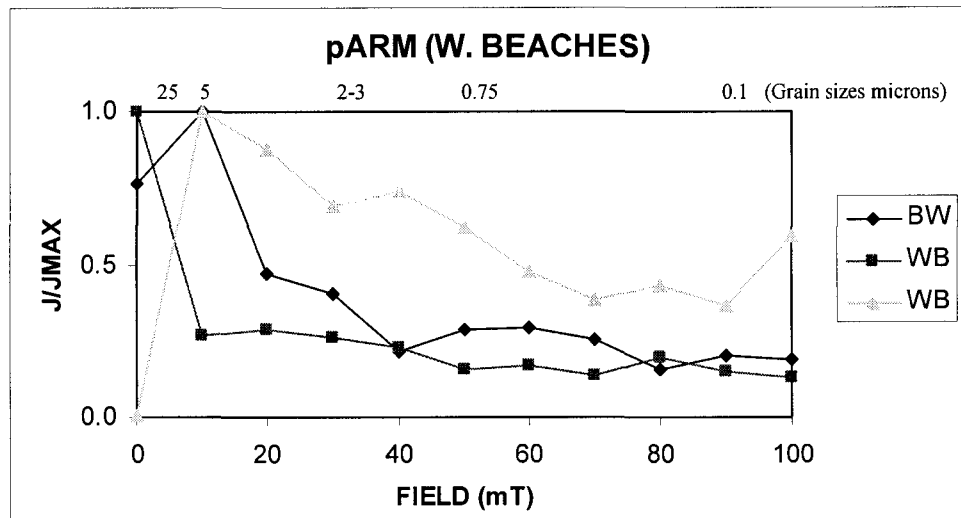


Figure 4.17: pARM spectra for sediments from other Western beaches.

F. EB, MEB AND WB (2004)

The magnetic grain size of sediment from MEB (2004) was approximately 5 microns. Sediment samples from EB, and WB (2004) showed evidence of high coercivity minerals. The spectra peak also indicated grain sizes of about 5 microns. Results were consistent with those of previous year.

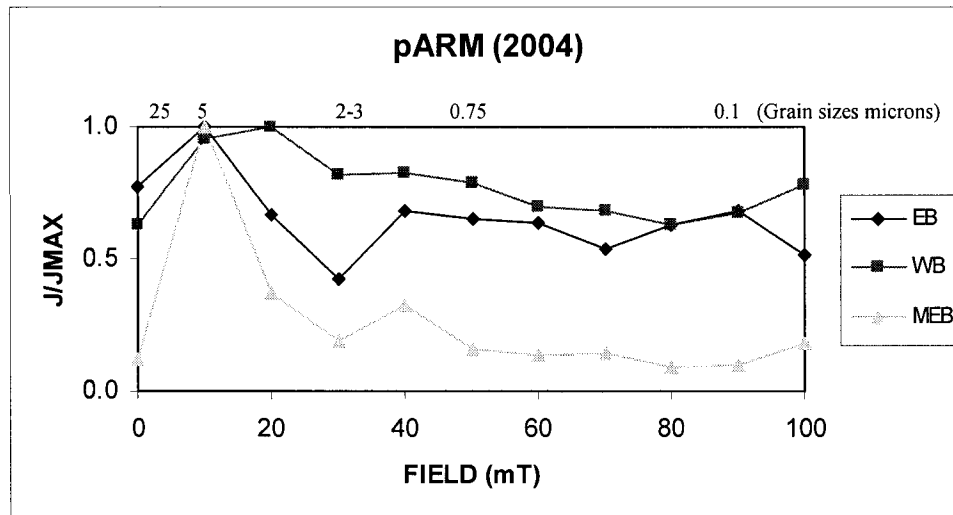


Figure 4.18: pARM spectra for sediments from other EB, MEB, WB

G. Wheatley

For the Wheatley sediments, the sample numbers represent their distance from the shoreline. Thus P1 is the furthest from the shoreline and P6 the closest. In all cases, samples P1, P2, and P3 were sampled from the bluffs; while P4, P5, and P6 were sampled from the beach sands.

The effective magnetic grain sizes of the samples were between 0.75-5 microns (Figure 4.19-4.21). Some samples also showed evidence of high coercivity minerals (Figure 4.20 samples P4 and P6). The majority of grains in samples closest to the shoreline (P6, P5, and P4) were larger than the majority of grains from the bluff samples. The effective magnetic grain sizes from the bluff samples were approximately less than 2 microns (samples P1, P2 and P3 in Figures. 4.19, 4.20, and 4.21), while magnetic grain sizes of the beach sediments were approximately 5 microns (see Figure 4.19 sample P5, Figure 4.20: P6, and Figure 4.21: P4). Some of the beach samples also showed evidence of high coercivity materials or lack any magnetic mineral, thus these samples (e.g. P4 and P6 in Figure 4.20) could not be magnetized.

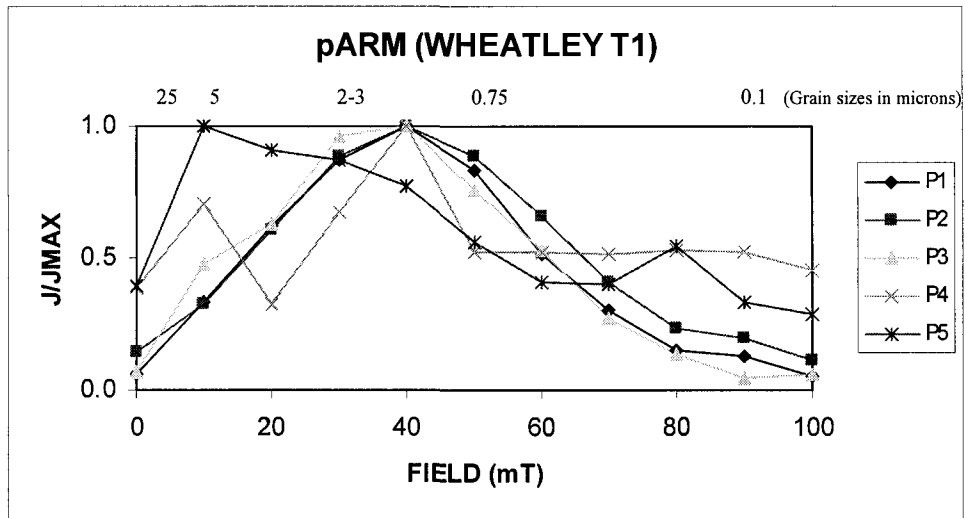


Figure 4.19: pARM spectra for Wheatley sediments, Transect 1.

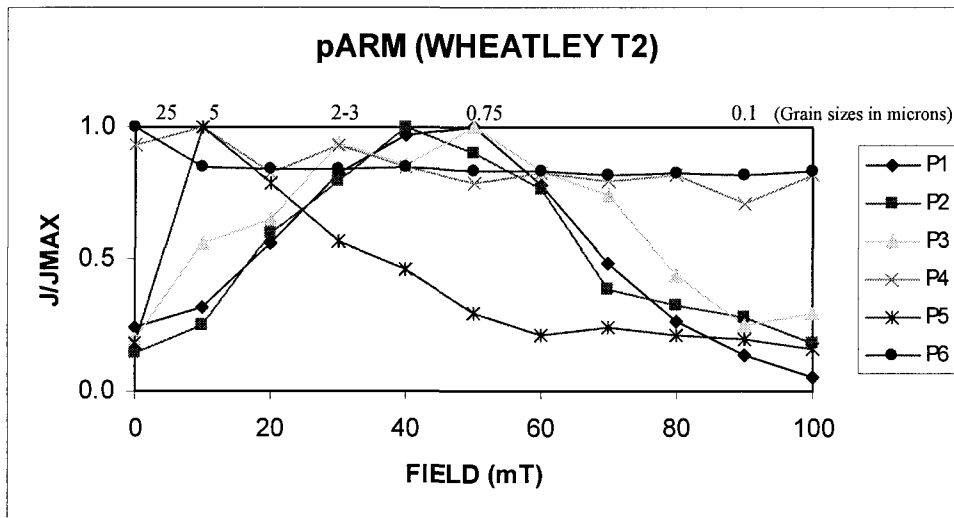


Figure 4.20: pARM spectra for Wheatley sediments, Transect 2.

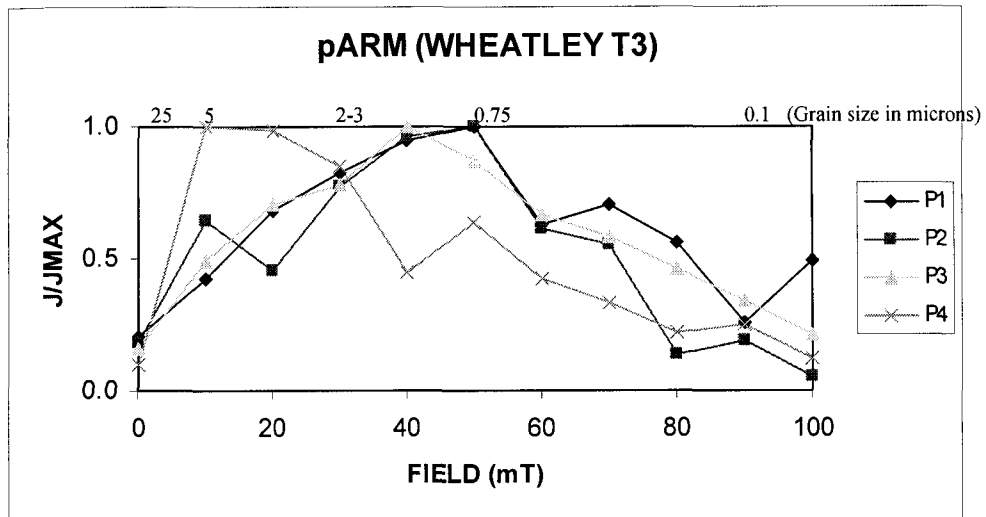


Figure 4.21: pARM spectra for Wheatley sediments, Transect 3.

G. Rondeau

The effective magnetic sediment grain size of the one sample collected from Rondeau Provincial Park Beaches was about 5 microns. There was very little evidence of higher coercivity material in it (Figure 4.22).

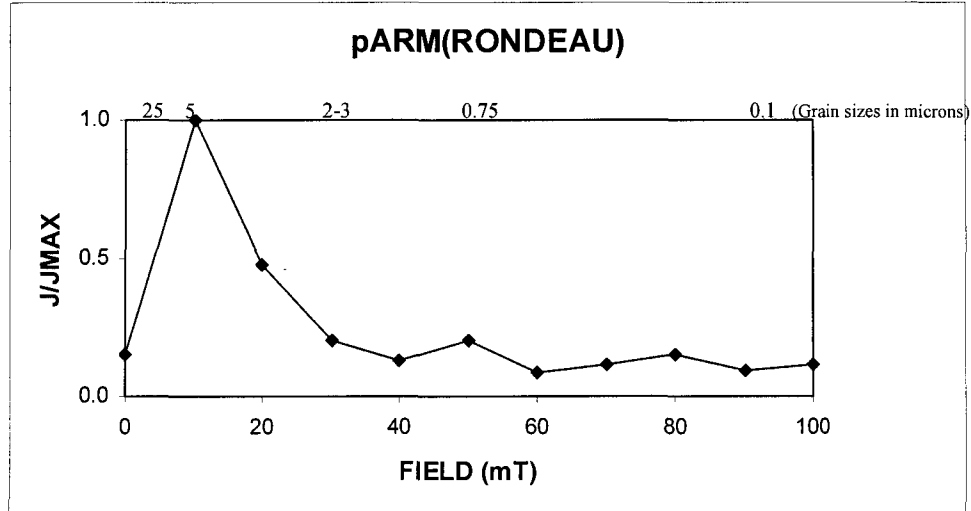


Figure 4.22: pARM spectra for sediment from Rondeau.

4.3. SIRM Analysis and Results

SIRM spectra for specimen were normalized with J at 1200mT. Below are the SIRM spectra for sediments from the western beaches of PPNP.

A. Sanctuary Beach and Other West Beaches

From the coercivity spectrum of the sediment samples from SB and other western side beaches, it can be deduced that magnetic minerals present in beach sand had low coercivity (for example, magnetite or pyrrhotite). The SIRM spectra below bear a close resemblance to those of magnetite (Symons and Cioppa, 2000). Samples were quickly saturated in low fields. Sediment samples domain size falls close to the pseudo-single domain magnetite grain sizes (PSD).

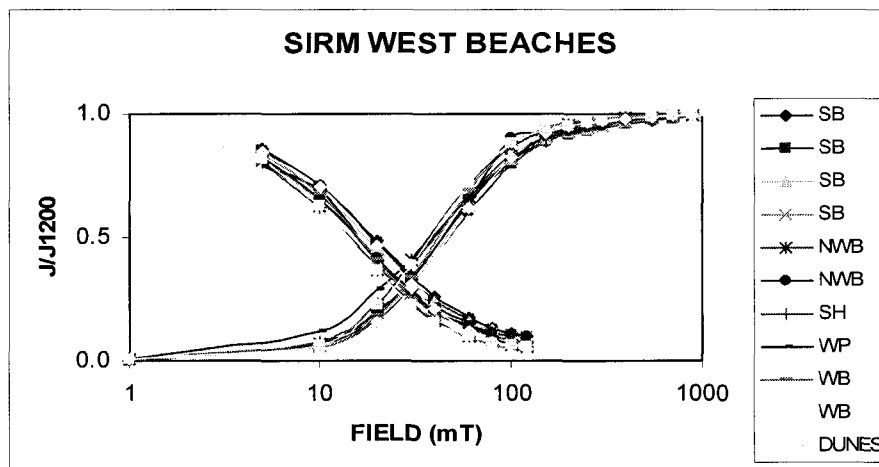


Figure 4.23: SIRM spectra for sediment samples from the Western beaches.

B. East beach

SIRM spectra for East beach sediments also falls close to the magnetite MD and PSD grain sizes. The magnetic minerals in this beach are of low coercivity. Samples taken at depths of 5-10cm were also similar to the surface EB samples. Both upper (Top sample) and lower (Lower sample) displayed very similar characteristics; there was no noticeable difference in magnetic characteristics or domain size. A couple of samples (see S7 and S2) displayed some evidence of high coercivity minerals.

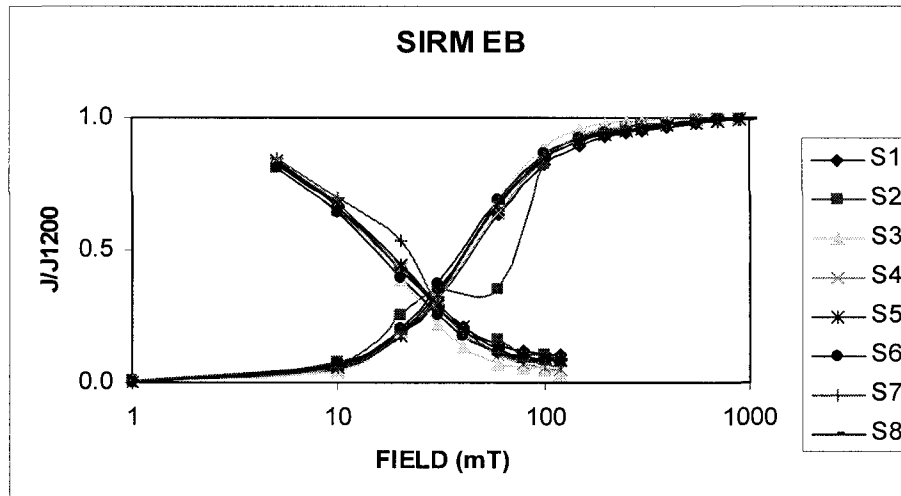


Figure 4.24: SIRM spectra for sediment samples from EB.

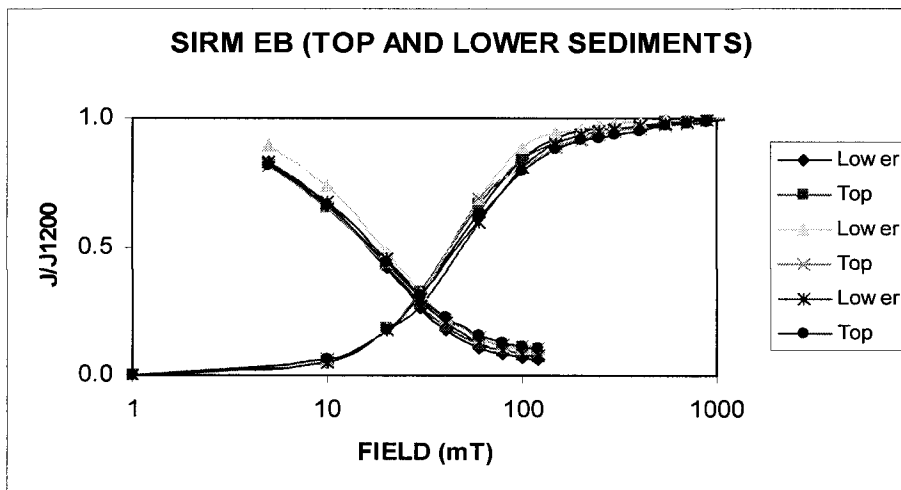


Figure 4.25: SIRM spectra for sediment from top and lower cores (EB).

C. MEB and NEB

The SIRM spectra for all samples from MEB fell close within the pseudo-single domain (PSD) magnetite grain size. The seized samples displayed some slight difference; the C samples (finer grains: $> 0.3\text{mm}$) had higher coercivity than the larger grains B samples ($>0.3<0.6\text{mm}$). Both samples fell within the pseudo-single domain magnetite spectra.

All the NEB sediments; core, sieved and other samples displayed very similar pattern in their spectra. All spectra fall closely within the PSD magnetite

spectra. Sample S3 was an exception (Figure 4.30); it showed some evidence of pyrrhotite.

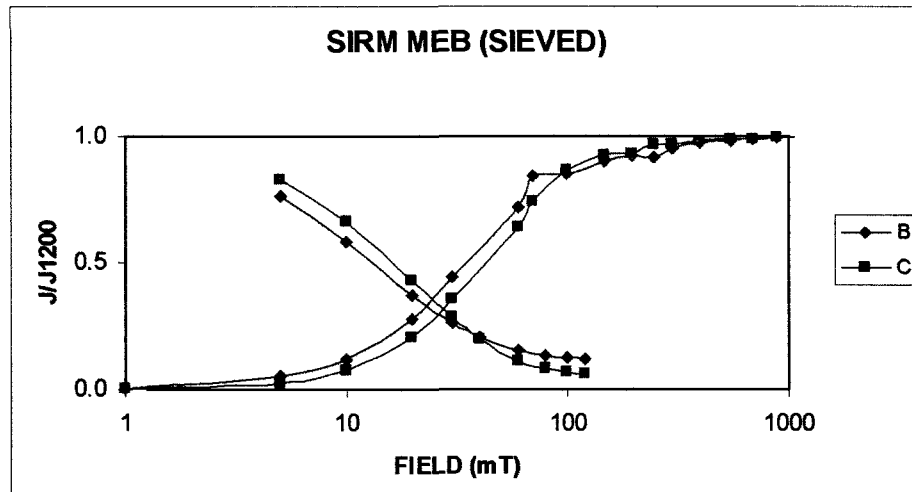


Figure 4.26: SIRM spectra for sieved sediments MEB.

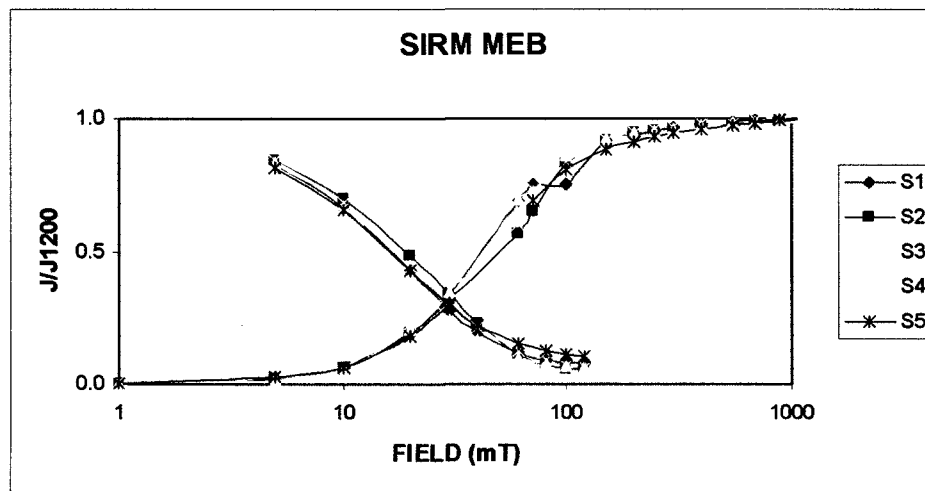


Figure 4.27: SIRM spectra for MEB sediment.

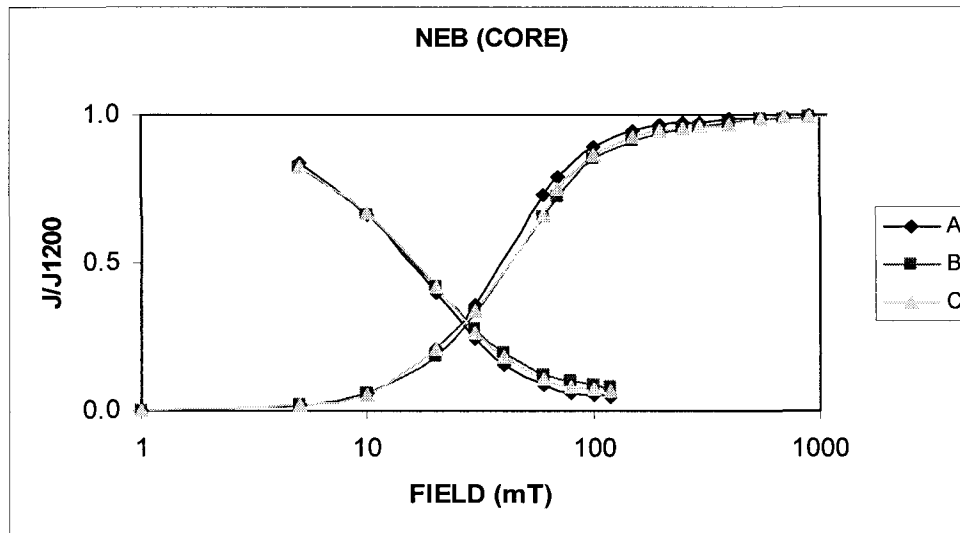


Figure 4.28: SIRM spectra for sediment from core samples NEB: (A is the top sediment, B in the centre and C the lowest sediment).

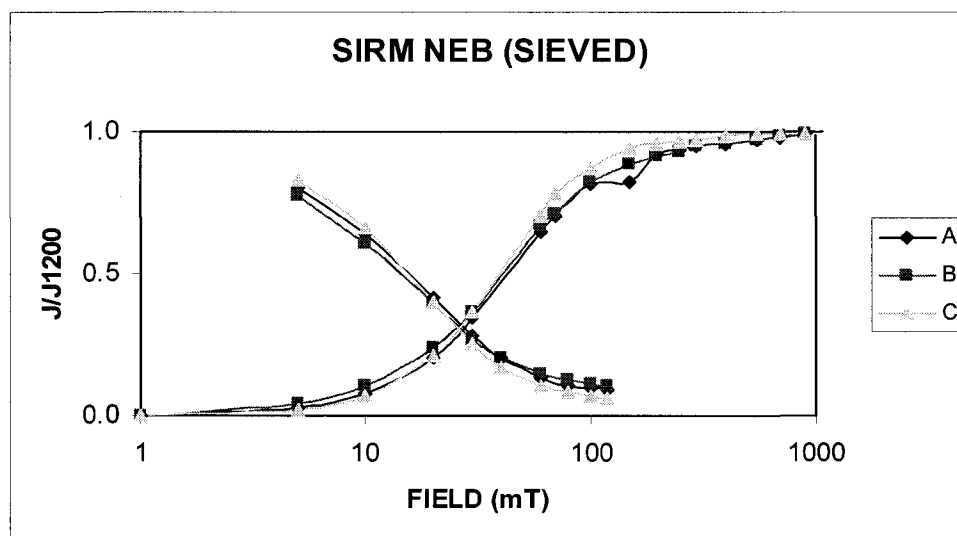


Figure 4.29: SIRM spectra for sieved sediment (NEB).

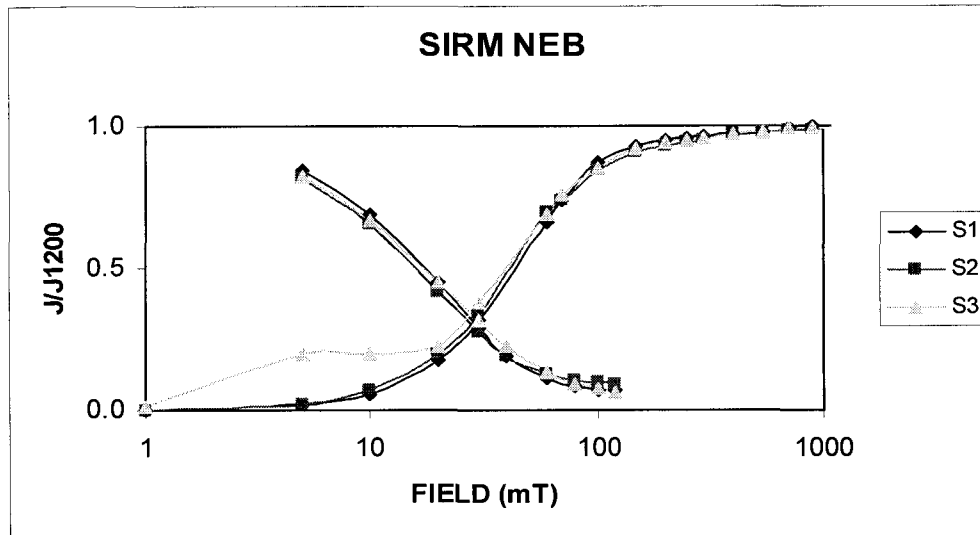


Figure 4.30: SIRM spectra for NEB sediment samples.

D. Wheatley

Samples from Wheatley showed a greater disparity than the sediment samples from PPNP beaches. In general, the grain sizes of sediments increased towards the shoreline. Samples furthest away from the shoreline had the smaller magnetic domain sizes, while those closest to the shoreline had larger magnetic grain sizes, consistent with the pARM results. Sediment grain sizes fell within the PSD and single domain (SD) magnetite spectra. The sediments closest to the shoreline (sand samples: P6, P5 and P4), all fell closely within the PSD magnetite spectra. Other samples (bluff samples: P1, P2 and P3) were all closely within the SD magnetite regions of the spectra.

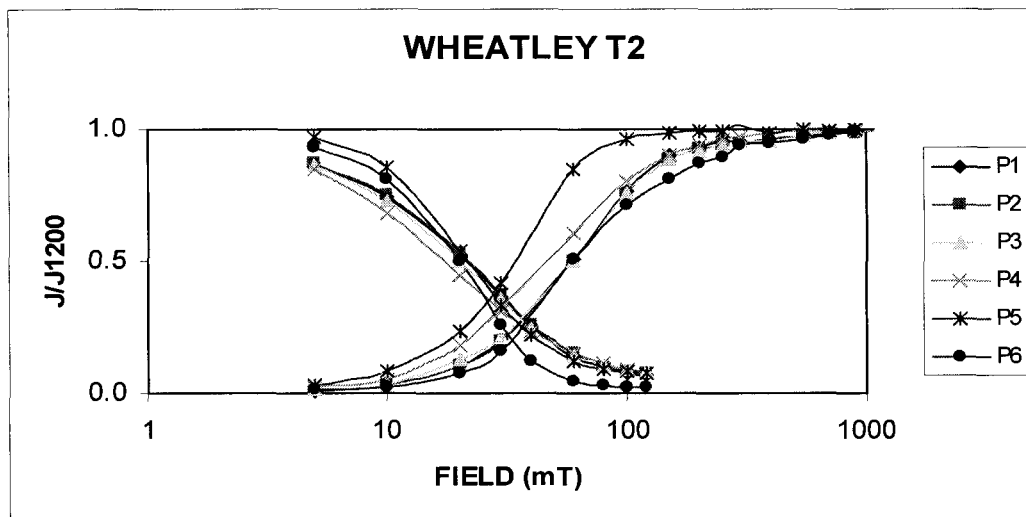


Figure 4.31: SIRM spectra for Wheatley sediment samples.

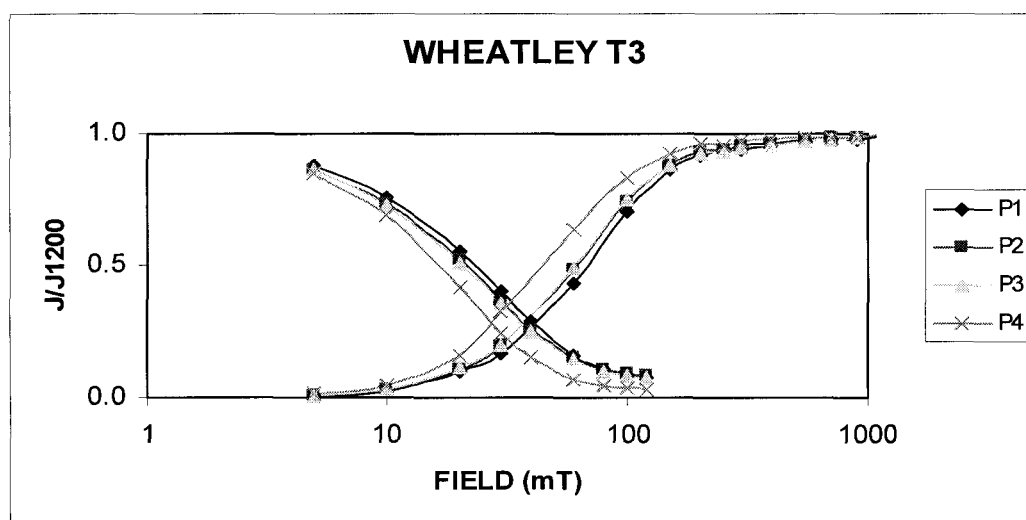


Figure 4.32: SIRM spectra for Wheatley sediment samples.

D. EB, WB, MEB and Rondeau (2004).

Samples from EB, WB, MEB and Rondeau were taken in 2004. The SIRM spectra are presented in Figure 4.33 below. All magnetic minerals in the four samples were of low coercivity. The MEB and Rondeau curves suggest that a small amount of high coercivity minerals might be present. EB and WB were very similar to each other, and there was no noticeable difference between the 2003 and 2004 spectra for EB and WB. The spectra for the four samples fell closely with PSD magnetite spectra.

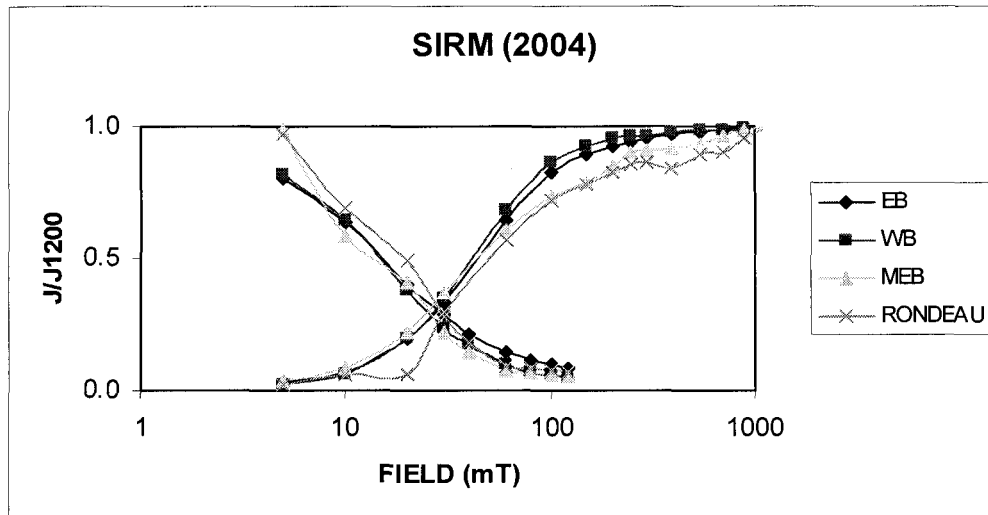


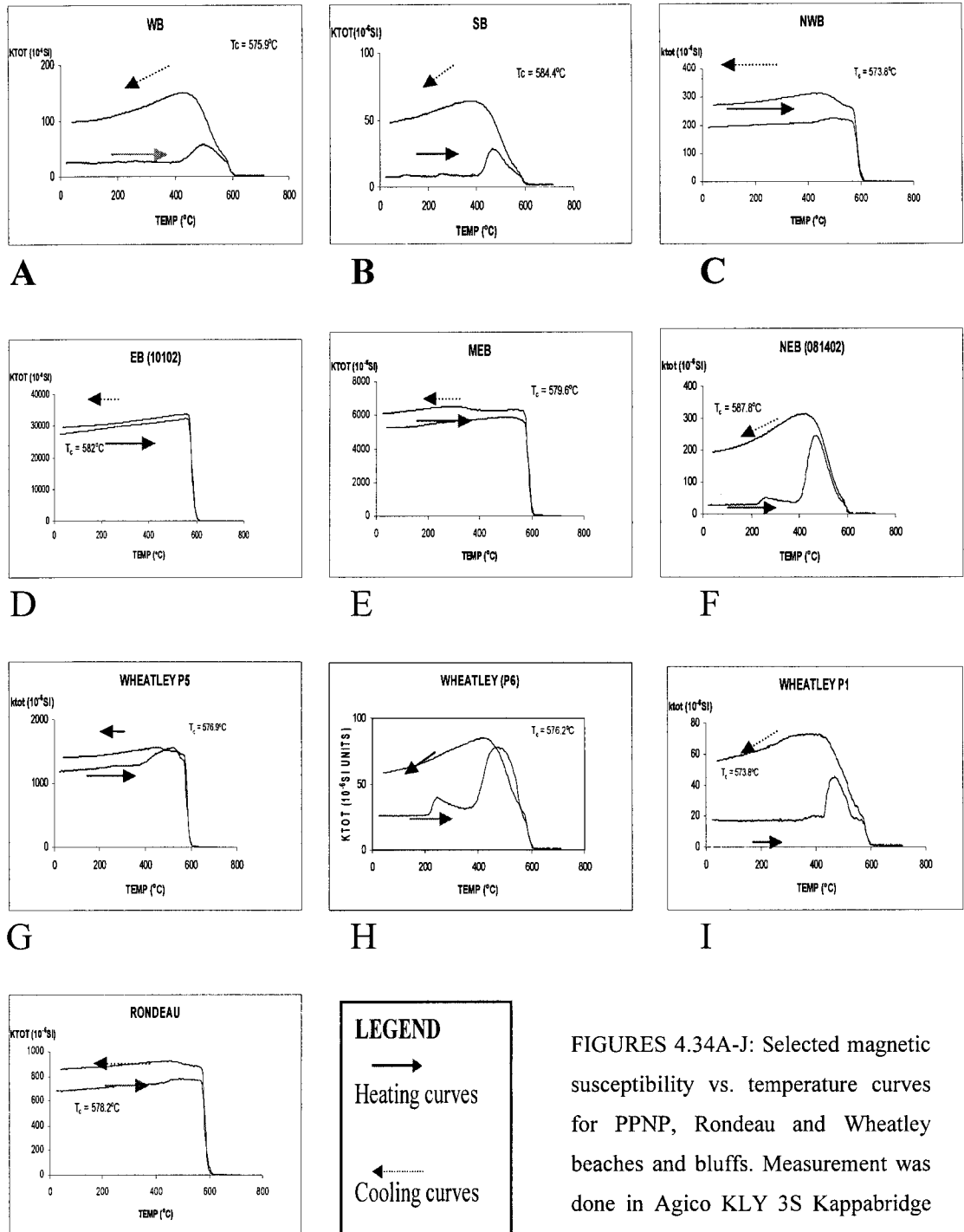
Figure 4.33: SIRM spectra for NEB sediment samples.

4.4. Susceptibility variation with temperature measurements

All the sediment samples from all beaches lost significant magnetic susceptibility between 572.2°C to 585.4°C indicating the presence of magnetite. The sediment samples with higher $KTOT$ [$>200 \times 10^{-6}SI$] showed a smoother curve over sediments with weaker magnetic susceptibility signals. The samples with the highest magnetic susceptibility signal displayed most similar (reversible) heating and cooling curves. All sediment samples with lower magnetic initial susceptibility had similar characteristics in their curve pattern. In sediments with an initial magnetic susceptibility less than $200 \times (10^{-6}SI)$; there was a general increase in observed susceptibility between 400-450°C. This increase is lost as soon as the temperature approached 570°C or thereabout. The cooling curves (upper curve) were generally smoother than the heating curves. These observations can be attributed to changes in magnetic minerals induced by heating; this results to a conspicuous change in susceptibility. The magnetic phases are changed in such a way that they correspond to new temperature conditions acting for the time of heating. This curve type (see Figures. 4.34: A and B) is usually characterized by a situation when a new phase and strongly magnetic phase (usually magnetite) is created from less magnetic phases during heating (Hrouda et al., 2003).

The susceptibility vs. temperature curve of a single sample from Rondeau was very similar to the curves displayed by EB samples with higher magnetic susceptibility

(Figures 4.34, J and D). One sample from 2004 (EB) was identical to its 2003 counterparts.



FIGURES 4.34A-J: Selected magnetic susceptibility vs. temperature curves for PPNP, Rondeau and Wheatley beaches and bluffs. Measurement was done in Agico KLY 3S Kappabridge susceptibility meter/furnace extension in argon gas atmosphere. See section 4.4 above for discussion.

4.5. Magnetic ratios

The magnetic ratios were calculated from parameters. Below is the result of the S-ratio, and other magnetic ratios i.e. HIRM, ARM/SIRM, ARM/ χ , and σ_{RS} (saturation remanence to susceptibility ratios) calculations.

A. S-Ratios

The S-ratios at backfield 0.1T and 0.3T for samples from the PPNP beaches are summarized in the Table 4.3. $S_{0.1T}$ for all beaches at all seasons exceeds 0.70 except for Wheatley, where some samples had $S_{0.1T}$ values of 0.60. All samples had $S_{0.3T}$ greater than 0.80 and a few of the samples had 1.00 $S_{0.3T}$. This further indicates that minerals mostly present on this beaches sediments are of low coercivity, with a very minor contribution from high coercivity magnetic minerals (for example; hematite or goethite).

BEACHES	S-RATIOS AT -0.1T				S-RATIOS AT -0.3T			
	MIN	MAX	AVG.	SD	MIN	MAX	AVG.	SD
EB	0.70	0.91	0.74	0.076	0.89	0.99	0.92	0.033
MEB	0.75	0.81	0.77	0.028	0.93	1.00	0.96	0.030
NEB	0.72	0.99	0.79	0.093	0.91	1.00	0.94	0.030
ALL EASTERN BEACHES				0.076				0.032
WESTERN BEACHES	0.71	0.82	0.76	0.047	0.89	0.96	0.93	0.027
WHEATLEY	0.63	1.00	0.75	0.103	0.87	1.00	0.93	0.041
RONDEAU	0.83	0.83	0.83	-	0.98	0.98	0.98	-
EB04	0.72	0.72	0.72	-	0.92	0.92	0.92	-
MEB04	0.92	0.92	0.92	-	1.00	1.00	1.0	-
WB04	0.81	0.81	0.81	-	0.96	0.96	0.96	-

Table 4.3: Summary of $S_{-0.1T}$ and $S_{-0.3T}$

B. Other magnetic ratios and parameters

The samples HIRM, high and low coercivity ARM, saturation remanence (σ_{RM}), and mass specific susceptibility (χ) were calculated and are summarized in the Table 4.4. Ratios having significant variation will be discussed in Chapter Seven.

S/N	SAMPLE	WEIGHT(g)	total mass(δ *vol)	δ (kg/m ³)	δ (g/cc)	%OF SED	BULK SUS(k)
1	90101	14.3	14.3	0.0018	1.79	1	1.15E-01
2	90102	8.8	12.1	0.0015	1.51	0.73	1.78E-01
3	80302	10.4	10.6	0.0013	1.33	0.98	2.61E-02
4	80303	12.4	12.4	0.0016	1.55	1	8.21E-02
5	80301	10.9	10.9	0.0014	1.36	1	5.87E-01
6	81301	8.9	12	0.0015	1.5	0.74	4.26E-02
7	90501	10.4	10.7	0.0013	1.34	0.97	3.59E-03
8	81402	9.6	9.6	0.0012	1.2	1	3.64E-04
9	81403	9.9	9.9	0.0012	1.24	1	5.92E-04
10	81401	12.1	12.3	0.0015	1.54	0.98	4.00E-02
11	1T71	11.8	11.8	0.0015	1.48	1	2.66E-02
12	81201	10.9	10.9	0.0014	1.36	1	1.03E-02
13	2901	10.2	10.2	0.0013	1.28	1	8.62E-04
14	1T81	10.6	13.25	0.0017	1.66	0.8	1.28E-01
15	7501	9.3	9.6	0.0012	1.2	0.97	4.55E-04
16	3201	10.3	10.3	0.0013	1.29	1	5.25E-04
17	1B71	10	10.5	0.0013	1.31	0.95	2.74E-03
18	1101	11.8	11.9	0.0015	1.49	0.99	3.02E-02
19	3601	10.2	10.2	0.0013	1.28	1	3.30E-03
20	50101	11.8	11.8	0.0015	1.48	1	7.73E-04
21	90301	10.6	11	0.0014	1.38	0.96	1.13E-02
22	1401	11.8	12	0.0015	1.5	0.98	3.09E-02
23	4301	11.1	11.1	0.0014	1.39	1	5.53E-04
24	1201	9.7	9.9	0.0012	1.24	0.98	3.93E-04
25	1111	9.8	9.9	0.0012	1.24	0.99	7.12E-04
26	7801	10.2	10.5	0.0013	1.31	0.97	6.33E-04
27	1601	12.4	12.4	0.0016	1.55	1	3.54E-02
28	1B81	11.6	12.2	0.0015	1.53	0.95	1.10E-01
29	6101	11.2	11.2	0.0014	1.4	1	1.02E-03
30	C00001eb	0.3	15	0.0019	1.88	0.02	2.36E-03
31	C00002ME B	0.5	14.2	0.0018	1.78	0.04	5.37E-03
32	C00003WB	6.1	10.4	0.0013	1.3	0.59	2.34E-04
33	C00005R	5.9	9.8	0.0012	1.23	0.6	2.91E-03
34	W00011	4	7.2	0.0009	0.9	0.56	2.74E-04
35	W00012	4.2	7.2	0.0009	0.9	0.58	1.71E-04
36	W00013	4.3	7.2	0.0009	0.9	0.6	2.18E-04
37	W00014	6.1	10	0.0013	1.25	0.61	3.02E-04
38	W00015	6	10	0.0013	1.25	0.6	6.95E-04
39	W00021	4.5	7.2	0.0009	0.9	0.63	2.48E-04
40	W00022	5.7	7.2	0.0009	0.9	0.79	3.63E-04
41	W00023	4.5	7.2	0.0009	0.9	0.63	3.37E-04
42	W00024	6.5	10	0.0013	1.25	0.65	2.52E-04
43	W00025	6.4	10	0.0013	1.25	0.64	1.62E-02
44	W00026	6.9	10	0.0013	1.25	0.69	8.41E-04
45	W00031	3.1	7.2	0.0009	0.9	0.43	2.10E-04
46	W00032	3.2	7.2	0.0009	0.9	0.44	2.40E-04
47	W00033	4.5	7.2	0.0009	0.9	0.63	3.32E-04
48	W00034	6.7	10	0.0013	1.25	0.67	5.53E-04
49	W00035	6	10	0.0013	1.25	0.6	4.24E-04

Table 4.4

S/N	SAMPLE	CALC k	Ksi(P)	MASS SPEC 10 ⁻⁶ m ³ kg ⁻¹	ARM	Am ² kg-I ARM*1000	51/111
1	90101	1.649	0.1649	92.24	1.19E-03	1.19	0.89
2	90102	2.955	0.2955	195.36	1.34E-03	1.34	0.89
3	80302	0.282	0.0282	21.29	2.10E-04	0.21	0.84
4	80303	1.018	0.1018	65.7	6.97E-04	0.7	0.9
5	80301	6.395	0.6395	469.36	1.63E-05	0.02	0.72
6	81301	0.688	0.0688	45.9	5.70E-04	0.57	0.89
7	90501	0.04	0.004	2.95	6.65E-05	0.07	0.83
8	81402	0.003	0.0003	0.29	1.04E-05	0.01	0.73
9	81403	0.006	0.0006	0.47	1.16E-05	0.01	0.71
10	81401	0.501	0.0501	32.56	5.02E-04	0.5	0.9
11	1T71	0.314	0.0314	21.3	3.07E-04	0.31	0.9
12	81201	0.112	0.0112	8.25	1.28E-04	0.13	0.84
13	2901	0.009	0.0009	0.69	1.94E-05	0.02	0.82
14	1T81	2.122	0.2122	128.1	1.29E-03	1.29	0.91
15	7501	0.005	0.0005	0.38	1.41E-05	0.01	0.74
16	3201	0.005	0.0005	0.42	1.54E-05	0.02	0.91
17	1B71	0.03	0.003	2.3	4.75E-05	0.05	0.79
18	1101	0.362	0.0362	24.33	3.28E-04	0.33	0.93
19	3601	0.034	0.0034	2.64	2.82E-05	0.03	0.87
20	50101	0.009	0.0009	0.62	2.55E-05	0.03	0.78
21	90301	0.129	0.0129	9.41	1.45E-04	0.15	0.86
22	1401	0.377	0.0377	25.12	3.99E-04	0.4	0.87
23	4301	0.006	0.0006	0.44	2.19E-05	0.02	0.79
24	1201	0.004	0.0004	0.32	1.33E-05	0.01	0.77
25	1111	0.007	0.0007	0.58	1.39E-05	0.01	0.73
26	7801	0.007	0.0007	0.52	2.11E-05	0.02	0.83
27	1601	0.439	0.0439	28.32	5.75E-04	0.58	0.85
28	1B81	1.405	0.1405	92.13	1.13E-03	1.13	0.82
29	6101	0.011	0.0011	0.81	3.28E-05	0.03	0.8
30	C00001eb	1.77	0.177	94.4	1.63E-05	0.02	0.96
31	C00002MEB	2.164	0.2164	121.92	6.15E-05	0.06	1.06
32	C00003WB	0.004	0.0004	0.32	8.32E-06	0.01	0.85
33	C00005R	0.047	0.0047	3.86	2.76E-05	0.03	0.78
34	W00011	0.004	0.0004	0.39	2.63E-05	0.03	0.76
35	W00012	0.002	0.0002	0.23	1.42E-05	0.01	0.71
36	W00013	0.003	0.0003	0.29	2.43E-05	0.02	0.77
37	W00014	0.005	0.0005	0.4	9.99E-06	0.01	0.73
38	W00015	0.012	0.0012	0.93	2.01E-05	0.02	0.91
39	W00021	0.003	0.0003	0.32	1.84E-05	0.02	0.65
40	W00022	0.003	0.0003	0.37	2.05E-05	0.02	0.66
41	W00023	0.004	0.0004	0.43	1.30E-05	0.01	0.61
42	W00024	0.004	0.0004	0.31	1.20E-05	0.01	0.82
43	W00025	0.254	0.0254	20.3	1.44E-04	0.14	0.92

Table 4.4

S/N	SAMPLE	Am ² kg-1		ARM/SIRM	S _{-0.1T}	S _{0.3T}	HIRM
		101/111ARM	SIRMx1000				
1	90101	0.09	13.2	0.0902	0.81	1	0.03
2	90102	0.09	36.6	0.0366	0.75	0.93	0.0315
3	80302	0.14	2.99	0.0702	0.69	0.9	0.0028
4	80303	0.14	7.36	0.0947	0.73	0.91	0.007
5	80301	0.29	0.3	0.0543	0.77	0.94	0.0003
6	81301	0.08	9.45	0.0603	0.74	0.92	0.0091
7	90501	0.27	1.27	0.0524	0.75	0.95	0.0012
8	81402	0.18	0.312	0.0333	0.72	0.93	0.0003
9	81403	0.3	0.232	0.05	0.76	0.94	0.0002
10	81401	0.16	0.874	0.5744	0.99	1	0.0048
11	1T71	0.09	6.18	0.0497	0.73	0.9	0.0055
12	81201	0.13	2.84	0.0451	0.8	0.94	0.0028
13	2901	0.06	2.76	0.007	0.71	0.89	0.0026
14	1T81	0.12	15.8	0.0816	0.66	0.89	0.0149
15	7501	0.22	1.35	0.0104	0.81	0.96	0.0013
16	3201	0.25	1.75	0.0088	0.82	0.95	0.0017
17	1B71	0.17	8.19	0.0058	0.75	0.93	0.0079
18							
19	3601	0.11	3.8	0.0074	0.71	0.9	0.0036
20	50101	0.27	1.15	0.0222	0.81	0.94	0.0013
21	90301	0.22	4.06	0.0357	0.77	0.95	0.0039
22	1401	0.21	7.86	0.0508	0.75	0.94	0.0076
23	4301	0.25	0.781	0.028	0.73	0.93	0.0008
24	1201	0.31	1.32	0.0101	0.68	0.89	0.0037
25	1111	0.3	1.02	0.0136	0.91	0.99	0.001
26	7801	0.4	1.68	0.0126	0.74	0.96	0.0016
27	1601	0.09	13.2	0.0436	0.73	0.92	0.0127
28	1B81	0.17	8.35	0.1353	0.7	0.92	0.008
29	6101	0.22	1.54	0.0213	0.73	0.95	0.0015
30	C00001eb	0.29	5.67	0.0029	0.72	0.92	0.0028
31	C00002MEB	0.14	13.2	0.0047	0.92	1	0.0066
32	C00003WB	0.35	1.42	0.0059	0.81	0.96	0.0007
33	C00005R	0.12	6.18	0.0045	0.83	0.98	0.0031
34	W00011	0.23	1.57	0.0168	0.78	0.94	0.0008
35	W00012	0.3	0.933	0.0152	0.69	0.89	0.0005
36	W00013	0.24	1.25	0.0194	0.71	0.87	0.0006
37	W00014	0.28	2.1	0.0048	0.81	0.94	0.0011
38	W00015	0.19	5.01	0.004	0.84	0.97	0.0025
39	W00021	0.34	1.66	0.0111	0.7	0.91	0.0008
40	W00022	0.33	1.74	0.0118	0.68	0.9	0.0009
41	W00023	0.39	1.63	0.008	0.67	0.9	0.0008
42	W00024	0.48	2.54	0.0047	0.7	0.95	0.0013
43	W00025	0.15	33	0.0044	1	1	0.0165
44	W00026	1.01	13.5	0.0176	0.85	0.99	0.0068
45	W00031	0.41	1.04	0.0071	0.63	0.9	0.0005
46	W00032	0.39	0.884	0.0073	0.65	0.89	0.0004
47	W00033	0.39	1.5	0.0073	0.67	0.9	0.0008
48	W00034	0.23	3.27	0.0041	0.84	0.98	0.0016

Table 4.4: Ratio table and magnetic measurements summary.

CHAPTER 5

ANALYSIS AND PRESENTATION OF GEOSTATISTICAL SURFACE MODELS

5.1 Field magnetic susceptibility

A total of 1513 magnetic susceptibility data points were measured for summer 2003 and the same number for summer 2004 (for the individual beach total points see Tables 4.1 and 4.2). The database table used for mapping can be found on Appendix 5. For the EB random mapping, a total of 150 magnetic susceptibility point measurements were used for the surface creation. This chapter discusses the result of the Geostatistical Analyst surface creation and the result of the various steps of the surface creation.

5.2 Data exploration

In the data exploration method, the statistical and spatial properties of the data were explored using:

1. Histogram
2. Normal QQ plot
3. Trend Analysis.

5.2.1 Histograms

Most of the data sets were skewed and did not display evidence of normal distribution. The dataset from EB and EB random data were positively skewed without a log transformation. With a log transformation, the skewedness was reduced, but did not attain the shape of a normal distribution curve. In the surface fitting process, a log transformation was also applied for EB. In the NEB and MEB histogram, the data sets were also positively skewed. A log transformation produced a better but not a normal curve. In the surface fitting analysis, a log transformation was also applied.

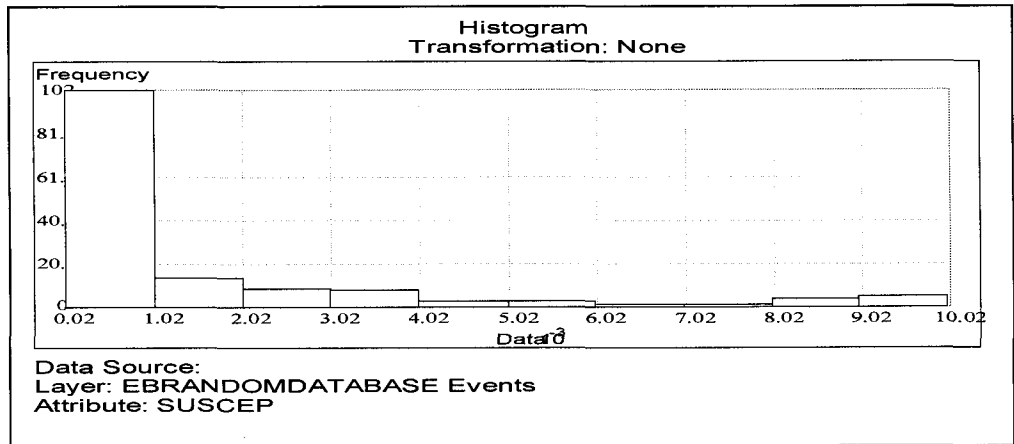


Figure 5.1: Histogram exploration for East beach dataset (no transformation).

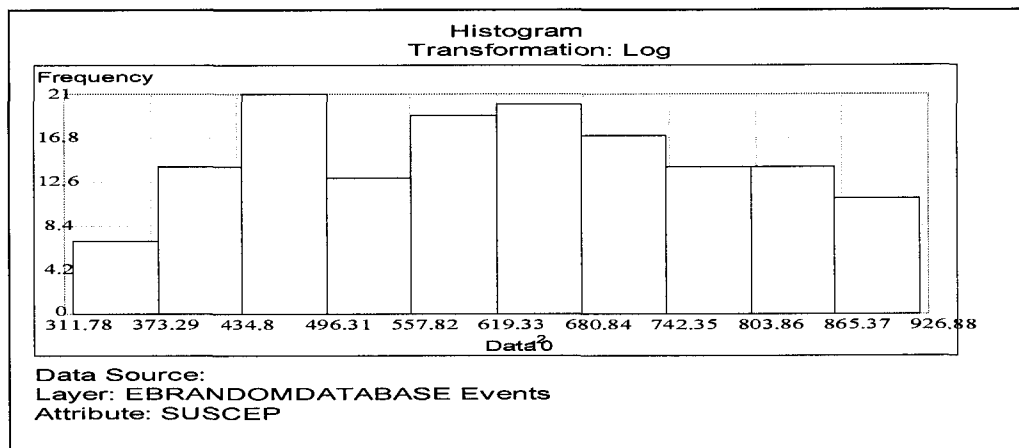


Figure 5.2: Histogram exploration for East beach dataset (log transformation)

The West Beaches displayed a better histogram distribution. The histogram for the WB was skewed, but a log transformation brought it very close to a normal distribution curve. Thus, during the surface creation, the log transformation was applied. The SB data distribution showed a positive low skewedness without the log transformation, and a much higher negative skewedness with the log transformation. Therefore, since the RMS error of the positively skewed distribution was lower than those of the negatively skewed distribution relatively without the negative of positive function, the surface model was created without the log transformation.

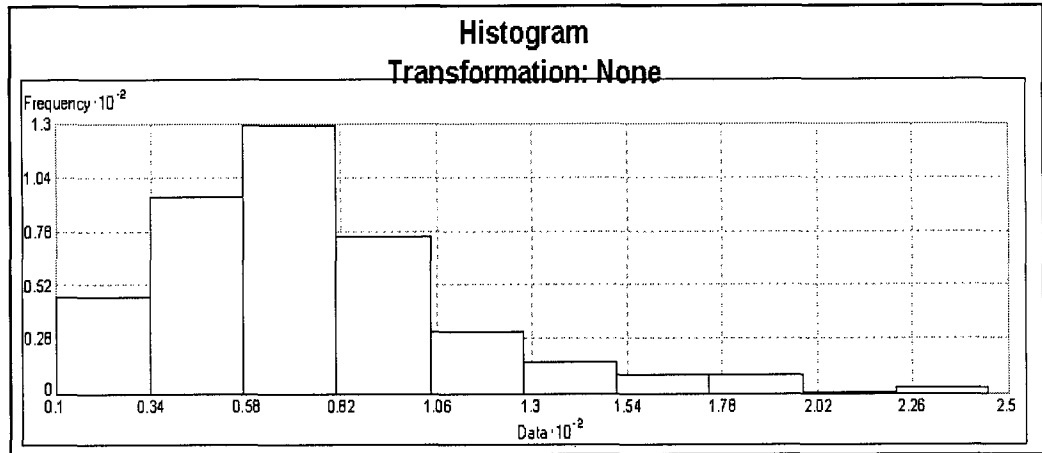


Figure 5.3: Histogram exploration for West beach dataset (no transformation).

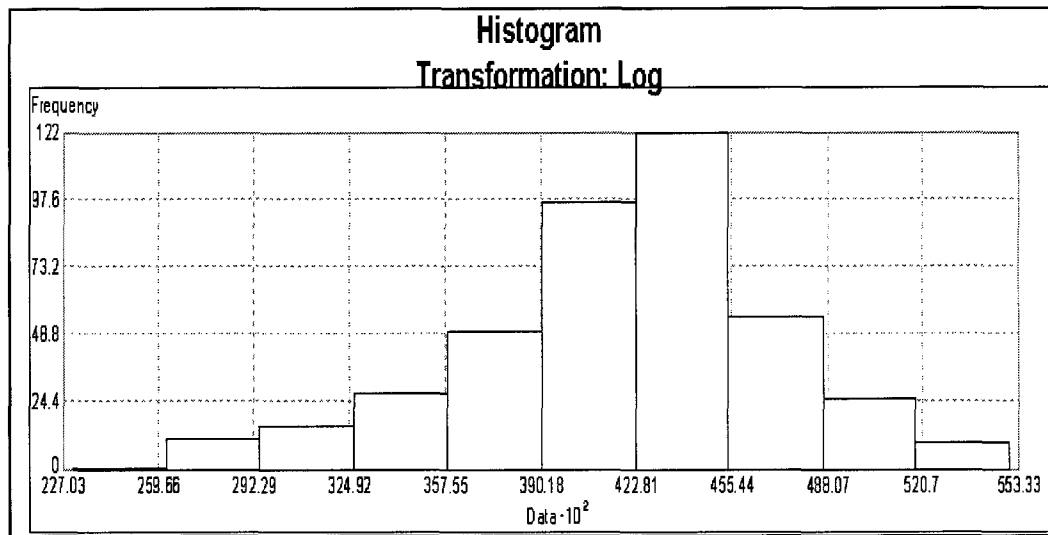


Figure 5.4: Histogram exploration for West beach dataset (log transformation)

5.2.2 Normal QQ plot

This technique compares the distribution of datasets to a standard normal distribution. Each beach group was done individually the results are shown. In the East beach, Middle-East beach, Northeast beach, and Sanctuary beach, applying log transformation in all these beaches provided a seemingly better fit to a standard normal distribution. The West beach differed; the data without a log transformation provided an almost perfect fit to a standard normal distribution. Below are the representative QQ Plot on the Eastern and Western beaches.

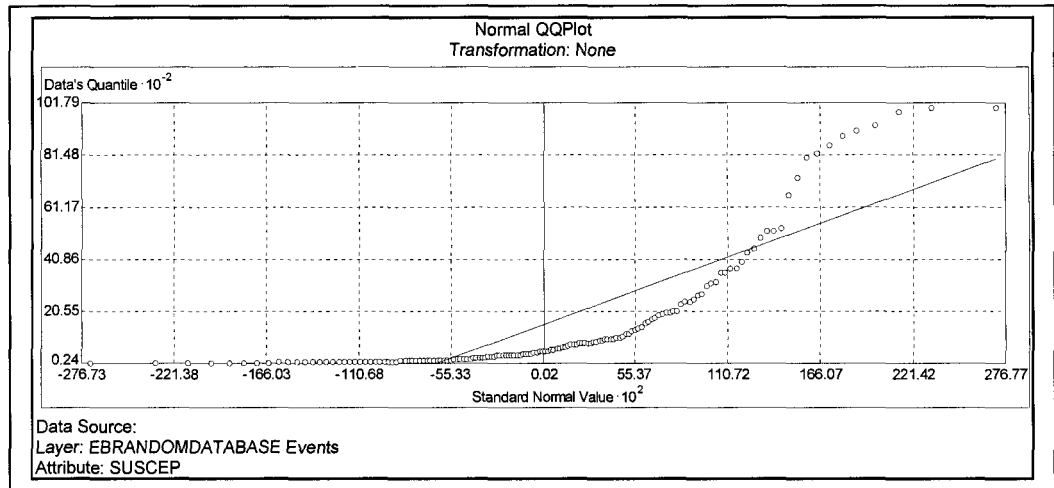


Figure 5.5: Normal QQ plots for EBR

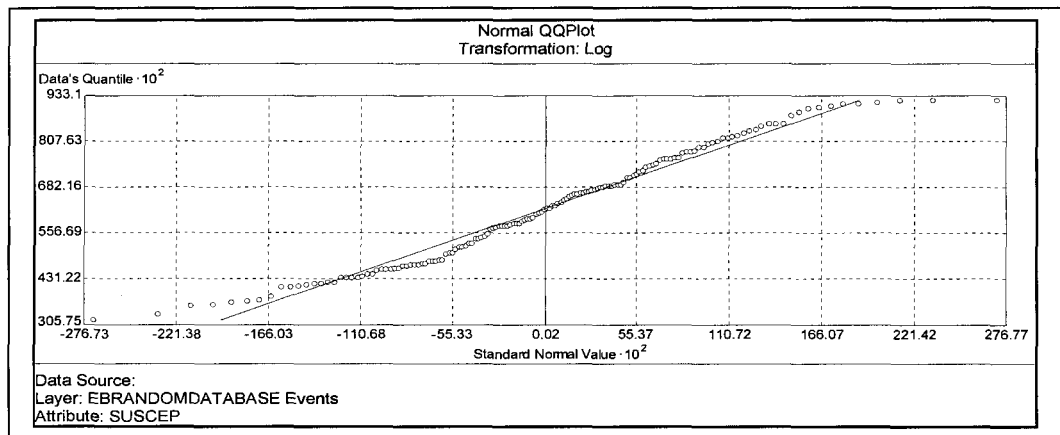


Figure 5.6: Normal QQ plots for EBR with log transformation

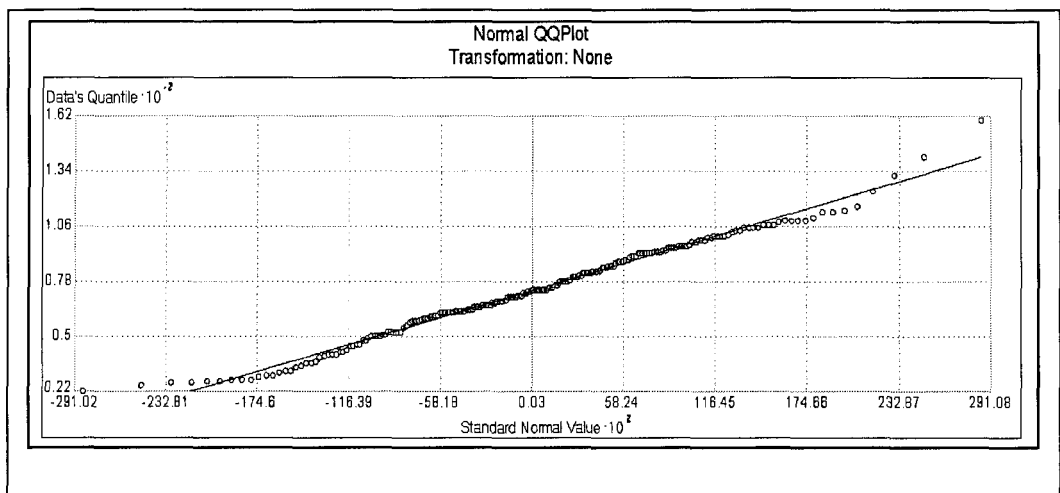


Figure 5.7: Normal QQ plot for SB (no transformation)

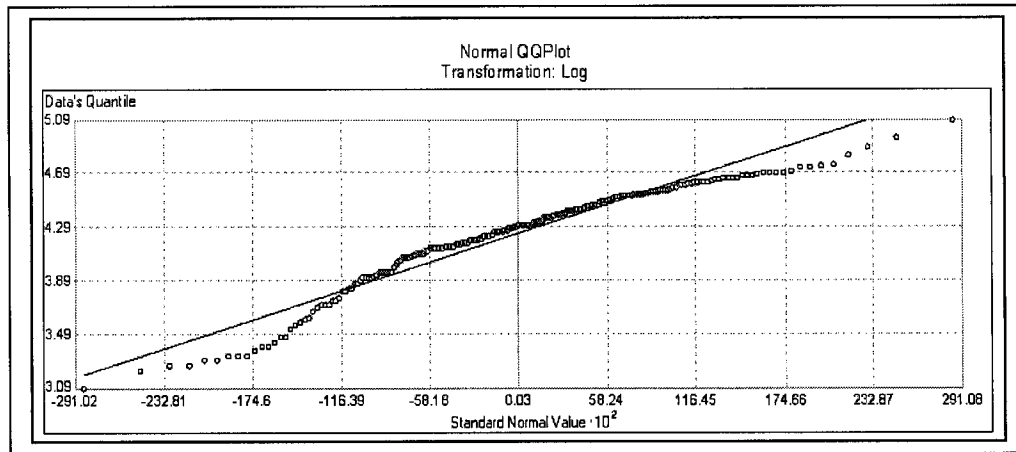


Figure 5.8: Normal QQ plot for SB (log transformation)

5.2.3 Trend analysis

Trend analysis identifies the presence or absence of trends in the input datasets in order to choose the appropriate mathematical transformation needed for the surface creation in Kriging. Although a visible trend may not be apparent initially, a rotation of the axis at 0-360° angles showed the presence of a trend in some of the datasets.

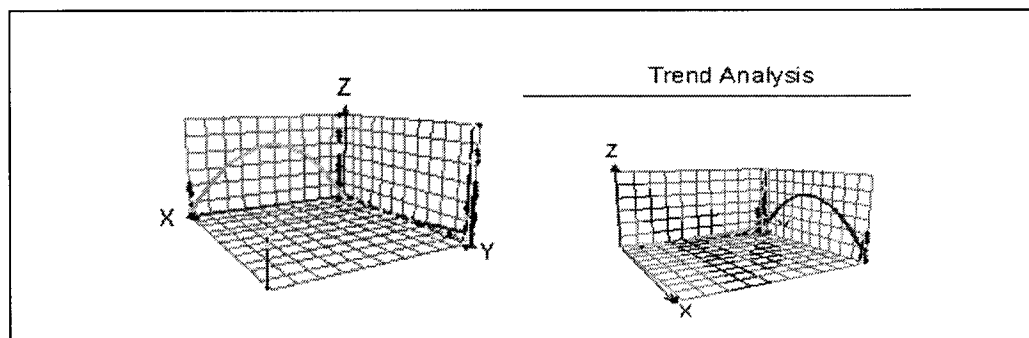


Figure 5.9: Trend analysis for East beach at different angles of rotation.

In the EB and MEB dataset, there was a u-shaped trend at the East-west trend line (green line) and north-south trend line (blue line) more like an inverted u-shape (Figure 5.9). Therefore, a second order trend removal was used for creating surface in the Kriging surface. In all other beaches, there was no noticeable trend, thus trend removal was not necessary.

5.3. Model fitting process

The data exploration revealed the nature of the data distribution. After the decisions on the transformation needed were made, the IDW and the Kriging functions were used to create a surface prediction map. The various transformation and model parameters for the datasets used to create the final surface model for each of the beaches are discussed below. The data used for the model fitting process were the magnetic susceptibility field data from summer 2003 for all beaches and a random sample from EB 2004.

5.3.1. Log transformation

A log transformation was used on data for EB, MEB, NEB and SB for the surface model fitting process (Kriging). This was done in order to have a data set that bore a closer resemblance to normal distribution, since the Kriging surface fitting model performs better with a data that has a normal distribution. The data set from WB was not log transformed during analysis; this was because it showed a relatively normal distribution without the transformation than it did with the log transformation.

5.3.2. Detrending

For Northeast Beach, Sanctuary Beach, West Beach, there was no trend removal during surface fitting process; since no obvious trend was noticed during data exploration.

5.4 Display of model result

A. East beach

The surface pattern displayed by the IDW model was consistent with field observation (figure 5.10). The Kriging model depicted a more uniform variation along a straight line; this was not the observation on this beach (Figure 5.11). Therefore, in terms of visual display and depiction of fact, the IDW model had a better performance. The IDW model also had a lower modelling error (RMS) than the Kriging model (see Table 5.1 for RMS values).

B. East beach random.

As a result of the high RMS error of model performance for EB, (Table 5.1), the random data collected from the third field work was used to create another surface model for EB, this as changed in order to ascertain that the errors did not result from parallel transect method of data collection. This dataset was not collected in transects, a random approach was used. The Kriging model showed an improvement in its display of surface magnetic susceptibility, and was similar to actual field observation. The mid point area with lower susceptibility was well depicted by both models; it was actually the entry point of the EB where low susceptibility were observed (see Figure 5.12).

C. MEB, NEB, SB and WB

For the MEB beach, the IDW model had a better performance both in depicting reality and in having a lower RMS error (Table 5.10). There was no much difference (in terms of depicting reality and model errors) between the IDW and Kriging performance for the NEB. The IDW model had a slightly better RMS error, although both were still quite high. For SB and WB, the model performances were very similar, with the IDW having slightly lower and better RMS errors. In all, the RMS errors observed for SB and WB were generally the lowest for all the beaches, therefore, the model produced is probably more accurate.

5.5. Models performance and prediction error table

Generally, the models with lower RMS errors are deemed to have performed better over the ones with higher RMS errors. A low RMS error was observed for the Western beaches, probably due to the fact that distribution of magnetic susceptibility was more uniform. Some RMS (e.g. EBR) values were very high, and the models would only be good for display, but not for prediction. In all, the surface depiction by IDW showed a higher consistency in depicting reality than Kriging, which had few a ambiguous depictions for some beaches.

S/N	BEACH	METHOD	MEAN	RMS	NO OF PARAMETERS
1	EB	IDW	2.32	804	277
		KRIGING	-109.8	971	277
2	MEB	IDW	12.7	1561	188
		KRIGING	26.7	1569	188
3	NEB	IDW	2.3	806	254
		KRIGING	-109.8	971.8	254
4	EBR	IDW	75.6	2197	150
		KRIGING	1.3	2212	150
5	SB	IDW	-2.8	30.4	318
		KRIGING	-0.3	34.6	318
6	WS	IDW	-1.5	16.3	145
		KRIGING	-0.4	16.1	145

Table 5.1: Model comparison and error report for all beaches.

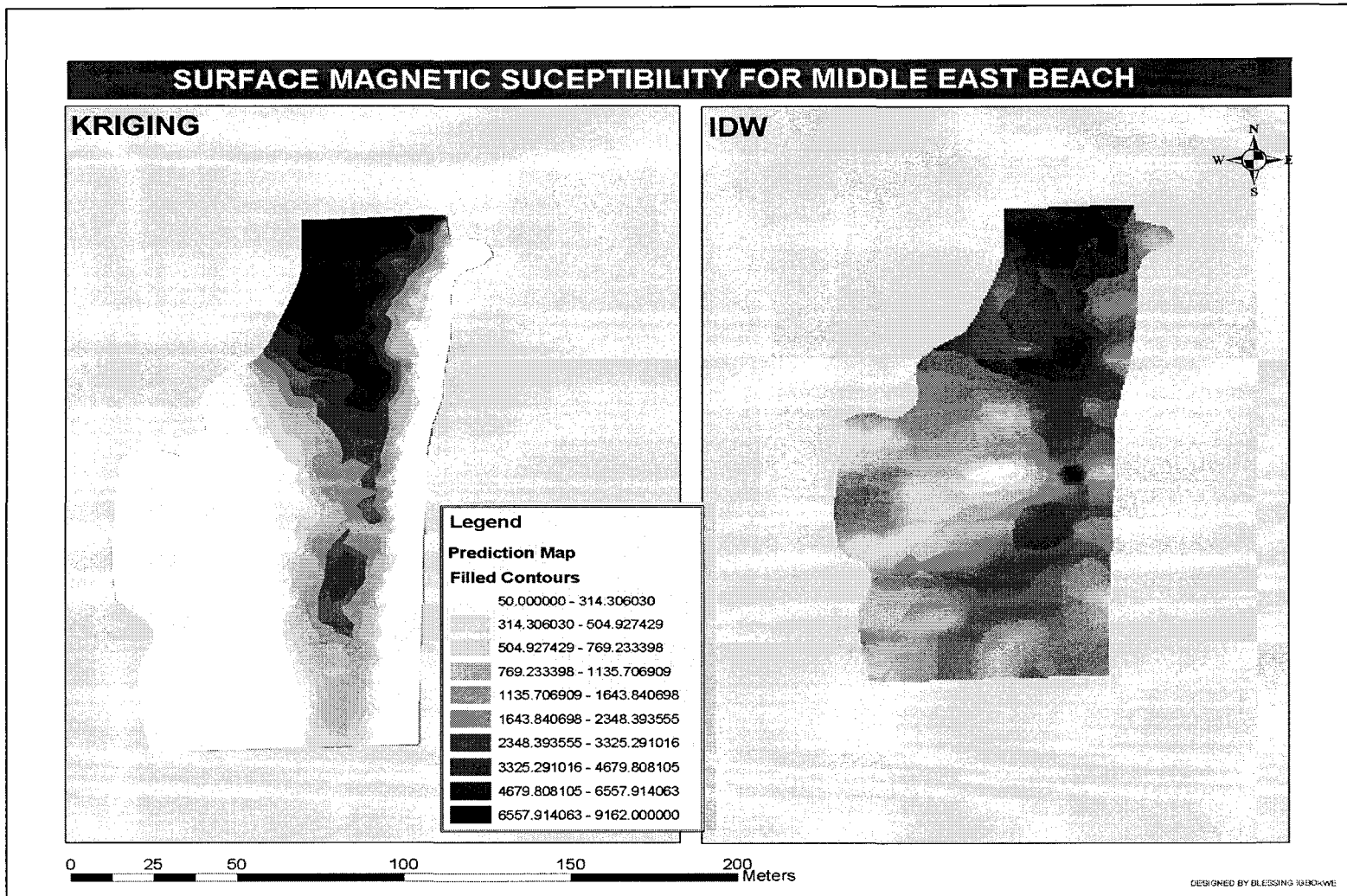


Figure 5.10: Kriging and IDW surface model for MEB.

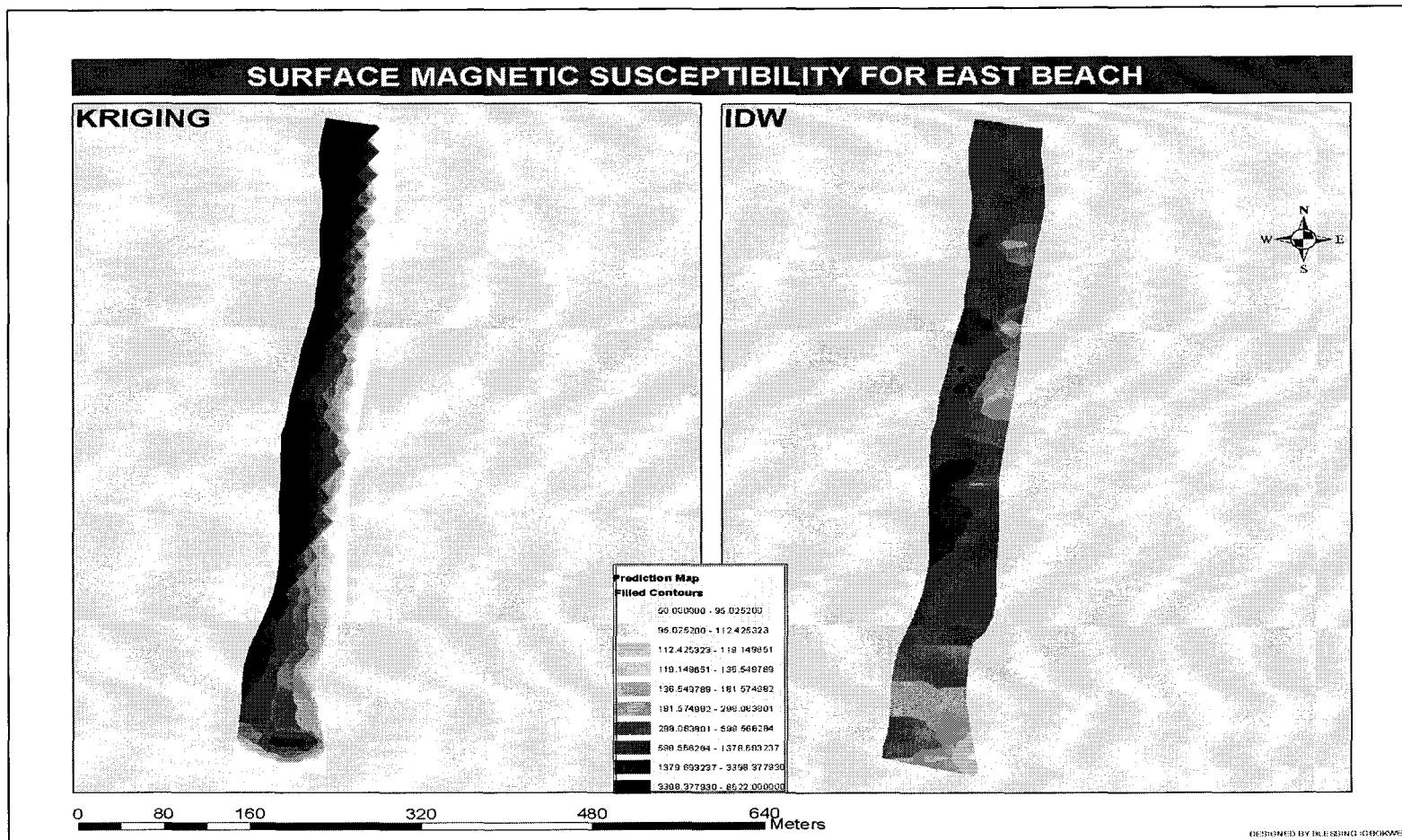


Figure 5.11:Kriging and IDW surface model for EB.

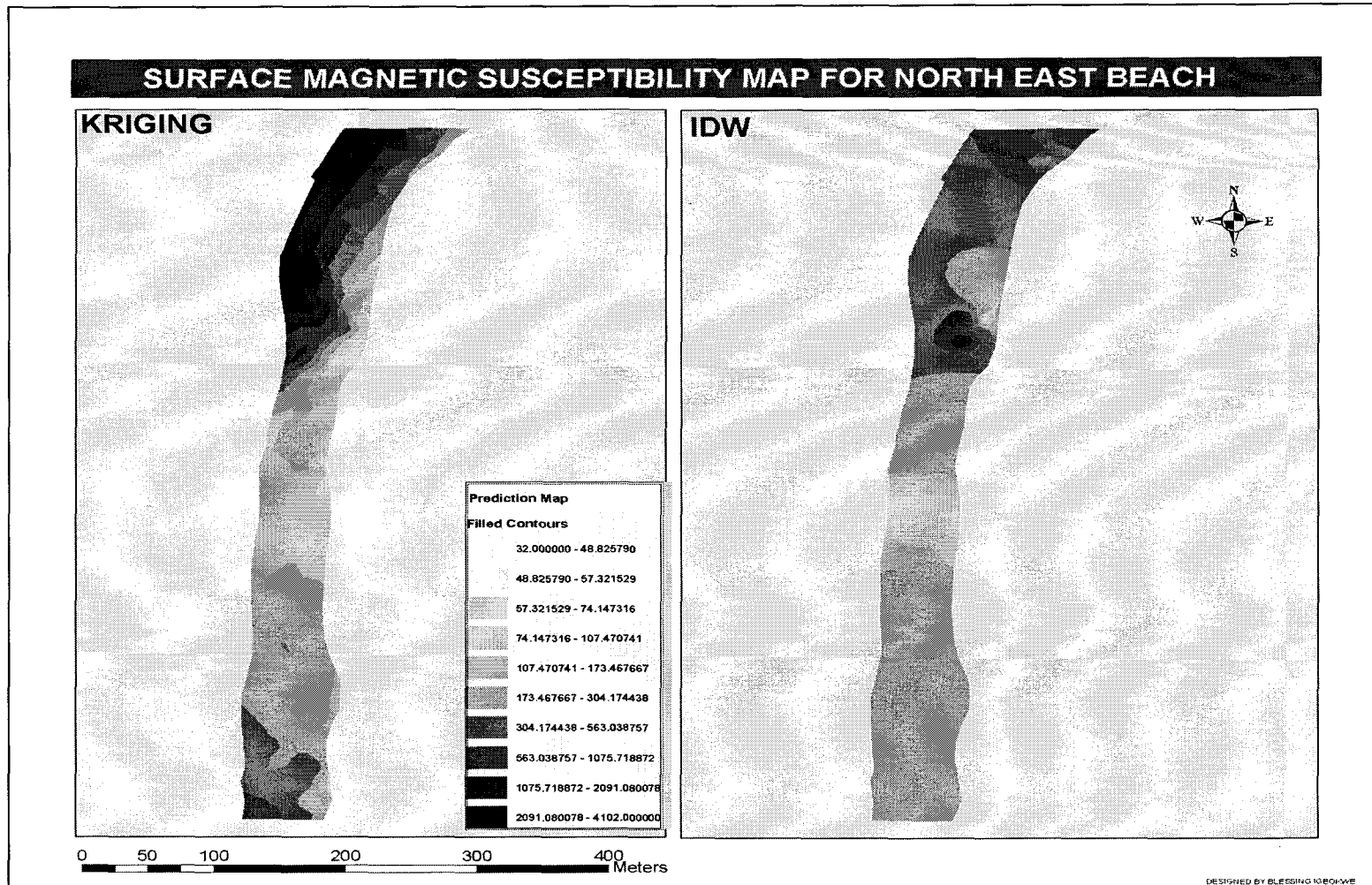


Figure 5.12: Kriging and IDW surface model for NEB

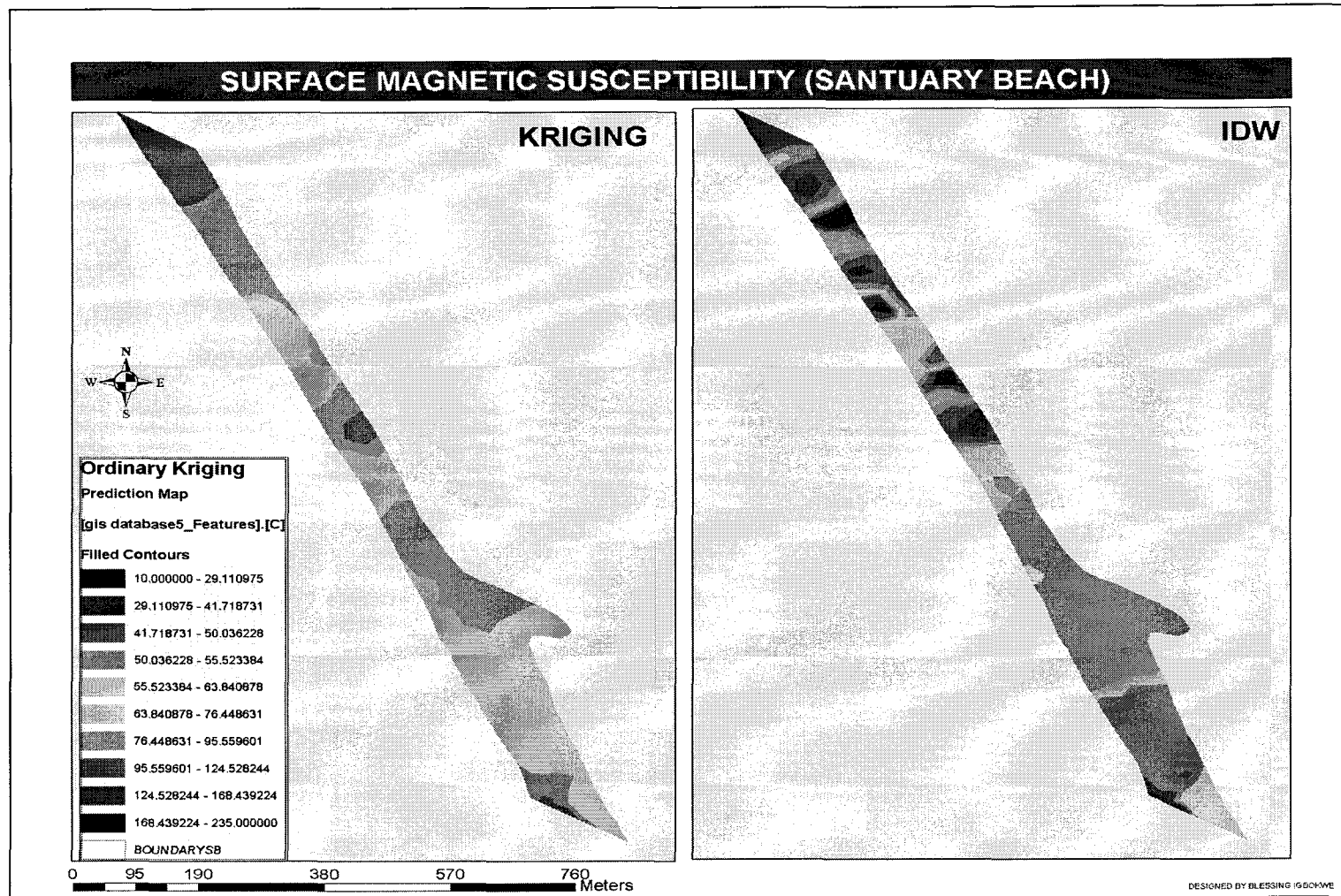


Figure 5.13: Kriging and IDW surface model for SB

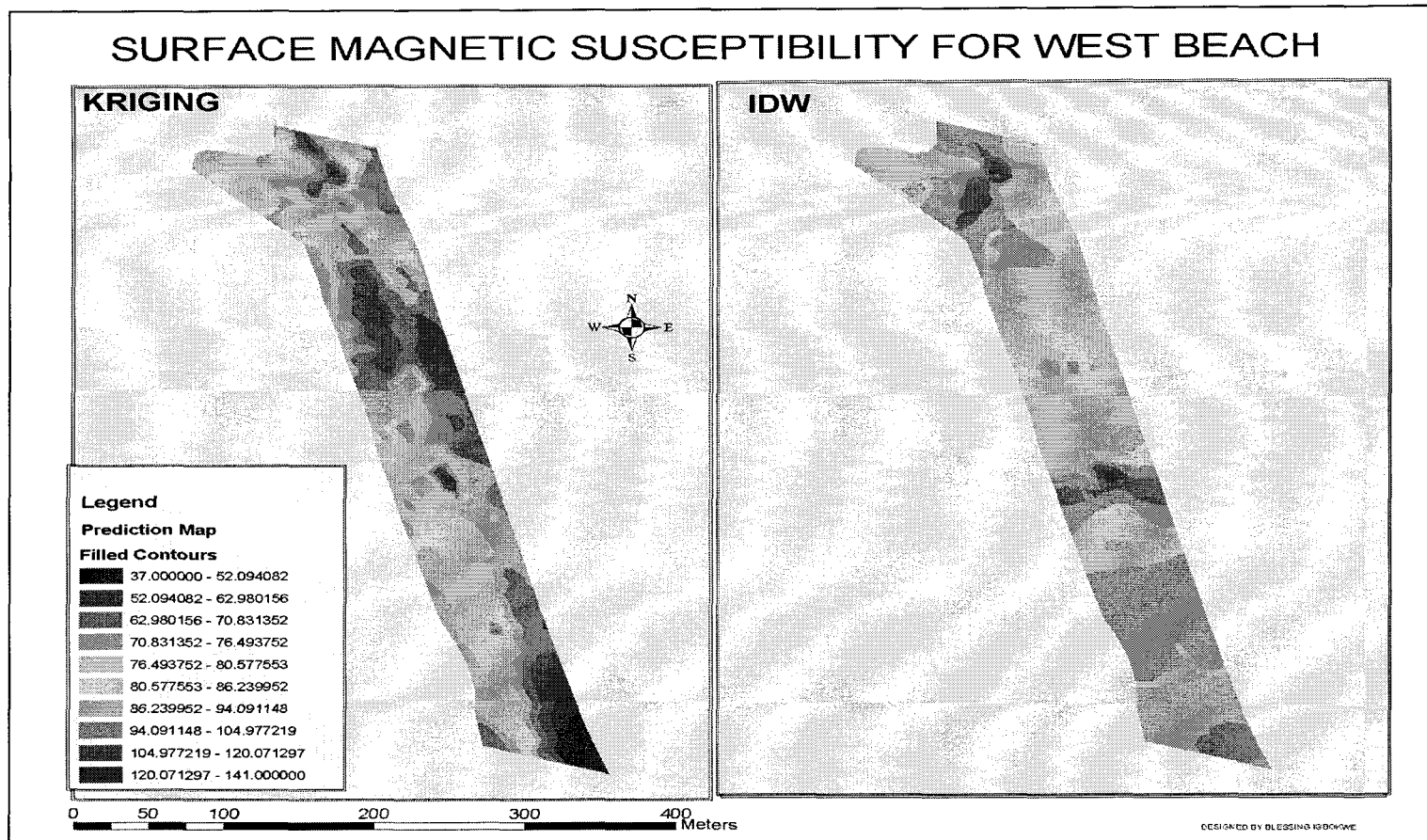


Figure 5.14: Kriging and IDW surface model for WB.

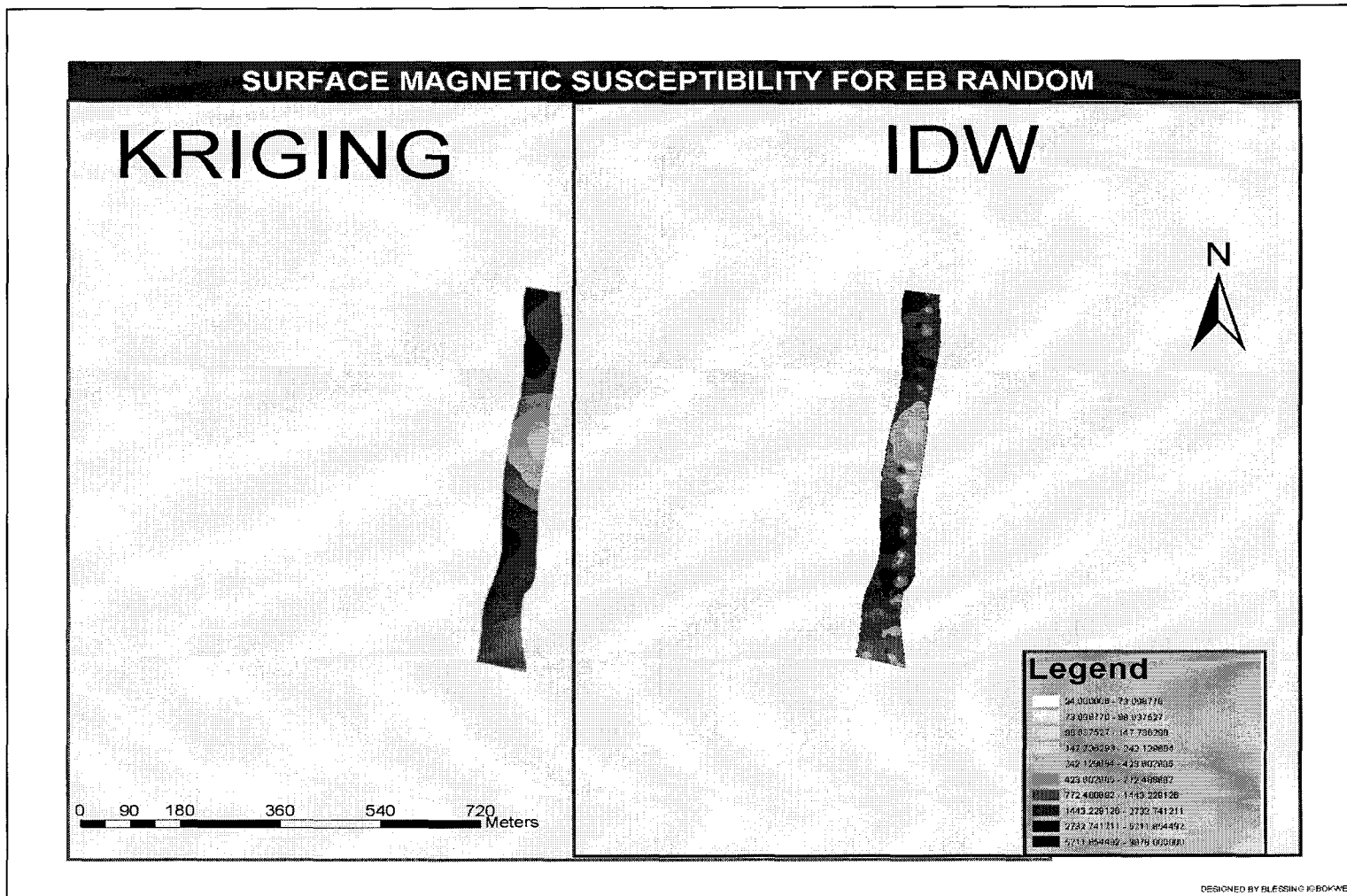


Figure 5.15: Kriging and IDW surface model for EB random data.

CHAPTER 6

TEST OF HYPOTHESES AND PRESENTATION OF STATISTICAL RESULTS

6.1 Hypothesis 1: Spatial variation

In order to quantify the spatial variability of magnetic susceptibility on PPNP beaches, statistical tests were used to test for significant difference in field susceptibility. All beaches were assigned variables from one through ten, data points from the same beachwear assigned the same variable and the test statistics were run on MINITAB using Kruskal Wallis (Freund, 1960). The hypothesis was tested at the 1% level of significance, and the test results are summarized in Table 6.1 below. The actual test statistics are displayed in Appendix (4). Hypothesis 1 stated: there is no significant difference in the susceptibility (χ) observed on the Eastern beaches and those observed on the Western beaches. The test statistics showed that there was a significant difference in the magnetic susceptibility observed at the Western beaches and those observed at the Eastern beaches for each of the two seasons 2003 and 2004. This difference could be as a result of varied rate of deposition and erosion in the West and East beaches.

	HYPOTHESES (Questions)	RESULT	TEST STATISTICS	CRITICAL H	DF	DECISION
1	Is there a significant difference in the susceptibility (χ) observed on the Eastern beaches and those observed on the Western beaches?		Kruskal Wallis			
a	EB, MEB, NEB, WB, WP, SB BW, DUNES, SH and NW (2003).	yes	604.81	6.635	1	Reject H0
b	EB, MEB, NEB, WB, WP, SB BW, DUNES, SH and NW (2004).	yes	550.09	6.635	1	Reject H0

Table 6.1: Test statistic summary for hypothesis 1

6.2 Hypothesis 2: Individual beach seasonal variability

As the magnetic susceptibility varied from beach to beach, in order to determine if the magnetic susceptibility at each data point varied over time, two datasets were compared: the magnetic susceptibility data from summer 2003 and those from 2004. The two data points from same beach were assigned two variables: 1 for 2003 and 2 for 2004 data points. Hypothesis 2 stated: there is no significant seasonal variation in magnetic susceptibility (χ) on the beaches. The test statistics showed that this hypothesis holds for NWB, WP and SB. In the other seven beaches, there was a significant seasonal variation.

	HYPOTHESIS (Question)	RESULT	TEST STATISTICS	DF	CRITICAL H	DECISION
2	Is there a significant temporal variation in magnetic susceptibility (χ) on the Beaches?		Kruskal Wallis			
a	MEB.	yes	64.84	1	6.635	Reject H0
b	EB.	yes	6.79	1	6.635	Reject H0
c	WB.	yes	27.06	1	6.635	Reject H0
d	NEB.	yes	141.34	1	6.635	Reject H0
e	WP Beach.	No	2.83	1	6.635	Accept H0
f	BW Beach.	yes	9.75	1	6.635	Reject H0
g	NW Beach.	No	1.51	1	6.635	Accept H0
h	SH Beach.	yes	33.33	1	6.635	Reject H0
i	Dunes.	yes	28.03	1	6.635	Reject H0
j	SB Beach	No	0.44	1	6.635	Accept H0

Table 6.2: Test statistics summary for hypothesis 2.

6.3 Hypothesis 3: Intrabeach variability

The summary statistics for hypothesis 3: there is no significant difference in susceptibility (χ) within the individual beach transects is presented in Table 6.3 below. Test statistics showed that for the following beaches; WP-2003 and 2004, BW-2003, Dunes 2003 and 2004, and SH 2003 and 2004 there was no significant difference within individual beach transect and across all transect on these beaches. For all the other beaches, there was a significant difference between the individual beach transects. This implies that, within some of the West beaches, the magnetic susceptibility was evenly

distributed, with a small range between the low and high values. But for all the East beaches, the range of magnetic susceptibility in individual beach was high.

	HYPOTHESES (Questions)	RESULT	TEST STATISTICS	CRITICAL H	DF	DECISION
3	Is there a significant difference in susceptibility (χ) within the individual beach transects?		Kruskal Wallis			
a	EB-2003	Yes	28.67	26.217	12	Reject H_0
b	EB-2004	Yes	90.22	26.217	12	Reject H_0
c	NEB-2003	Yes	59.67	36.191	19	Reject H_0
d	NEB-2004	Yes	89.51	36.191	19	Reject H_0
e	MEB-2003	Yes	45.35	18.475	7	Reject H_0
f	MEB-2004	Yes	59.23	18.475	7	Reject H_0
g	WB-2003	Yes	22.06	20.090	8	Reject H_0
h	WB-2004	Yes	23.26	20.090	8	Reject H_0
i	WP-2003	No	0.70	11.345	3	Accept H_0
J	WP-2004	No	1.82	11.345	3	Accept H_0
k	BW-2003	No	6.17	9.210	2	Accept H_0
l	BW-2004	Yes	9.32	9.210	2	Reject H_0
m	Dunes-2003	No	0.31	9.210	2	Accept H_0
n	Dunes-2004	No	3.69	9.210	2	Accept H_0
o	SH-2003	No	2.74	9.210	2	Accept H_0
p	SH-2004	No	2.60	9.210	2	Accept H_0
q	SB-2003	Yes	34.73	21.666	9	Reject H_0
r	SB-2004	Yes	26.03	21.666	9	Reject H_0
s	NW-2003	Yes	66.29	18.475	7	Reject H_0
t	NW-2004	Yes	35.93	18.475	7	Reject H_0

Table 6.3: Test statistics summary for hypothesis 3

CHAPTER 7

DISCUSSION OF RESULTS, FINDINGS AND CONCLUSIONS

The initial observations on Point Pelee National Park (PPNP) beaches indicated the following:

1. An overall higher magnetic susceptibility values on the Eastern beaches and a fairly low uniform susceptibility on the western beaches.
2. Vivid colour (black and red) of sediments with high magnetic susceptibility values on the Eastern shores of the PPNP.
3. A thin laminate of magnetite, distinctly coloured, about 1cm thick on the Eastern beaches.
4. A pattern in the distribution of the high susceptibility zones on the Eastern beaches: higher away from the shoreline (closer to the vegetation front).

The variations from beach to beach indicated that there could be an underlying process responsible for the observed difference in magnetic susceptibility on the West and East beaches. A number of plausible reasons could be suggested as explanations for the observed variations which include: (i) erosion; (ii) seasonal sediments transported by waves of water; (iii) one time depositional event from a huge storm; (iv) microbiological activities (due to magnetotactic bacteria activities within the lake or pond); (v) beach nourishment on the Eastern side; and, (vi) wave action causing sediment sorting due to grain density of heavy minerals, making them less easily transported than the lighter grain sediments (Trenhaile, 1997). The source of sediments on PPNP western and Eastern beaches could be from different sources (Figure 2.1) as a result of sediment movement and transport (Trenhaile et al., 2000). If this is so, then the variation in magnetic susceptibility may be credited to different sediment source areas.

7.1. Objectives

In order to provide an explanation for the magnetic susceptibility variation, the following objectives were set for this research;

1. To use a Geographic Information System (GIS) in mapping and displaying the magnetic susceptibility of Point Pelee beaches and its attributes in order to show

the spatial variation at a glance and produce a map that can be easily updated with new data.

2. To determine the magnetic mineralogy at each beach and to delineate the effective grain size of the major magnetic minerals present in the beach sediment that caused the observed susceptibility variation.
3. To determine if the source of the sediments on the various beaches are the same through comparison of the sediments magnetic characteristics.
4. To ascertain if the magnetic susceptibility on the beaches is temporal.
5. To characterize and compare sediments from potential source/area suggested by Trenhaile et al., (2000) i.e. PPNP and bluffs of Wheatley the beach sediment.
6. To examine physical processes like weathering, erosion, sediment transport, deposition and beach nourishment as potential causes of the magnetic susceptibility variation observed on the west and the East beaches.

The following subsections discuss the extent to which these objectives have been achieved.

7.2. GIS model, display and results implication

The surface magnetic susceptibility for the Eastern beaches was mapped for each beach, and the Western beaches were divided into two areas. In order to see if GIS could be used for surface modeling and mapping, two methods were applied: IDW and Kriging. Both used the Geostatistical Analyst which is an extension of ESRI ARCMAP/ARCINFO. Both models were characterized by very high RMS errors for the Eastern beaches (Tables 5.3). This suggests that neither model was suited for surface magnetic susceptibility prediction at these locations. The modeling and RMS errors were much lower for the Western beaches; and thus, these models would be more suitable for surface magnetic susceptibility predictions. This difference could potentially be attributed to the significantly greater variation in magnetic susceptibility on the Eastern beaches as opposed to a more uniform magnetic susceptibility on the Western beaches (magnetic susceptibility field observation, 2003/2004), or could be potentially attributed to the sampling method (parallel transects, perpendicular to the shoreline).

In order to test this idea, that is the effect of the sampling method, it was suggested during the thesis proposal and a term paper that analyzed the field data (61-582, 61-574) that the sampling method should be changed to random type. A random sampling of East beach was done, however, the surface model result showed no improvement over the original method of data collection in transects. The RMS error for this particular method was higher than the RMS errors of the models made with the original set of data. This result indicates that the original method of data collection (i.e. 1m interval on vertical transects) was not the reason for the high model and RMS errors observed on the Eastern beaches. The high modeling and RMS errors probably resulted from the high variability of χ over very short distances. Thus an ideal sampling methodology has not been determined.

7.3. Magnetic mineralogy and granulometry

The determination of magnetic mineralogy rested on SIRM acquisition and demagnetization spectra, Curie temperature analysis (T_c), as well as several magnetic parameters (s-ratios and HIRM). In determining the magnetic granulometry, individual sample coercivity spectra were plotted on a graph of J/J_{900} (magnetic intensity/intensity at 900mT) against field. These graphs were compared to the Symons and Cioppa (2000) templates. Normalized pARM acquisition curves (Jackson et al., 1988) were also used for estimating the effective grain sizes of the magnetic minerals.

7.3.1. Magnetic mineralogy

Temperature dependence of magnetic susceptibility (T - χ) curves were obtained from heating the samples from room temperature (25°C) to 700°C in an argon atmosphere. The results showed that the χ of all samples decreased significantly between 530°C and 580°C, indicating that the magnetic carriers were probably titanomagnetite and magnetite. Although all samples showed a χ of almost zero at ~580°C, the shapes of the T - χ curves were variable. Some curves showed a bump in their heating curve that resembles a Hopkinson peak, which is a maximum in susceptibility experienced just below the T_c (Kwon, 2002).

The Hopkinson phenomenon may be explained in terms of the relationship $\chi(T) \propto M_s(T)/K(T)$, where M_s is the spontaneous magnetization and K is the magnetic anisotropy. Both M_s and K decrease with increasing temperature. At low temperatures, these two effects cancel out and χ remain roughly constant. As T approaches T_c both M_s and K approaches 0. Since K decreases at a faster rate than M_s , thermal fluctuations at T close to T_c give rise to a peak in susceptibility known as the Hopkinson peak (Harrison and Putnis, 1999). Three distinct types of heating/cooling curves were noticeable. The first type of heating/cooling curve (Figure 7.1A) showed a very gradual increase in χ until $\sim 220^\circ\text{C}$ (point A1), peaking at $\sim 250^\circ\text{C}$ (point A2). After these peaks, χ does not decrease below the original values. The χ values then decrease gradually until about 400°C (point A3), above which temperature there is a very sharp increase in χ to $\sim 500^\circ\text{C}$ (point A4). The gain in χ at a peak of $\sim 500^\circ\text{C}$ is greater than 100% of the original values. Magnetic susceptibility generally dropped to almost zero between $\sim 575\text{-}580^\circ\text{C}$ (point A5). The features seen in this curve are not typical of a homogenous material. The broad peak at 500°C is not likely a Hopkinson peak, which would be observed just before the sample attained its T_c (Harrison and Putnis, 1999). Thus, the most likely explanation is the presence of multiple magnetic minerals (e.g. pyrrhotite: $T_c = 350^\circ\text{C}$; Hrouda and Zapletal, 2003; Konty and De Wall, 2000).

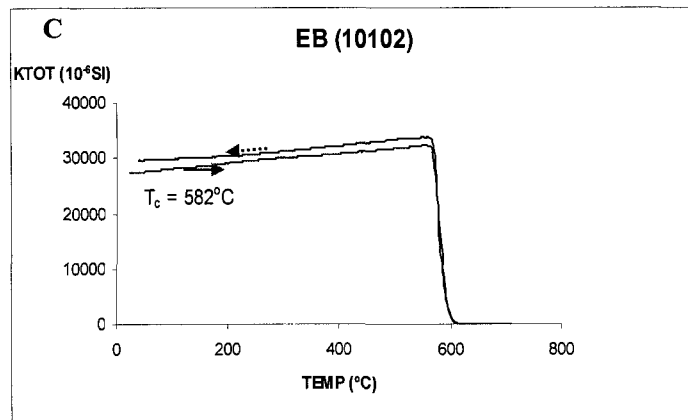
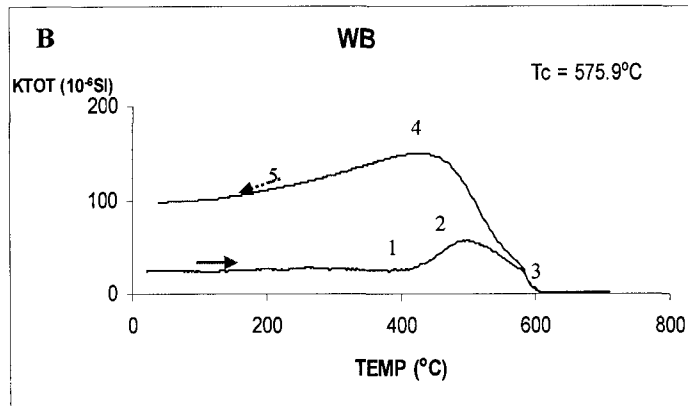
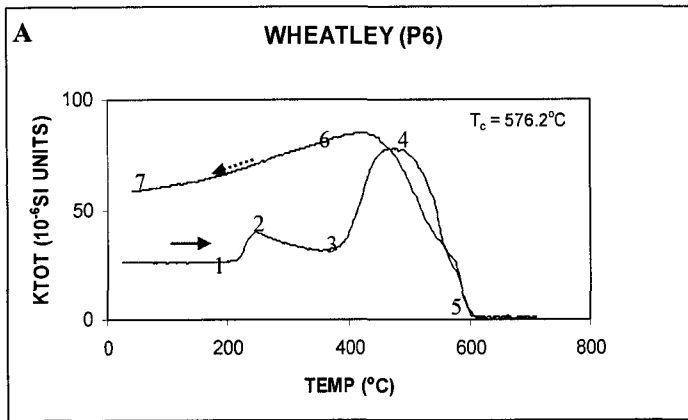


Fig. 7.1: Susceptibility vs. temperature heating and cooling curves for A. Wheatley (bluff sample), B. West Beach sample, and C. East Beach sample. Heating and cooling occurred in an argon atmosphere.

The second type of curve (Figure 7.1B) showed less variation in the heating phase than Type A. The χ was uniform until the temperature approached $\sim 400^{\circ}\text{C}$ (point B1), after which a sharp increase in χ occurs and peaks at $\sim 500^{\circ}\text{C}$ (point B2). The χ then reduces to almost zero at $\sim 580^{\circ}\text{C}$ (point B3). The cooling curve for Type B (points B4-5) was similar to the cooling curves of Type A (point A6-7). For samples that displayed these two types of curves, there was a gain ($> 100\%$) in overall magnetic susceptibility when the samples were returned to room temperature. This increase supports an interpretation that the minor peaks in the heating curves were due to the production of new magnetic phases rather than a Hopkinson peak of a pre-existing ferromagnetic phase which would be expected to return to its original value (Zhu et al., 2000, in Liu et al., 2003). The samples displaying type A and B curves could also be reflecting variable titanomagnetite compositions.

The third and final type had an almost totally reversible heating and cooling curves. In general, these samples had very high initial χ values (Figure 7.1C). The T_c of these samples was consistent with magnetite, with a very sharp drop in χ at $\sim 580^{\circ}\text{C}$. The multiple peaks characterizing the heating and cooling curves of types A and B were absent. The total gain in magnetic susceptibility after heating and cooling was generally less than 20% of the original total, as opposed to greater than 100% gain in types A and B. Hrouda et al. (2003) suggested that this type of reversible curve (Figure 7.1C) was characteristic of coarse-grained (multi-domain) magnetite. The samples displaying this type of curve are more likely to be composed of relatively homogeneous magnetite of a uniform grain size.

The SIRM and back field IRM values are useful parameters for estimating the relative enrichment of low coercivity or high coercivity minerals in a sample. In general HIRM values are high if the concentration of high coercivity minerals is high and vice versa. The ranges of HIRM observed in the beach are summarized below: all the values observed are low. There is no observable pattern or areas of high values, and the distribution appears to be even. Therefore, no particular area can be pinpointed to have a unique concentration of high coercivity material.

Beach	Range
EB	0.0010-0.0149
MEB	0.0012-0.0315
NEB	0.0002-0.0048
Western beaches	0.0008-0.0036
Wheatley bluff	0.0004-0.0009
Wheatley beach	0.0011-0.0165
Rondeau	0.0031

Table 7.1: HIRM values obtained from SIRM and IRM values.

The $S_{-0.3T}$ values confirmed this conclusion. Samples with an $S_{-0.3T}$ of 1 contain only magnetite or pyrrhotite (low coercivity minerals); lower values indicate the contribution of the contribution of “harder” magnetic minerals which are not saturated at in a field of 0.3T (see section 3.5.6 on magnetic ratios). This ratio serves to discriminate magnetite (or other easily saturated magnetic minerals such as pyrrhotite) from hematite and goethite which are not easily saturated in a field of 0.3T. The observed values were 0.9 or greater for most samples, and a 1.0 for a few samples. The combination of the T_c and these parameters strongly indicate the presence of magnetite.

The $S_{-0.1T}$ parameter indicative of the presence of relatively fine (SD) and coarse (PSD and MD) grain magnetite: the higher the value, the greater the proportion of coarse magnetite. $S_{-0.1T}$ ranges from 0 to one. One indicates very low coercivity and larger grain sizes and lower values of $S_{-0.1T}$ indicate higher coercivity and smaller grain size. The most disparate results were seen in the Wheatley bluff samples. Almost 90% of the Wheatley bluff samples displayed an $S_{-0.1T}$ value of less than 0.7; while more than 90% of PPNP samples displayed an $S_{-0.1T}$ of higher than 90% (see tables 4.2 and 4.4 on $S_{-0.1T}$ and $S_{-0.3T}$ for summary and samples values). This result suggests that the Wheatley bluff samples may contain relatively higher coercivity and, most probably, smaller grain size minerals than the PPNP, RPP and the Wheatley beach samples. The samples of the PPNP and RPP gave higher values of $S_{-0.1T}$ than the samples from the Wheatley bluffs; since coercivity of SD magnetite are higher than those of PSD and MD magnetite, the $S_{-0.1T}$

values for Wheatley bluffs suggest that the samples may contain SD magnetite while the PPNP and RPP may contain PSD or MD magnetite.

7.3.2. Magnetic granulometry

The pARM acquisition curves used for estimating the relative magnetic grain sizes of samples from PPNP beaches were relatively uniform (section 4.2, A-E). The pARM peaked at relatively low fields of about (10mT). This corresponded to grain size range of ~5 to >25 microns (Jackson et al., 1988) in all the beaches. Overall, most of the samples from the western beaches had effective magnetic grain sizes in the range of 25 microns. However, grain sizes of ~5 microns were also observed in WB and BW, which were closer to the Eastern beaches than the other beaches at the west side.

The Eastern beaches (EB, MEB and NEB), had grain sizes ranging from ~5-25 microns. About 80% of the samples had grain sizes of ~5 microns, while the other 20% had grain sizes of ~25 microns or greater (Figures. 4.6, 4.8 and 4.11). In the MEB, the effective magnetic grain sizes were mainly in the 5 microns range. In the MEB sieved samples, (mesh size-<0.6mm and >0.3mm (Figures 4.13 and 4.14) the coarse grain samples (<0.6mm grains) displayed evidence of very little magnetic minerals present, since some of the samples did not peak or could not be demagnetized. For NEB, grain sizes also ranged from ~5-25 microns with little evidence of high coercivity magnetic material in the sieved samples. For the lone sample obtained from RPP beach, the effective magnetic grain size was ~5 microns (Figure 4.22).

The pARM curves of samples from the Wheatley area showed greater variability. Two sample sets were collected, one from the bluffs and the other from the beach. The sample sets from the bluff (Figures. 4.19, 4.20, and 4.21) had the smallest effective magnetic grain sizes of all samples measured. Grain sizes for this group were less than 2 microns with little evidence of high coercivity minerals apparent. The set of samples from the beach (Figures. 4.19, 4.20 and 4.21) displayed evidence of larger magnetic grain sizes of ~5 microns, similar to those of PPNP beaches and RPP. From this set of samples, some showed evidence for very high coercivity minerals (e.g. hematite and goethite or very fine grained magnetite); the pARM curve was a straight line indicating that there were no low coercivity minerals to be magnetized. In summary, the bluff samples (clayey

sediments) had smaller magnetic grain sizes, whereas the beach sands collected at the base of the bluffs were similar to those of PPNP. This is probably because finer grains are carried offshore as suspended loads, into the lake and the coarser ones are left on the beaches (Trenhaile, 1997).

The SIRM acquisition and demagnetization plots for Western, Eastern and RPP beaches (Figures. 4.23, 4.24, 4.27, 4.30 and 4.33) showed no significant variation in magnetic mineralogy. All plots displayed characteristics of PSD magnetite. With the assumption that magnetite was the dominant magnetic mineral, as suggested by the Curie temperature, S-ratios and SIRM measurement; a template fit of SIRM acquisition and demagnetization plots on the Symons and Cioppa (2000) magnetite template showed that the magnetic domain sizes of samples were consistent with PSD and SD magnetite. For PPNP, the results clustered in the PSD grain size range. However, the Wheatley samples showed a noticeable difference in grain sizes. The bluff samples fell mainly within the SD grain size (Figure 7.1), while the beach sands fell within the PSD grain size. The Eastern beaches were also within the PSD range while all samples from the west beaches were consistent with the PSD grainsize. Magnetic domain sizes in PPNP beaches were similar to those on Wheatley and Rondeau beaches, but different from those of the Wheatley bluffs. The effective magnetic mineral grain size in PPNP was uniform, both over the West and the Eastern beaches. Grain sizes were in the range of ~5-25 microns. Magnetic domain sizes were all PSD magnetite.

The apparent difference in magnetic grain sizes in the Wheatley pARM spectra was visible in the SIRM spectra. The two sets of samples showed distinct SIRM curves. The bluff samples plot displayed characteristics of SD magnetite, while the beach samples displayed characteristics of PSD grain sizes which were similar to the PPNP and RPP samples.

In summary, from the temperature dependence of magnetic susceptibility and SIRM acquisition curves, the characteristics of the magnetic minerals causing high susceptibility in PPNP Eastern beaches were consistent with those of magnetite. All of PPNP beaches displayed very similar values. Therefore, the higher values of magnetic susceptibility observed in the Eastern beaches were mainly due to a higher concentration of the magnetic minerals.

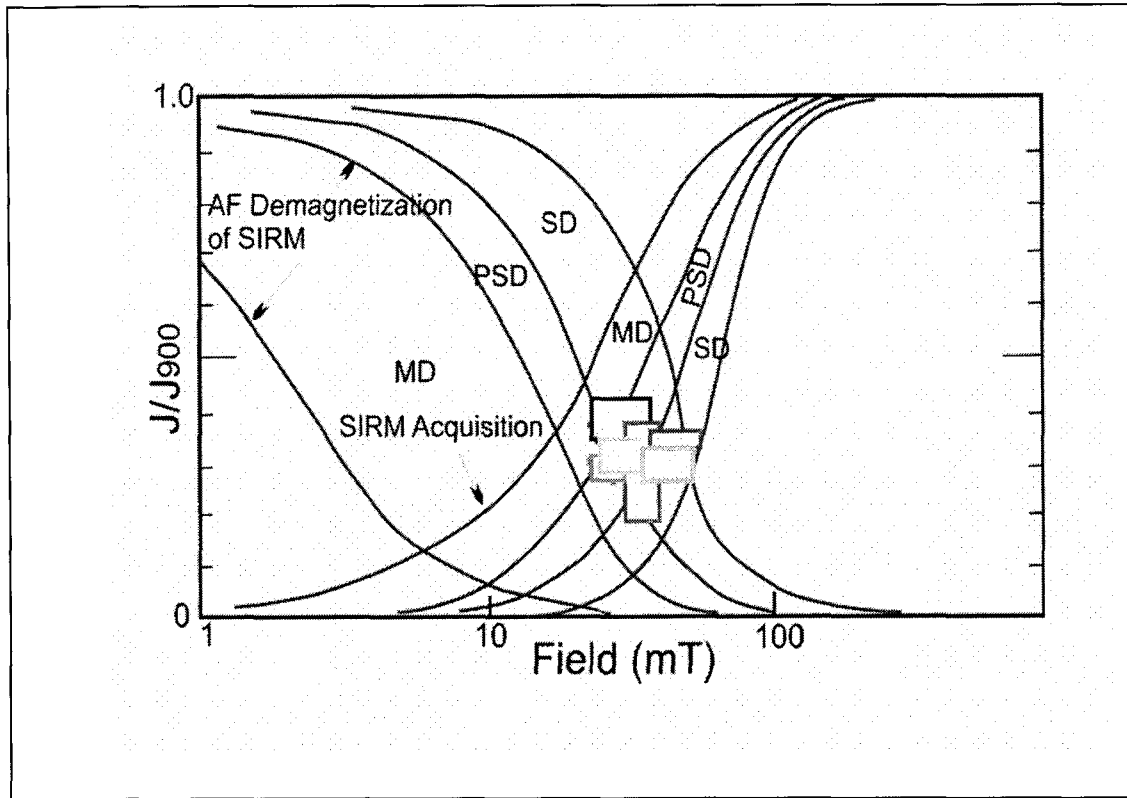


Figure 7.2: Magnetic domain sizes for samples from the various beaches plotted on the Symons and Cioppa (2000) templates.

7.4. Seasonal variation of magnetic susceptibility in PPNP

In order to determine if the variation observed in the spring and mid summer was seasonal or consistent over time, a hypothesis was formulated;

There is no significant temporal variation in magnetic susceptibility (χ) on the PPNP Beaches (section 6.1). This hypothesis was statistically tested with the Kruskal Wallis (a non-parametric) test by comparing the field magnetic susceptibility measurements made in summer 2003 and summer 2004. The result showed that for all the beaches but SB, NWB and WP (Table 6.2 on test of hypothesis), there was a significant year to year variation in the observed field magnetic susceptibility. This variation could be due to the following:

- i. Since the high magnetic susceptibility minerals were mainly on the sand surface, processes like sediment movement/transport by ice or rain water,

and erosion could be causing relocation of original sediment and replacement by some less susceptible sediment.

- ii. The GPS ten meter accuracy level could allow measurements to be made at points anywhere within a 10 meter radius of the previous summer position. Since χ varied widely over very short distances in the Eastern beaches, this error margin in GPS could have caused the variations observed. Notwithstanding, the general pattern of increasing susceptibility toward the vegetation was still apparent in both fall measurements.

In order to ascertain the temporal variability on the Eastern beach with higher degree of accuracy and avoid GPS error, high accuracy GPS, in the range ten centimetres or less would have to be employed.

7.5. Spatial variation and comparison of beaches

The spatial variation in beach sediment characteristics can be attributed to several possible mechanisms, including the mechanical and chemical breakdown, more rapid transport of grains of one size than the other, longshore variations in wave energy, the addition or loss of sediment, and mixing of two or more distinct sediment populations (Trenhaile, 2000). During the sample collection, the wave pattern varied, wave energy varied from one day to the other, but mostly, it was observed to be high on the Eastern shores on most days of data collection. Since wave energy observation was not part of the study scope, it was never measured or monitored closely for adequate comparison.

Some of the magnetic parameters (Curie temperature, magnetic susceptibility- Π and grain sizes) measured varied from beach to beach, while others were relatively constant over the whole areas sampled. In order to have a comprehensive spatial comparison, magnetic parameters (Curie temperature, χ and grain sizes), were summarized and mapped for the major sites of study. The maps display a representative average value for each study site.

7.5.1. Comparison of magnetic ratios, mineralogy, and granulometry-spatial variation

The variation of $S_{-0.3mT}$ over the whole study area was relatively very small. In the Eastern beaches, values ranged from 0.89-1.00 with about 10% of the samples having a value of less than 0.9. For Wheatley and the Western beaches also, values ranged from 0.89-1.00. For the $S_{-0.1mT}$, there was a much wider range in the distribution. Values in the Eastern beaches ranged from 0.66-0.99, with about 90% of the samples falling between 0.66-0.75. A similar pattern of $S_{-0.1T}$ magnitude was observed in the western beaches. For the Wheatley bluff samples, there was a greater uniformity in the $S_{-0.1T}$ magnitude which ranged from 0.63-0.78 with more than 90% of the values less than 0.7. For the Wheatley beach sands, the magnitude ranged from 0.70-1.00 with a majority within 0.80-0.84 range. The distribution of S_{-1T} and $S_{-0.3T}$ in the West and East beaches not only confirms the conclusion that the magnetic mineralogy is dominated by magnetite with very little amount of hematite (Liu et al., 2003) but also shows that magnetic mineralogy was homogeneous with a roughly constant ratio of $S_{-0.1T}$ and $S_{-0.3T}$. Since the ratios were relatively uniform over Eastern and Western beaches, this suggested that the source of magnetic minerals on the Eastern beaches same and the source of sediment on the Western beaches is also the same. The Wheatley bluffs showed a relatively wider range in its $S_{-0.1T}$ values with relatively lower values than the beach samples. Therefore, the $S_{-0.1T}$ magnitude suggest that the magnetic fractions in beaches are primarily of coarse grains while the bluffs are of finer grains (Liu el, 2003), which is in agreement with the conclusion drawn earlier that the magnetic minerals are in the PSD and SD states.

As discussed previously, the dominant magnetic mineral in all the beaches was magnetite. However, the domain sizes estimated from the SIRM curves differed slightly (Figure 7.3). All areas except for the Wheatley bluffs had PSD magnetite, while Wheatley bluff had SD magnetite. For RPP, PPNP and Wheatley beaches, magnetite grain sizes all fell within ~5-25micron sizes; these areas were also comprised of PSD magnetite (Figure 7.4).

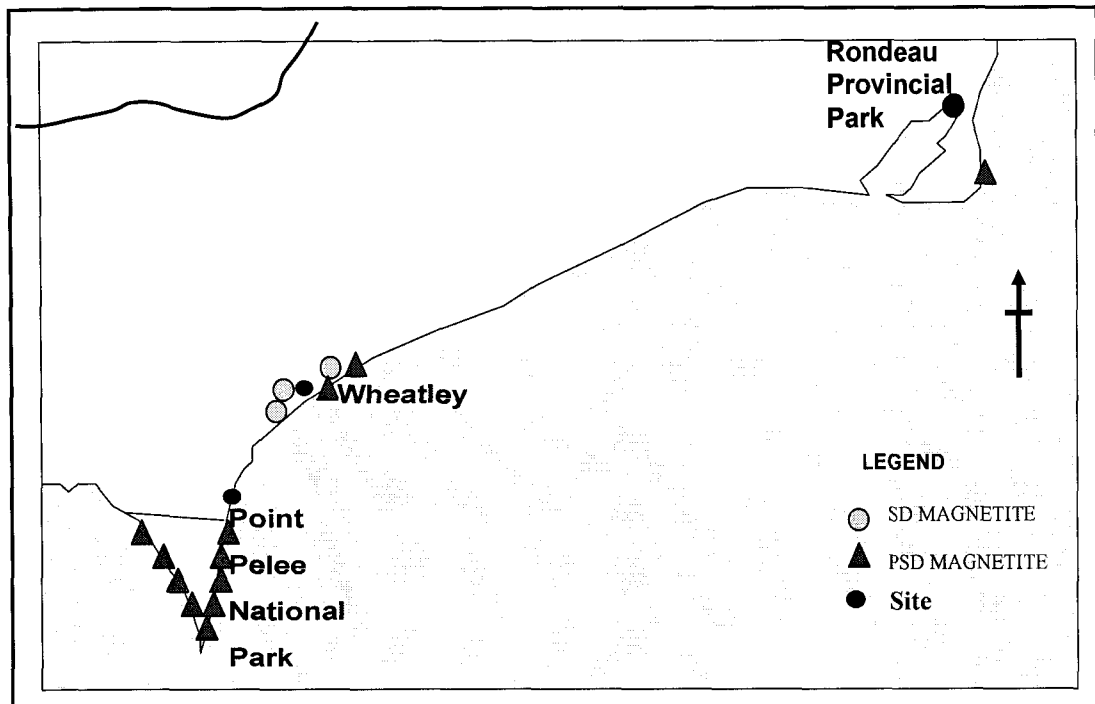


Figure 7.3: Spatial distribution of magnetic mineralogy from SIRM analysis. Samples generally falls under two categories: SD and PSD magnetite.

On the Wheatley bluffs, the grain size also varied, the majority of the samples displayed a grain size of $\sim 0.75\text{-}2\mu\text{m}$ as would be expected since they were mainly clayey material.

In terms of spatial distribution of T- χ types of curve (Figure 7.5), there were some interesting observations. All the EB and MEB samples displayed only type C curve. For the core samples from EB, there was no noticeable difference between the upper and lower sediment T- χ curves. The NEB samples displayed both type A and C curves; all surface samples in NEB displayed type C curve but the lower sediments of the core samples on NEB [080402 (middle) and 081403 (lower)] displayed a type A curve. This observation could be indicative of diagenesis of the underlying sediments (surface alteration of underlying sediment as a result of exposure to surface processes: sorting, chemical reactions or addition of sediments).

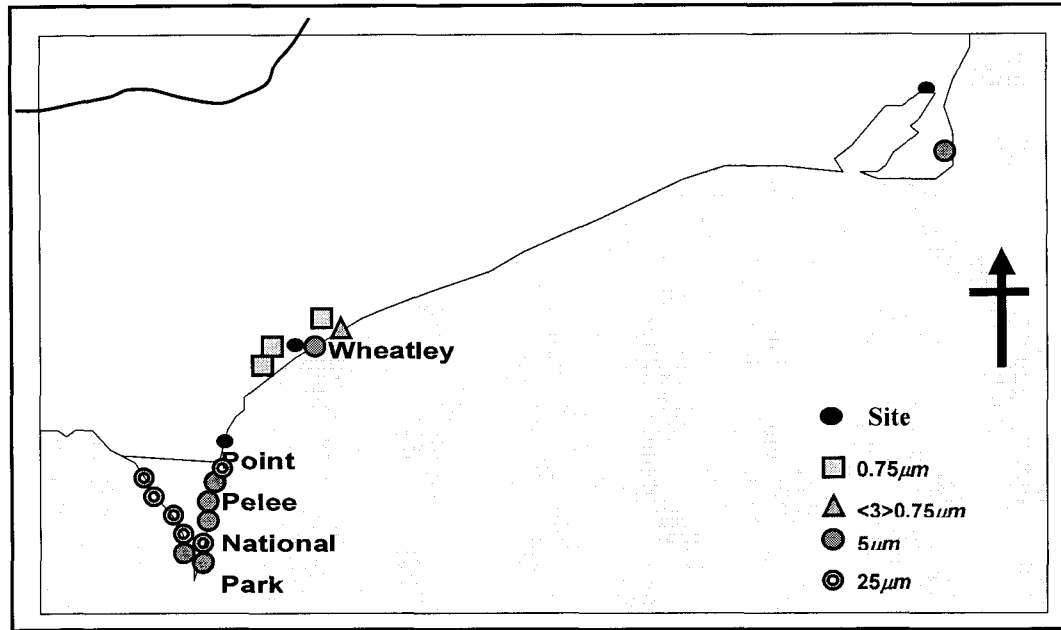


Figure 7.4: Spatial distribution of magnetic grain size from PARM analysis. There is a noticeable variation in beach sand grain size.

The SB, WB, and SH all displayed type B curves (Figure 7.5), while NWB displayed a type C curve similar to those of Eastern side beaches and RPP. A majority of the samples on the western side of the PPNP beach displayed type B T- χ curves. All of the Wheatley bluff samples displayed type A curves, and some Wheatley beach samples displayed type C curve. The single representative sample from RPP displayed a type C curve. The similarity of the T- χ curves from the RRP, EB, MEB, the top sediments of NEB, and the Wheatley beach might be an indicator of similar surface processes or an identical sediment source. The similarity of the western side beaches T- Π curves is indicative of similar sediment source and processes on the Western beaches, but distinct from those affecting the Eastern beaches.

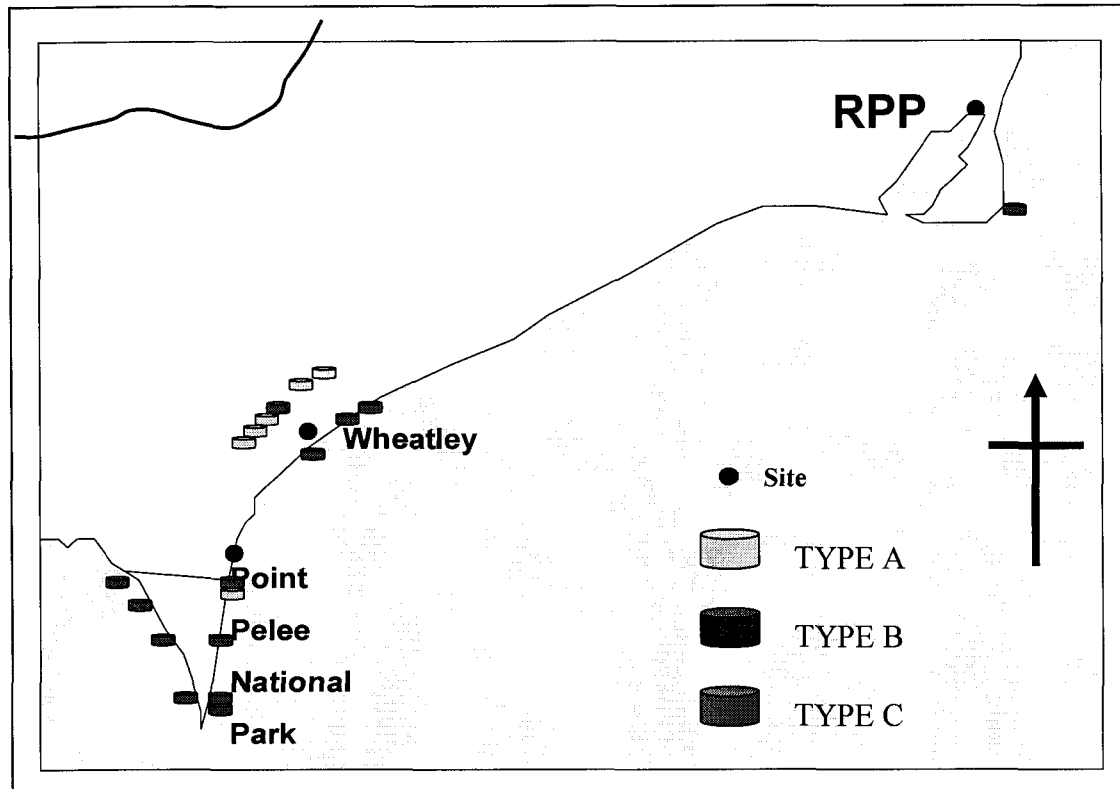


Figure 7.5.: Spatial Distribution of T- χ type curves. The stacked cylinders represent core samples, while single cylinders are surface samples.

7.5.2. Magnetic susceptibility (χ) – spatial variation

The χ (both mass and volume specific) is an indicator of ferrimagnetic mineral concentration, and also varied spatially. The highest values were observed in EB, NEB and MEB (see table 4.4; Π_{mass} spec.). The most noticeable variations were between the Eastern and Western beaches. Values in the Eastern beaches ranged from $0.42\text{-}121 \cdot 10^{-6} \text{ m}^3/\text{kg}$, while values in the Western beaches ranged from $0.42\text{-}2.64 \cdot 10^{-6} \text{ (m}^3/\text{kg)}$. In Wheatley, the χ ranged from $0.23\text{-}20.3 \cdot 10^{-6} \text{ (m}^3/\text{kg)}$. The high range was observed on the beach while the bluff showed a relatively uniform average of $\sim 0.55 \cdot 10^{-6} \text{ (m}^3/\text{kg)}$. The single sample from RPP had a value of $3.86 \cdot 10^{-6} \text{ (m}^3/\text{kg)}$.

The observed field magnetic susceptibility distribution was also consistent with sample mass specific susceptibility (Figure 7.6: the summary of field magnetic susceptibility distribution for all study areas). The field magnetic susceptibility (volume specific) taken on all beaches used for study showed its highest values in the Eastern beaches ($8888 \cdot 10^{-6} \text{ SI units}$) and lowest values were observed in the bluffs of Wheatley

($\sim 7 \times 10^{-6}$ SI units). The beach sand in Wheatley showed higher values than the bluff samples ($\sim 789 \times 10^{-6}$ SI units). Since volume specific magnetic susceptibility value is dependent on concentration (Dearing, 1994), the values from the beach samples suggest that the concentration of magnetic minerals is highest on the Eastern beaches (EB, MEB and NEB), relatively low on the Western beaches, high on Wheatley and RPP beaches, and lowest for the Wheatley Bluffs. Although concentration is low on the Wheatley bluffs, on eroding, the fine grained sediments on Wheatley bluff could easily be carried offshore leaving a higher concentration of magnetic minerals on the beach. The higher concentration on the Eastern shores could be attributed a lower amount of sediment source and lack of quartz sand because of the till clay bluffs to NE beach. While the West side have lots of sand sourced from the north western glacio-fluvial sediments. Coakley, (1977) suggested that the Point Pelee was pivoting towards the west, suggesting that erosion on the East side was occurring concurrently with a net accretion of the west side. Thus, one explanation for the variation could be that the higher rate of accretion on the West beaches might dilute the magnetic mineral concentration due to a more sand rich sediment source (the sandy bluffs on NW), and the erosion or lack of deposition on the Eastern side due to lack of sand on the NE bluffs.

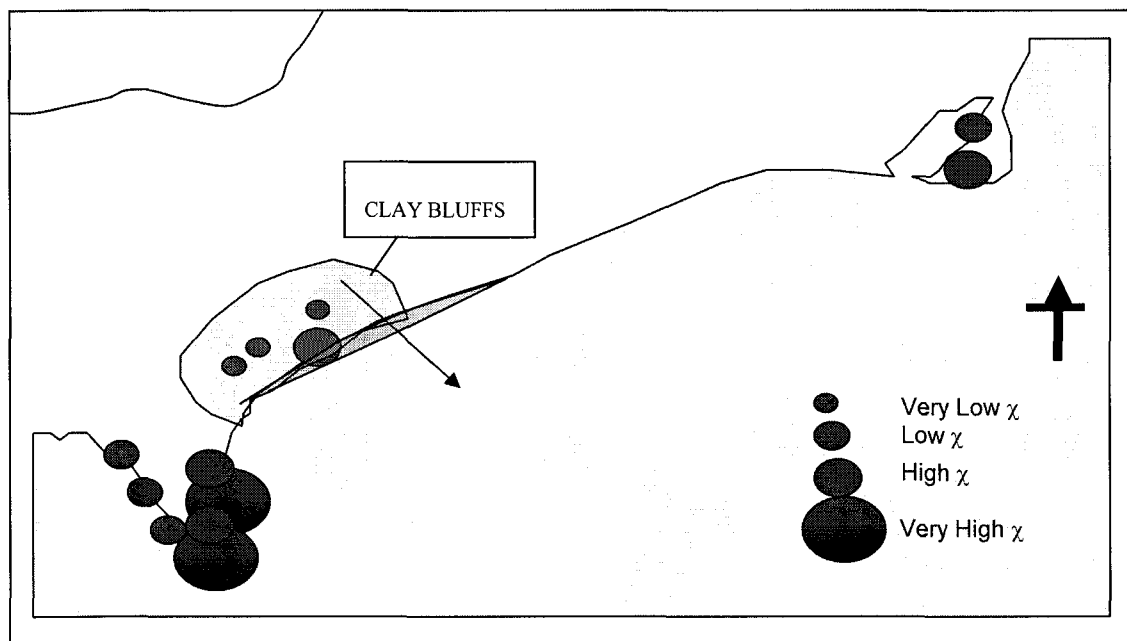


Figure 7.6: Spatial distribution of field magnetic susceptibility (volume specific) at PPNP and surrounding areas. Clay in the bluffs of Wheatley is washed into the lake, smaller grain sizes are also carried away.

The observations on the PPNP Eastern beaches and RPP, which is also a cusped foreland, actually suggest that the same process (or processes) may be in operation on the two cusped forelands. The western side of the RPP cusped foreland was not sampled because there was no apparent beach, and it was composed of marshes and bays.

7.6. Sediment transport and beach processes: an explanation for the high magnetite concentration on beaches

To explain the high concentration of magnetite on the Eastern beaches, it is necessary to understand beach processes that could cause such observation. Materials on the beach come from different sources. Most sediment is local, and sometimes transported, generally by longshore transport, from distant locations (Trenhaile, 1997). Sediments can also be obtained from materials stored in depositional features through erosion, for example, the erosion of the Wheatley bluffs can add sediments to the beaches. Sediments carried into deep water are permanently lost to the coastal system while it remains at its present level (Trenhaile, 1997).

Spatial variations in beach sediment characteristics are common in PPNP. The areas with the high concentration of magnetite are distinctly coloured on the Eastern beaches. Trenhaile (1997) attributed spatial changes in beach sediment characteristics to several possible mechanisms, including mechanical and chemical breakdown, more rapid transport of grains of one size than the other, longshore variation in wave energy, the addition and loss of sediment, and mixing of two or more distinct sediment populations.

The main magnetic mineral causing the high magnetic susceptibility on the Eastern beaches is magnetite. Magnetite is a heavy mineral, with a density of 5200kgm^{-3} . Observation shows that heavy minerals tend to concentrate locally on beaches forming bands and streaks near high tide zone (Trenhaile, 1997). Magnetite concentration found in PPNP in the Eastern beaches formed streaks and thin laminates that are observable at some points on the surface of the beach and at other points just beneath the surface. No streaks or laminates were observed on RPP beach. This observed layer of laminate under the surface is about 1cm in thickness. "Swash laminates are thought to develop as a result of the shearing of dense concentrations of coarse and fine grains by backwash. Shear sorting causes the coarser, or lighter, grains to migrate upwards into the zone of lower

shear, while finer or heavier, grains move downward, into the zone of maximum shear at the bed. Selective longshore transport of lower density minerals may also concentrate heavy minerals in erosive lag deposit” (Trenhaile, 1997). A possible explanation for the magnetite concentration and laminate in PPNP could be by shear sorting and selective longshore transport of lower density minerals and thus a concentration of high density magnetite on the beaches.

Another cusplate foreland was sampled to see if the observation on PPNP beaches held true for other cusplate forelands around Lake Erie. There was also a concentration of magnetite on the southern part of the Eastern shores of RPP, but the laminates present in some parts of PPNP were absent in this cusplate foreland. A difference in wave energy could easily cause a spatial variation between these two cusplate forelands. The similarity in the characteristics of the magnetic sediment of PPNP and those of RPP might indicate one thing, a common source rock, if the source rock is identified; the direction of longshore transport could be determined (Trenhaile, 1997).

Another factor that cannot be overlooked is the natural processes on the beaches. Trenhaile (1997) pointed to the fact that heavy minerals tend to be concentrated on beaches (as result of a tendency to be less easily transported due to its density), often forming bands or streaks near the high tide zones. LaValle et al. (2001) pointed out the fact that as a result of the continuous and accelerated shoreline erosion along the Eastern beach of PPNP, there was a sediment nourishment program instituted along the central portion of the NEB in 1979. It is possible that the sediment used for the nourishment might have had a high concentration of magnetic minerals. If this were the case, then the PPNP beaches could be the source of the high magnetic susceptibility minerals. But this is probably not be the case, as the cusplate foreland formation processes suggest sediment transport cells into the cusplate forelands and not away from the cusplate foreland (Trenhaile et al., 2000).

For the winter sediment study in PPNP, the magnetic susceptibility values on the beaches showed a similar pattern to that observed in the summer. The lower values could be attributed to the extreme cold temperature, which may have altered the instrument sensitivity.

7.7. Sediment source/origin of magnetic sediment on PPNP beaches

In order to determine if the source of the magnetic sediments was the same for all beaches, the sediment magnetic characteristics were compared. The magnetic signature of the beach sands suggested similar but not identical magnetic minerals on both the East and the West beaches. The Curie temperatures for all samples indicated magnetite, and SIRM acquisition curves indicated PSD magnetite. Both the East and the West beaches had identical SIRM acquisition plots. PARM spectra showed magnetic grain sizes of ~5 and 25 microns to be consistent in all beaches. The beaches on the eastern side had majority of its sample grain size in the 5 microns range (see Figure 7.3.), while the grain size of those on the western side were mainly in the 25 microns range; a very small percentage of the west beach samples had grain sizes in the 5 microns range. The $S_{-0.1T}$ and $S_{-0.3T}$ were also identical; almost all sediments attained more than 90% of their IRM at 300mT and greater than 70% of IRM at 100mT (Table 4.2); this indicates a dominance of low coercivity minerals on both the Eastern and Western sides of the beach, with very little contribution from high coercivity minerals. The major variation was seen in the T- χ curves. The Western beaches all showed similar curves, which were visibly different from those Eastern beaches (see Figure 7.1B). Thus, although the magnetic mineral was recognized to be magnetite, they were apparently of different compositions. This could signify different sources or alteration of minerals. The similarity of the entire Western beach T- χ curves and their distinction from the Eastern beaches suggest that the Western beaches have a different source of sediment budget. This corroborates the observation from Trenhaile et al. (2000) that the sediment budget for the Western beaches is a different source from those of the Eastern beaches.

Trenhaile et al. (2000) suggested the northern part of the NEB (Alma) as a possible source of sediment. In order to confirm this, samples from the north of Wheatley were taken and their magnetic mineralogy and granulometry was compared to those of PPNP beaches (Figures 7.3, 7.4, and 7.5). It is immediately obvious that their sediments did not have identical characteristics. The effective magnetic grain sizes determined by pARM analysis for Wheatley Bluff were between 0.75- < 2 microns, while those of PPNP beaches were between 5->25 microns. There was also a significant variation in magnetic domain sizes, determined by SIRM spectra analysis; while sediments from

PPNP fell within the PSD range, sediments from the Wheatley Bluffs fell within the SD range. Magnetic susceptibility also varied, all time low was observed in the bluff, while all time high was observed in PPNP. The reason for the variation was probably because sampling did not cover the required area (Alma) but was just in Wheatley. Since susceptibility is indicative of magnetic mineral concentration (in terms of magnetite), it can be assumed that PPNP Eastern beaches had the highest concentration of magnetic minerals and the Wheatley bluff had the lowest concentration. The samples from the north of Wheatley were mainly clayey material; therefore, the grain sizes are too small to be part of the beach sand as they are washed away and lost to the lake. Another explanation could be that after the erosion of the Wheatley bluff, smaller grain are washed into the lake, while larger magnetic grains are left on the beaches as a result of sediment sorting. Taking sediment samples further northeast may be necessary in order to ascertain the sediment (sand) source at PPNP Eastern beaches.

The observed high magnetic susceptibility in PPNP Eastern beaches, RPP and the low susceptibility on the Western beaches could be explained by the following:

- ❖ The rate of material removal (erosion) from Eastern side of the cusped forelands could be higher than those of the western side thereby causing a concentration of heavy minerals on the East sides of the cusped forelands.
- ❖ The higher concentration of magnetic material could not have resulted from the sediment nourishment program of 1978 instituted along the central portion of the Northeast beach (Lavalle et al., 2001). Since sediment transport from PPNP to RPP is not plausible.

The similar observation in PPNP and RPP could suggest two things:

- a. Similar beach processes on the cusped forelands; which could be selective longshore transport of lower density minerals and shear sorting on the beaches.
- b. The similar mineralogy (magnetite) on PPNP and RPP may suggest a similar parent source.

Right now, the processes are not clear, and one can not determine with certainty the origins of these magnetic sediments. Further investigations into outcrops around south-

western Ontario, further north of Port Alma and north of Kingsville might help in understanding sediment distribution and origin of magnetite sediments in the East side of the PPNP beaches.

7.8. Summary and conclusion

The GIS mapping of PPNP showed at a glance that the same pattern of increasing magnetic susceptibility occurred in all the Eastern beaches. The Western beaches showed a very uniform low magnetic susceptibility distribution; there were no areas of extreme highs or lows. The main aim for mapping magnetic susceptibility in PPNP was to show its distribution at a glance. This objective was partially achieved. This was because the beaches covered only a small area along the shoreline relative to the whole of PPNP. A complete mapping of PPNP may be necessary in order to view the varying magnetic susceptibility of the PPNP as a whole.

The magnetic sediment analysis from the T_C , SIRM and pARM analysis suggested that the sediments in RPP and PPNP Eastern beaches have similar magnetic sediments which are PSD magnetite with grain sizes of about 5 microns. It also suggested that the Western beach and the Eastern beach had different magnetic minerals; indicating different sediment source.

The significant different in magnetic susceptibility observed on the East beaches and the West beaches could be indicative of entirely different physical process for the two beach sides as discussed earlier. It could be indicative of varied rate of sediment budget, with the Eastern beach experiencing a faster sediment removal or lower rate of sediment deposition than the Western beaches. The high magnetic mineral concentration on the East side corroborated this conclusion that selective erosion of less dense sediment may have resulted to a concentration of magnetite. As a whole, this observation points to the fact that the East beaches might be residing at a rate faster than the West beaches.

In the Western beaches, the transects showed less variation than on the Eastern beaches. The hypothesis set to test for temporal changes in magnetic susceptibility on the beaches reveal that the field magnetic susceptibility observed on the West beaches were stable and more consistent over time than the those of the Eastern beaches. Fifty percent of the West beaches showed no significant variation from one transect to the other. While

all the East beaches showed a significant variation in beach transects, again, more intense erosion could cause this observation. The temporal variation determined from hypothesis 2 may indicate dominant short term physical process as a significant difference in magnetic susceptibility was observed on the East beaches within the summers of 2003 and 2004.

There was also a temporal variation but similar pattern in magnetic susceptibility on the East beaches. This observation could be attributed to the GPS ten meter error since there was a high transect variability, a ten meter error will cause readings to be made in areas not previously recorded. The GPS error was not very noticeable in the West beaches because transect measurements were not significantly different.

In order to conclude that the process in PPNP could be unique or common to cusped forelands in the Lake Erie region, RPP was sampled. The similar pattern of magnetic susceptibility distribution on RPP Eastern beach suggested a similar process. The west bank was not sampled because it is a swamp. The lack of samples from the west side of RPP makes it difficult to conclusively say that the two cusped forelands are identical in processes. The sediment magnetic property analysis from both cusped forelands indicated that both cusped forelands had similar magnetic minerals, this observation could be suggestive of a common parent rock source of magnetite for these two cusped forelands.

REFERENCES

- Akram H., Yoshida M., and Ahmad M.N.** 1998. "Rock magnetic properties of the late Pleistocene Loess-Paleosol deposits in the Haro River Area, Attock basin, Pakistan: Is magnetic susceptibility a proxy measure of paleoclimate?" *Earth Planets Space*, 50, 129-131, pp 129-139.
- Boyce J., Pozza M., and Morris B.** 2001. "High resolution magnetic mapping of contaminated sediments in urbanized environments." *The Leading Edge*, pp 886-890.
- Boyko T, Scholger R and Holl S.** 2001. "Magnetic susceptibility mapping of forest top Soil: reproducibility and implications for environmental monitoring." *The Geological Society of America, Environmental Geosciences*. Hynes Convention.
- Caithcheon G.G.** 1998. "The significance of various sediment magnetic mineral fractions for tracing sediment sources in Kilimicat Creek." *Elsevier: Catena*, vol. 32, pp 131-142.
- Coakley J.P.** 1977. Processes in sediment deposition and shoreline changes in the Point Pelee area, Ontario. *Fisheries and Environment Canada. Scientific Series No. 79*.
- Dearing J.A.** 1999. Environmental magnetic susceptibility: Using the Bartington MS2 System, Chi Publisher.
- Dekkers M.J.** 1997. "Environmental magnetism: an introduction." *Geology en Mijnbouw*, v76, pp 163-182.
- Duck R.W., Rowan J.S., Jenkins P.A., and Youngs I.** 2001. "A multi-method study of bedload provenance and transport pathways in an estuarine channel." *Phys. Chem. Earth (B)*, vol. 26, no 9, pp 747-752.
- Environment Systems Research Institute, Inc.** 1997. Understanding GIS the ARC/INFO method; Self Study Work Book. Redlands, CA, U.S.A.
- Environment Systems Research Institute, Inc.** 2001. Using ArcGIS Geostatistical Analyst. Redlands, CA, U.S.A.
- Freund J.E.** 1960. Modern Elementary Statistic. 2ed. Prentice Hall Inc.
- Gruszowski K.E., Foster I.D.L., Lees J.A., and Charlesworth S.M.** 2003. "Sediment Source and transport pathways in a rural catchment, Herefordshire, UK." *Hydrological Process*. 17, Issue 13 pp2665-2681.

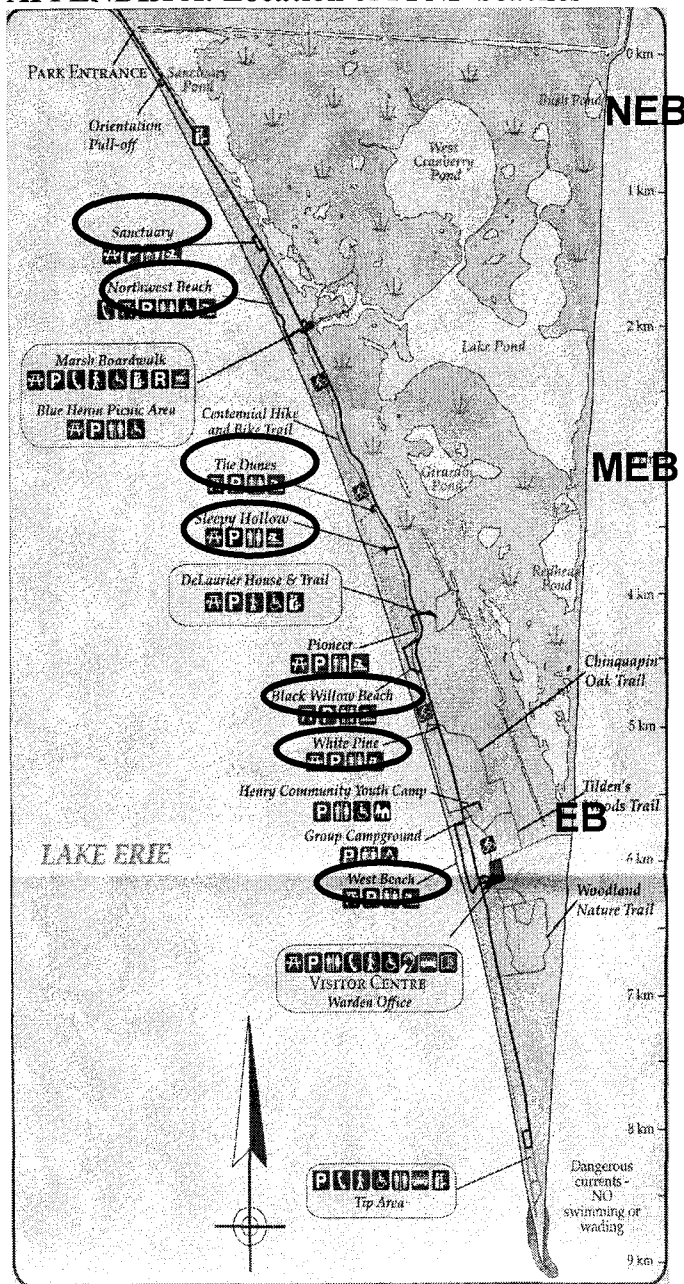
- Guo B., Zhu R., Bai L. and Florindo F.** 2001. "Rock magnetic properties of a loess-paleosol couple along an N-S transect in the chinese loess plateau." *Science in China (Series D)*, vol. 44, no. 12, pp1099-1108.
- Hanesch M. and Schoger R.** 2002. "Mapping of road side pollution." *Journal of Geochemical Exploration*, vol. 42, issue. 8, pp857-870.
- Harrison R.J., and Putnis A.** 1999. "Determination of the mechanism of cation ordering in magnesioferrite ($MgFe_2O_4$) from the time and temperature-dependence of magnetic susceptibility". *Phys Chem Minerals*, 26:322-332.
- Hoffman V., Knab M., and Appel E.** 1999. "Magnetic susceptibility mapping of road side pollution." *Journal of Geochemical Exploration*, vol. 66. , pp313 –326.
- Hrouda F., Muller P, and Hanak J.** 2003. "Repeated progressive heating in susceptibility vs. temperature investigation: a new palaeotemperature indicator?" *Physics and Chemistry of the Earth*, 28, pp 653-657.
- Hrouda F. and Zapletal K.** 2003. "Thermomagnetic curves of selected minerals and monomineralic fractions." AGICO Print No. 24.
- Jackson M., Gruber W., Marvin J. and Banajee S.K.** 1988. "Partial anhysteresis remanence and its anisotropy: application and grainsize-dependence." *Geophysical Research Letters*, vol. 15, no. 5, pp 440-443.
- Konty A. and De Wall H.** 2000. "Case studies on the use of temperature-dependent susceptibility for the characterisation of magneteto-mineralogical changes during metamorphism." *Phys. Chem. Earth (A)*, vol. 25, no. 5, pp 421-429.
- Konty A., De Wall H., Sharp T.G., and Posfai M.** 2000. "Mineralogy and magnetic behaviour of pyrrhotite from a 260°C section at the KTB drilling site, Germany." *American Mineralogist*, vol. 85, pp1416-1427.
- Kwon H.W.** 2002. Experimental study of Hopkinson effect in HDDR-treated $Nd_{15}Fe_{77}B_8$ and $Sm_2Fe_{17}N_x$ materials. *Elsevier:Journal of Magnetism and Magnetic Materials*, vol. 239, pp447-449.
- LaValle P.D., Lakhani V.C., and Trenhaile A.S.** 2001. "Space-time series modelling of beach and shoreline data." *Elsevier-Environmental Modelling and Software*, vol. 16, pp 299-307.

- Liu J, Zhu R, and Li G.** 2003. "Rock magnetic properties of the fine-grained sediment on the outer shelf of the East China Sea: implication for provenance. *ELSEVIER: MARINE GEOLOGY*, v193, pp 195-206.
- Lo C.P., and Yeung A.K.W.** 2002. Concepts and Techniques of Geographic Information Systems, Prentice Hall.
- McCubbin D, Leonard K.S., Maher B.A., and Hamiton E.I.** 2000. "Association of ^{210}Pb (^{210}Pb), $^{239+240}\text{Pu}$ and ^{241}Am with different mineral fractions of a beach sand at seascale Cumbria, UK." *ELSEVIER: The Science of the Total Environment*, vol. 254, pp1-15.
- Moore V.G.** 1978. The Penguin Dictionary of Geography. Penguin Books LTD.
- Morgan M.K.** 2002. "Soil Magnetic Susceptibility and Pollution Mapping of Camp Henry in Point Pelee National park." Earth science, University of Windsor.
- Moskowitz B.M., Frankel R.B., and Bazylnski D.A.** 1993. "Rock magnetic criteria for the detection of biogenic magnetite." *EPSL*, vol. 120, pp 283-300.
- Ollier C. (2ed)** 1984. Weathering, Longman Group Ltd.
- Peters C. and Dekkers M.J.** 2003. Selected room temperature magnetic parameters as a function of mineralogy, concentration and grain size. *Phys. and Chem. Of the Earth*, vol. 28, pp659-667.
- Reynolds J.M.** 1998. An Introduction to applied and Environmental Geophysics, John Wiley.
- Richter C., Blum, P., and Rohl U.** 2001. "Data report: magnetic properties and XRF scanner data of site 1075 (Lower Congo Basin)." *Proceedings of Ocean Drilling Program, Scientific Result*, vol. 175, pp1-11.
- Richer C., Valet J.P., and Solheid R.A.** 1997. "Rock magnetic properties of sediments from Ceara Rise (site 929): implications for the origin of magnetic susceptibility signal." *Proceedings of Ocean Drilling Program, Scientific Result*, pp169-179.
- Royall D.** 2001. "Use of mineral magnetic measurements to investigate soil erosion and sediment delivery in a small agricultural catchment in limestone terrain." *Catena*, vol. 46, pp15-34.

- Rukavina N.A., and St. Jacques D.A.** 1978. "Lake Erie nearshore sediment, Point Pelee to Port Burwell, Ontario." *Fisheries and Environment Canada. Scientific Series No. 99.*
- Salome L. and Meynaider L.** 2004. "Magnetic properties of rivers sands and rocks from Martinique island: tracers of weathering?" *Phys. and Chem. of the Earth, vol. 2,* pp 933-945.
- Schibler L.; Boyko T.; Ferdyn M.; Gadja B.; Holl S.; Jordanova N.; Rosler W.; and Team M.** 2002. "Top soil magnetic susceptibility mapping: data reproducibility and compatibility, measurement strategy." *Studia Geophysica et Geodaetica,* vol. 46, issue 1, pp 43-57.
- Solheid P.A., Banerjee S.K., Richer C and Valet J.P.** 1997. "High-resolution rock magnetic study of Ceara Rise sediments at site 925." *Proceedings of Ocean Drilling Program, Scientific Result,* vol. 154, pp181-186.
- Solheid P.A., and Yamazaki T.** 2001. "Data report: evidence of the dissolution of fine grained magnetic minerals from measurements of natural and laboratory-induced remanent magnetizations at site 1077." *Proceedings of Ocean Drilling Program: Scientific Result,* vol. 175, pp1-10.
- Stoner J.S., Richer C, and Roberts A.P.** 1998. Data report: high resolution study of magnetic properties of sapropel- bearing sediments from sites 966, 967, and 969, Eastern Mediterranean Sea." *Proceedings of Ocean Drilling Program, Scientific Result,* vol. 160,- pp75-82.
- Symons D.T.A and Cioppa M.T.** 2000. "Crossover plots: A useful method for plotting SIRM data in paleomagnetism." *Geophysical Research letters,* vol. 27, no. 112, pp1779-1782.
- Termier H. and Termier G,** 1963. *Erosion and Sedimentation.* D. Van Nostrand, London.
- Thompson R., and Oldfield F.,** 1986. *Environmental Magnetism.* Allen and Unwin.
- Torii M., Lee T.Q., Fukuma K., Mishima T., Yamazaki T., Oda H., and Ishikawa N. 2001. "Mineral magnetic study of the Kaklimakan desert sands and its relevance to the Chinese loess." *Geophys. J. Int., vol. 146,* pp416-424.

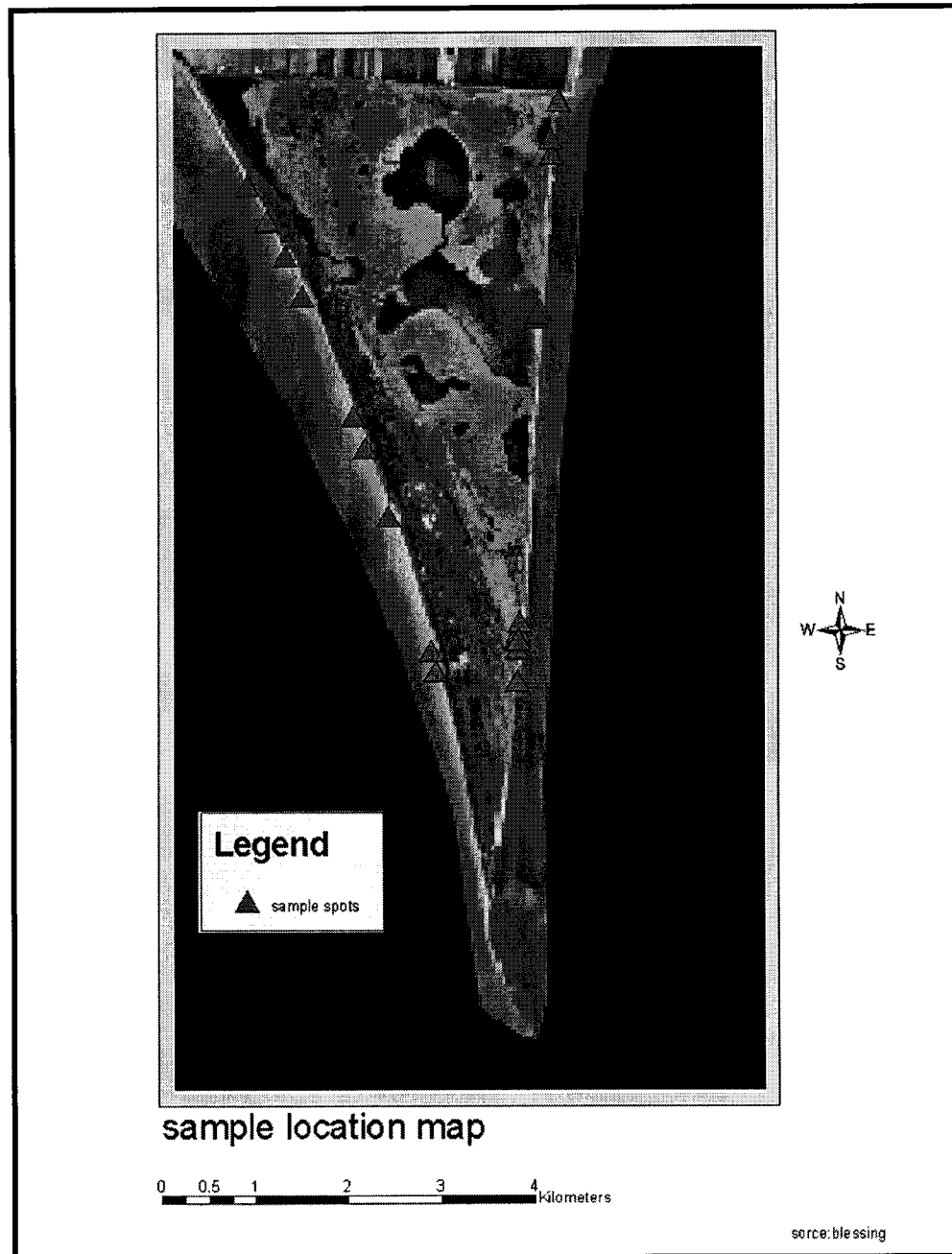
- Trenhaile A.S.** 1997. Coastal Dynamics and Landforms. Oxford University Press, Oxford.
- Trenhaile A.S., Lavallo P.D., and Lakhan V.C.** 2000. "Canadian landform examples- 39. Point Pelee-A Large Cuspate Foreland on Lake Erie." *The Canadian Geographer*, vol. 44, no. 2, pp191-195.
- Varga L.K., Franco V., Kakay A Kovacs G., and Mazaleyrat F.** 2001. "The role of internal and external demagnetizing effects in nanocrystalline alloys." *IEEE Transaction on Magnetics*, vol. 37, no. 4, pp 2229-2231.
- Van Oorschot I.H.M.** 2001. "Chemical distinction between lithogenic and pedogenic iron oxides in environmental magnetism. A search for the perfect solution." *Geologica Ultraiectina*, 208, pp 73-89.
- Ventura E, Nearing M.A., and Norton D.** 2001. "Developing a Magnetic Tracer to Study Soil Erosion." *Catena*, vol. 43, pp 277-291.
- Wasson R.J., Caitcheon g., Murray A.S., McCulloch M. and Quade J.** 2002. "Sourcing sediment using multiple tracers in the catchment of Lake Argyle, northwestern Australia." *Environmental Management*, vol. 29, no. 5, pp 634-646.
- Weiers R. M.** 1991. Introduction to Business Statistics, the Dryden Press.
- Yu Y., Dunlop D.J., and Ozdemir O.** 2002. "Partial anhysteretic remanent magnetisation in magnetite: reciprocity." *Journals of Geophysical Research*, vol. 107, no. B10, Pp1-9.
- Zhu R., Kazansky A., Matasova G., Guo B., Zykina V., Petrosky E., and Jordanova N.** 2000. "Rock-magnetic investigation of Siberia loess and its implication." *Chinese Science Bulletin*, v45, no 23, pp2182-2197.

APPENDIX A: Location of PPNP beaches



LEGEND	
SB-	Sanctuary beach
NWB-	Northwest beach
D-	Dunes
SH-	Sleepy Hollow
BW-	Black Willow
WP-	White Pine
WB-	West beach
NEB-	Northeast beach
MEB-	Middle-east beach
EB-	East beach

APPENDIX B: Points where sediment samples were collected in PPNP



APPENDIX C: Parameters used for calculating magnetic ratios

	MASS (g)FOR CALCULATING DENSITY
MEB	14.2
RONDEAU	9.8
WHEATLEY FINE	10
WESTB	10.4
EB	15
WHEATLEYCCOARSE	7.2
Volume	8cc

APENDIX D: Test of hypotheses

6.1 Hypothesis (1)

NULL

There is no significant difference in the susceptibility (χ) observed on the Eastern Beaches and those observed on the Western Beaches.

$H_0: 0\chi_{EB}=0\chi_{MED}=0\chi_{NEB}=0\chi_{SB}=0\chi_{SH}=0\chi_{WP}=0\chi_{D}=0\chi_{WB}=0\chi_{SH}=0\chi_{BW}$ (2003/04)

ALTERNATE

There is a significant difference in the susceptibility (χ) observed on the Eastern Beaches and those observed on the Western Beaches.

$H_1: 0\chi_{EB} \neq 0\chi_{MED} \neq 0\chi_{NEB} \neq 0\chi_{SB} \neq 0\chi_{SH} \neq 0\chi_{WP} \neq 0\chi_{D} \neq 0\chi_{WB} \neq 0\chi_{SH} \neq 0\chi_{BW}$

Magnetic susceptibility values from all beaches grouped into western (SH, NWB, BW, DUNES, SB, WP and WB) and eastern beaches (EB, MEB and NEB) gave the test statistics result below:

Kruskal-Wallis Test on All Ten Beaches (03)

1474 cases were used
2 cases contained missing values

Kruskal-Wallis Test on 10BEACHES03

C39	N	Median	Ave Rank	Z
1	646	68.50	428.8	-24.59
2	828	238.75	978.3	24.59
Overall	1474		737.5	

H = 604.80 DF = 1 P = 0.000

H = 604.81 DF = 1 P = 0.000 (adjusted for ties)

DECISION

Computed H = 604.81

Theoretical H = 6.635

Since computed H is higher than theoretical H, we do not accept the null hypothesis that states: "There is no significant difference in the susceptibility (χ) observed on the Eastern Beaches and those observed on the Western Beaches" for summer 2003.

Kruskal-Wallis Test: ALL TEN BEACHES 04

Kruskal-Wallis Test on 10BEACHES04

C37	N	Median	Ave Rank	Z
1	364	172.75	1045.7	15.16
2	203	314.00	1113.9	13.02
3	262	38.75	464.5	-11.69
4	151	62.00	639.2	-3.25
5	59	41.00	369.0	-6.88
6	32	66.00	712.4	-0.47
7	43	56.50	539.5	-3.21
8	54	62.00	627.5	-2.08
9	182	58.00	597.7	-5.00
10	144	55.50	564.9	-5.34
Overall	1494		747.5	

H = 550.07 DF = 9 P = 0.000

H = 550.09 DF = 9 P = 0.000 (adjusted for ties)

DECISION

COMPUTED H = 550.09

THEORETICAL H = 21.666

Therefore, we do not accept the null hypothesis that states: “There is no significant difference in the susceptibility (χ) observed on the Eastern Beaches and those observed on the Western Beaches” for summer 2004.

6.2 Hypothesis (2)

NULL

There is no significant seasonal variation in magnetic susceptibility (χ) on the beaches.

H₀: $0\chi_{(Bi)} \text{ May03} = 0\chi_{(Bi)} \text{ May04}$

ALTERNATE

There is no significant seasonal variation in magnetic susceptibility (χ) on the

H₁: $0\chi_{(Bi)} \text{ May03} \neq 0\chi_{(Bi)} \text{ May04}$

(Where Bi = EB, MEB ...WB)

Magnetic susceptibility data from two seasons (summer 2003 and 2004) for individual beaches were used for these test statistics. Below are the test statistics and results.

Kruskal-Wallis Test: MEB0304

Kruskal-Wallis Test on MEB0304

C2	N	Median	Ave Rank	Z
1	203	1480.0	250.4	8.05
2	203	328.5	156.6	-8.05
Overall	406		203.5	

H = 64.84 DF = 1 P = 0.000

H = 64.84 DF = 1 P = 0.000 (adjusted for ties)

DECISION

COMPUTED H =64.84

THEORETICAL H = 6.635

Therefore, we do not accept the null hypothesis that states: “There is no significant seasonal variation in magnetic susceptibility (χ) on MEB.”

Kruskal-Wallis Test: EB0304

Kruskal-Wallis Test on EB0304

C4	N	Median	Ave Rank	Z
1	364	200.5	384.8	2.61
2	364	172.8	344.2	-2.61
Overall	728		364.5	

H = 6.79 DF = 1 P = 0.009

H = 6.79 DF = 1 P = 0.009 (adjusted for ties)

DECISION

COMPUTED H = 6.79

THEORETICAL H = 6.635

Theoretical H is lower than computed H, therefore, we do not accept the null hypothesis that states: "There is no significant seasonal variation in magnetic susceptibility (χ) on EB."

Kruskal-Wallis Test: WB0304

Kruskal-Wallis Test on WB0304

C6	N	Median	Ave Rank	Z
1	151	74.00	177.6	5.20
2	151	62.00	125.4	-5.20
Overall	302		151.5	

H = 27.05 DF = 1 P = 0.000
H = 27.06 DF = 1 P = 0.000 (adjusted for ties)

DECISION

COMPUTED H =27.05

THEORETICAL H = 6.635

Computed H is greater than theoretical H, therefore, we do not accept the null hypothesis that states: "There is no significant seasonal variation in magnetic susceptibility (χ) on WB."

Kruskal-Wallis Test: SB0304

Kruskal-Wallis Test on SB03

C8	N	Median	Ave Rank	Z
1	188	61.50	192.2	0.66
2	188	58.00	184.8	-0.66
Overall	376		188.5	

H = 0.44 DF = 1 P = 0.507
H = 0.44 DF = 1 P = 0.507 (adjusted for ties)

DECISION

COMPUTED H =0.44

THEORETICAL H = 6.635

Since computed H is less than theoretical H, we do not reject the null hypothesis that states: "There is no significant seasonal variation in magnetic susceptibility (χ) on SB."

Kruskal-Wallis Test: NEB0304

Kruskal-Wallis Test on NEB0304

C10	N	Median	Ave Rank	Z
1	262	118.00	341.1	11.89
2	262	39.25	183.9	-11.89

Overall 524 262.5

H = 141.34 DF = 1 P = 0.000

H = 141.34 DF = 1 P = 0.000 (adjusted for ties)

DECISION

COMPUTED H = 141.34

THEORETICAL H = 6.635

Since computed H is greater than theoretical H, we do not accept the null hypothesis that states: "There is no significant seasonal variation in magnetic susceptibility (χ) on NEB."

Kruskal-Wallis Test: WP0304

Kruskal-Wallis Test on WP0304

C14	N	Median	Ave Rank	Z
1	59	49.00	64.8	1.68
2	59	41.00	54.2	-1.68
Overall	118		59.5	

H = 2.83 DF = 1 P = 0.093

H = 2.83 DF = 1 P = 0.093 (adjusted for ties)

DECISION

COMPUTED H = 2.83

THEORETICAL H = 6.635

Since computed H is less than theoretical H, we do not reject the null hypothesis that states: "There is no significant seasonal variation in magnetic susceptibility (χ) on WP."

Kruskal-Wallis Test: BW0304

Kruskal-Wallis Test on BW0304

C16	N	Median	Ave Rank	Z
1	32	87.00	39.8	3.12
2	32	66.00	25.2	-3.12
Overall	64		32.5	

H = 9.75 DF = 1 P = 0.002

H = 9.75 DF = 1 P = 0.002 (adjusted for ties)

DECISION

COMPUTED H = 9.75

THEORETICAL H = 6.635

Since computed H is greater than theoretical H, we do not accept the null hypothesis that states: "There is no significant seasonal variation in magnetic susceptibility (χ) on BW."

Kruskal-Wallis Test: NW0304

Kruskal-Wallis Test on NW0304

C18	N	Median	Ave Rank	Z
1	144	63.00	150.5	1.23
2	144	55.50	138.5	-1.23

Overall 288 144.5

H = 1.51 DF = 1 P = 0.219

H = 1.51 DF = 1 P = 0.219 (adjusted for ties)

DECISION

COMPUTED H = 1.51

THEORETICAL H = 6.635

Since computed H is less than theoretical H, we do not reject the null hypothesis that states: "There is no significant seasonal variation in magnetic susceptibility (χ) on NW."

Kruskal-Wallis Test: SH0304

Kruskal-Wallis Test on SH03

C20	N	Median	Ave Rank	Z
1	54	88.50	71.9	5.77
2	54	62.00	37.1	-5.77
Overall	108		54.5	

H = 33.32 DF = 1 P = 0.000

H = 33.33 DF = 1 P = 0.000 (adjusted for ties)

DECISION

COMPUTED H = 33.32

THEORETICAL H = 6.635

Since computed H is greater than theoretical H, we do not accept the null hypothesis that states: "There is no significant seasonal variation in magnetic susceptibility (χ) on SH."

Kruskal-Wallis Test: DUNES0304

Kruskal-Wallis Test on DUNES03

C22	N	Median	Ave Rank	Z
1	43	83.50	57.8	5.29
2	43	56.50	29.2	-5.29
Overall	86		43.5	

H = 28.03 DF = 1 P = 0.000

H = 28.04 DF = 1 P = 0.000 (adjusted for ties)

DECISION

COMPUTED H = 28.04

THEORETICAL H = 6.635

Since computed H is greater than theoretical H, we do not accept the null hypothesis that states: "There is no significant seasonal variation in magnetic susceptibility (χ) on DUNES."

6.3 Hypothesis (3)

NULL

There is no significant difference in susceptibility (χ) within the individual beach transects.

ALTERNATE

There is a significant difference in susceptibility (χ) within the individual beach transects. To test for this hypothesis, transects from each beach were compared within individual beach; data from same transect were treated as a group. Below are the test statistics and the results for each beach in the two seasons considered.

Kruskal-Wallis Test: EB03

Kruskal-Wallis Test on EB03

C11	N	Median	Ave Rank	Z
1	25	235.5	177.9	-0.20
2	27	176.5	173.2	-0.45
3	30	244.3	184.4	0.13
4	31	307.5	213.5	1.75
5	31	545.5	216.5	1.92
6	30	168.3	177.6	-0.24
7	31	181.5	192.6	0.59
8	24	137.5	151.4	-1.48
9	20	200.3	170.9	-0.49
10	19	434.5	200.7	0.80
11	26	387.5	240.3	2.94
12	23	111.5	137.2	-2.12
13	46	151.8	141.6	-2.79
Overall	363		182.0	

H = 28.67 DF = 12 P = 0.004
H = 28.67 DF = 12 P = 0.004 (adjusted for ties)

DECISION

COMPUTED H = 28.67

THEORETICAL H = 26.217

Computed H exceeds the theoretical H, there, we do not accept the null hypothesis which states: "There is no significant difference in susceptibility (χ) within the individual beach transects (EB03)."

Kruskal-Wallis Test: EB04 Transects

Kruskal-Wallis Test on EB04

C8	N	Median	Ave Rank	Z
1	26	98.50	110.7	-3.61
2	27	66.50	109.6	-3.74
3	30	131.50	132.3	-2.73
4	31	123.00	138.5	-2.43
5	31	150.50	144.8	-2.09
6	30	192.00	198.3	0.86
7	31	417.00	209.2	1.48
8	24	132.25	164.3	-0.88
9	20	662.00	257.0	3.26
10	19	189.50	209.5	1.15
11	26	1476.25	291.4	5.48
12	23	123.00	205.3	1.07
13	46	510.75	218.4	2.47
Overall	364		182.5	

H = 90.22 DF = 12 P = 0.000
H = 90.22 DF = 12 P = 0.000 (adjusted for ties)

DECISION

COMPUTED H = 90.22

THEORETICAL H = 26.217

Computed H exceeds the theoretical H, there, we do not accept the null hypothesis which states: "There is no significant difference in susceptibility (χ) within the individual beach transects (EB04)."

Kruskal-Wallis Test: NEB03 Transects

Kruskal-Wallis Test on NEB03

C17	N	Median	Ave Rank	Z
1	9	246.50	163.8	1.33
2	9	241.00	162.0	1.25
3	9	260.00	179.9	1.98
4	8	263.25	169.6	1.47
5	9	77.50	89.1	-1.70
6	9	76.00	84.1	-1.90
7	10	68.50	77.8	-2.27
8	15	98.00	151.9	1.10
9	16	66.75	109.6	-1.17
10	17	53.50	84.8	-2.61
11	13	49.50	43.7	-4.28
12	11	189.50	144.2	0.59
13	14	88.00	122.9	-0.41
14	16	90.00	126.3	-0.26
15	15	156.00	156.4	1.34
16	15	162.00	159.1	1.48
17	15	241.00	167.5	1.93
18	16	239.25	168.7	2.06
19	18	186.25	146.8	0.92
20	17	117.50	117.3	-0.77
Overall	261		131.0	

H = 59.67 DF = 19 P = 0.000
H = 59.67 DF = 19 P = 0.000 (adjusted for ties)

DECISION

COMPUTED H = 59.67

THEORETICAL H = 36.191

Computed H exceeds the theoretical H, there, we do not accept the null hypothesis which states: "There is no significant difference in susceptibility (χ) within the individual beach transects (NEB03)."

Kruskal-Wallis Test: NEB04

Kruskal-Wallis Test on NEB04

C15	N	Median	Ave Rank	Z
1	9	33.50	85.9	-1.84
2	9	48.50	159.4	1.12
3	9	45.50	151.7	0.81
4	8	53.50	146.2	0.56

5	9	35.00	108.5	-0.93
6	9	49.50	156.1	0.99
7	10	99.25	175.0	1.85
8	15	178.00	216.5	4.48
9	16	105.50	198.5	3.65
10	17	129.50	191.7	3.39
11	13	84.00	183.7	2.55
12	11	30.50	93.1	-1.72
13	14	30.00	98.7	-1.66
14	16	36.25	120.8	-0.58
15	15	34.00	115.4	-0.85
16	15	28.50	84.9	-2.45
17	15	30.50	90.4	-2.16
18	16	34.75	98.6	-1.79
19	18	28.25	83.5	-2.79
20	18	34.50	96.0	-2.06
Overall	262		131.5	

H = 89.49 DF = 19 P = 0.000

H = 89.51 DF = 19 P = 0.000 (adjusted for ties)

DECISION

COMPUTED H = 89.51

THEORETICAL H = 36.191

Computed H exceeds the theoretical H, there, we do not accept the null hypothesis which states: "There is no significant difference in susceptibility (χ) within the individual beach transects (NEB04)."

Kruskal-Wallis Test: MEB03 Transects

Kruskal-Wallis Test on MEB03

C19	N	Median	Ave Rank	Z
1	15	2288.5	120.9	1.30
2	12	1155.3	88.1	-0.85
3	42	3192.3	146.6	5.53
4	36	1394.8	101.6	-0.04
5	38	581.0	68.2	-3.94
6	18	2591.8	113.4	0.87
7	18	1403.5	81.6	-1.55
8	24	963.3	79.9	-1.96
Overall	203		102.0	

H = 45.35 DF = 7 P = 0.000

H = 45.35 DF = 7 P = 0.000 (adjusted for ties)

DECISION

COMPUTED H = 45.35

THEORETICAL H = 18.475

Computed H exceeds the theoretical H, there, we do not accept the null hypothesis which states: "There is no significant difference in susceptibility (χ) within the individual beach transects (MEB03)."

Kruskal-Wallis Test: MEB04 Transects

Kruskal-Wallis Test on MEB03

C13	N	Median	Ave Rank	Z
1	15	357.5	101.2	-0.06
2	12	530.5	111.5	0.57

3	42	1937.0	158.3	6.97
4	36	334.0	92.4	-1.08
5	38	256.0	90.1	-1.39
6	18	291.5	71.5	-2.31
7	18	148.8	53.6	-3.66
8	24	268.8	91.8	-0.91
Overall	203		102.0	

H = 59.23 DF = 7 P = 0.000
H = 59.23 DF = 7 P = 0.000 (adjusted for ties)

DECISION

COMPUTED H = 59.23

THEORETICAL H = 18.475

Computed H exceeds the theoretical H, there, we do not accept the null hypothesis which states: "There is no significant difference in susceptibility (χ) within the individual beach transects (MEB04)."

Kruskal-Wallis Test: WB03 Transects

Kruskal-Wallis Test on wb01

C2	N	Median	Ave Rank	Z
1	16	75.00	75.1	-0.09
2	16	67.00	54.8	-2.05
3	16	69.25	59.7	-1.58
4	16	67.25	71.9	-0.40
5	17	80.50	87.9	1.20
6	17	81.50	87.6	1.16
7	17	73.50	62.9	-1.32
8	19	68.00	70.2	-0.62
9	17	94.50	112.1	3.61
Overall	151		76.0	

H = 22.05 DF = 8 P = 0.005
H = 22.06 DF = 8 P = 0.005 (adjusted for ties)

DECISION

COMPUTED H = 22.05

THEORETICAL H = 20.090

Computed H exceeds the theoretical H, there, we do not accept the null hypothesis which states: "There is no significant difference in susceptibility (χ) within the individual beach transects (WB03)."

Kruskal-Wallis Test: WB04 Transects

Kruskal-Wallis Test on wb04

C5	N	Median	Ave Rank	Z
1	16	62.50	73.2	-0.27
2	16	53.00	61.2	-1.44
3	16	56.50	70.5	-0.53
4	16	54.00	46.3	-2.87
5	17	54.00	56.7	-1.93
6	17	75.00	92.9	1.69
7	17	79.00	95.6	1.96

8	19	71.00	90.6	1.55
9	17	74.00	92.3	1.63
Overall	151		76.0	

H = 23.26 DF = 8 P = 0.003
H = 23.26 DF = 8 P = 0.003 (adjusted for ties)

DECISION

COMPUTED H = 23.26
THEORETICAL H = 20.090

Computed H exceeds the theoretical H, there, we do not accept the null hypothesis which states: “There is no significant difference in susceptibility (χ) within the individual beach transects (WB04). “

Kruskal-Wallis Test: WP03 Transects

Kruskal-Wallis Test on wp03

C8	N	Median	Ave Rank	Z
1	17	60.50	31.4	0.38
2	15	50.00	30.4	0.11
3	14	38.50	26.7	-0.82
4	13	49.00	31.3	0.30
Overall	59		30.0	

H = 0.70 DF = 3 P = 0.874
H = 0.70 DF = 3 P = 0.874 (adjusted for ties)

DECISION

COMPUTED H = 0.70
THEORETICAL H = 11.345

Computed H is less than theoretical H, there, we do not reject the null hypothesis which states: “There is no significant difference in susceptibility (χ) within the individual beach transects (MEB03). “

Kruskal-Wallis Test: WP04 Transects

Kruskal-Wallis Test on wp04

C10	N	Median	Ave Rank	Z
1	17	40.00	26.6	-0.95
2	15	36.50	29.1	-0.23
3	14	51.75	34.9	1.22
4	13	40.50	30.1	0.03
Overall	59		30.0	

H = 1.82 DF = 3 P = 0.610
H = 1.82 DF = 3 P = 0.610 (adjusted for ties)

DECISION

COMPUTED H = 1.82
THEORETICAL H = 11.345

Computed H exceeds the theoretical H, there, we do not reject the null hypothesis which states: "There is no significant difference in susceptibility (χ) within the individual beach transects (WP04)."

Kruskal-Wallis Test: BW03 Transects

Kruskal-Wallis Test on bw03

C12	N	Median	Ave Rank	Z
1	13	97.50	19.8	1.65
2	9	89.00	18.4	0.73
3	10	71.25	10.5	-2.46
Overall	32		16.5	

H = 6.16 DF = 2 P = 0.046
H = 6.17 DF = 2 P = 0.046 (adjusted for ties)

DECISION

COMPUTED H = 6.17
THEORETICAL H = 9.210

Computed H is less than the theoretical H, there, we do not reject the null hypothesis which states: "There is no significant difference in susceptibility (χ) within the individual beach transects (BW03)."

Kruskal-Wallis Test: BW04

Kruskal-Wallis Test on bw04

C14	N	Median	Ave Rank	Z
1	13	65.50	15.0	-0.73
2	9	88.00	24.2	2.91
3	10	59.75	11.5	-2.05
Overall	32		16.5	

H = 9.31 DF = 2 P = 0.010
H = 9.32 DF = 2 P = 0.009 (adjusted for ties)

DECISION

COMPUTED H = 9.31
THEORETICAL H = 9.210

Computed H is greater than the theoretical H, there, we do accept the null hypothesis which states: "There is no significant difference in susceptibility (χ) within the individual beach transects (BW04)."

Kruskal-Wallis Test: DUNES03 Transects

Kruskal-Wallis Test on d03

C16	N	Median	Ave Rank	Z
1	22	82.50	22.1	0.05
2	11	89.00	23.4	0.42
3	10	78.75	20.3	-0.49

Overall 43 22.0

H = 0.31 DF = 2 P = 0.855

H = 0.31 DF = 2 P = 0.855 (adjusted for ties)

DECISION

COMPUTED H = 0.31

THEORETICAL H = 9.210

Computed H is less than the theoretical H, there, we do not reject the null hypothesis which states: "There is no significant difference in susceptibility (χ) within the individual beach transects (DUNES03)."

Kruskal-Wallis Test: DUNES04 Transects

Kruskal-Wallis Test on d04

C18	N	Median	Ave Rank	Z
1	22	60.75	23.5	0.83
2	11	68.00	24.9	0.89
3	10	42.00	15.4	-1.90
Overall	43		22.0	

H = 3.69 DF = 2 P = 0.158

H = 3.69 DF = 2 P = 0.158 (adjusted for ties)

DECISION

COMPUTED H = 3.69

THEORETICAL H = 9.210

Computed H is less than the theoretical H, there, we do not reject the null hypothesis which states: "There is no significant difference in susceptibility (χ) within the individual beach transects (DUNES04)."

Kruskal-Wallis Test: SH03 Transects

Kruskal-Wallis Test on sh03

C21	N	Median	Ave Rank	Z
1	24	85.50	24.9	-1.09
2	16	99.00	32.9	1.65
3	14	83.25	25.8	-0.48
Overall	54		27.5	

H = 2.74 DF = 2 P = 0.254

H = 2.74 DF = 2 P = 0.254 (adjusted for ties)

DECISION

COMPUTED H = 2.74

THEORETICAL H = 9.210

Computed H is less than the theoretical H, there, we do not reject the null hypothesis which states: "There is no significant difference in susceptibility (χ) within the individual beach transects (SH03)."

Kruskal-Wallis Test: SH04

Kruskal-Wallis Test on sh04

C23	N	Median	Ave Rank	Z
1	24	67.75	30.7	1.32
2	16	61.75	27.4	-0.02
3	14	57.25	22.1	-1.48
Overall	54		27.5	

H = 2.60 DF = 2 P = 0.273

H = 2.60 DF = 2 P = 0.273 (adjusted for ties)

DECISION

COMPUTED H = 2.60

THEORETICAL H = 9.210

Computed H is less than the theoretical H, there, we do not reject the null hypothesis which states: "There is no significant difference in susceptibility (χ) within the individual beach transects (SH04)."

Kruskal-Wallis Test: SB03 Transects

Kruskal-Wallis Test on sb03

C26	N	Median	Ave Rank	Z
1	15	20.00	43.9	-3.66
2	16	52.50	82.1	-0.75
3	17	59.50	94.1	0.22
4	13	50.50	68.0	-1.67
5	15	61.00	99.6	0.62
6	16	57.25	92.6	0.09
7	23	56.00	82.7	-0.86
8	16	51.75	73.3	-1.45
9	27	103.50	127.1	3.80
10	24	71.75	113.2	2.17
Overall	182		91.5	

H = 34.73 DF = 9 P = 0.000

H = 34.73 DF = 9 P = 0.000 (adjusted for ties)

DECISION

COMPUTED H = 34.73

THEORETICAL H = 21.666

Computed H is greater than the theoretical H, there, we do not accept the null hypothesis which states: "There is no significant difference in susceptibility (χ) within the individual beach transects (SB03)".

Kruskal-Wallis Test: SB04 Transects

Kruskal-Wallis Test on sb04

C28	N	Median	Ave Rank	Z
1	15	36.00	65.4	-2.01
2	16	50.00	78.6	-1.03
3	17	72.00	100.2	0.72
4	13	44.50	63.3	-2.00
5	15	45.50	66.8	-1.90
6	16	55.00	78.5	-1.03
7	23	80.50	122.6	3.03
8	16	53.75	85.8	-0.45
9	27	76.50	111.6	2.15

10	24	74.75	101.0	0.94
Overall	182		91.5	

H = 26.03 DF = 9 P = 0.002
H = 26.03 DF = 9 P = 0.002 (adjusted for ties)

DECISION

COMPUTED H = 26.03

THEORETICAL H = 21.666

Computed H is greater than the theoretical H, there, we do not accept the null hypothesis which states: "There is no significant difference in susceptibility (χ) within the individual beach transects (SB04)."

Kruskal-Wallis Test: NWB03 Transects

Kruskal-Wallis Test on nw03

C31	N	Median	Ave Rank	Z
1	22	54.50	49.0	-2.88
2	22	47.50	51.9	-2.52
3	14	46.00	41.7	-2.91
4	11	52.00	42.8	-2.46
5	22	72.75	90.9	2.24
6	21	80.00	109.0	4.33
7	20	90.25	112.0	4.56
8	12	51.50	53.4	-1.66
Overall	144		72.5	

H = 66.29 DF = 7 P = 0.000
H = 66.30 DF = 7 P = 0.000 (adjusted for ties)

DECISION

COMPUTED H = 66.29

THEORETICAL H = 18.475

Computed H is greater than the theoretical H, there, we do not accept the null hypothesis which states: "There is no significant difference in susceptibility (χ) within the individual beach transects (NWB03)."

Kruskal-Wallis Test: nw04

Kruskal-Wallis Test on nw04

C33	N	Median	Ave Rank	Z
1	22	49.50	54.4	-2.22
2	22	44.25	47.6	-3.04
3	14	54.50	68.4	-0.39
4	11	51.00	55.3	-1.42
5	22	76.00	95.8	2.84
6	21	61.00	84.8	1.46
7	20	80.00	103.9	3.62
8	12	51.50	55.6	-1.47
Overall	144		72.5	

H = 35.93 DF = 7 P = 0.000

H = 35.94 DF = 7 P = 0.000 (adjusted for ties)

DECISION

COMPUTED H = 35.93

THEORETICAL H = 18.475

Computed H is greater than the theoretical H, there, we do not accept the null hypothesis which states: "There is no significant difference in susceptibility (χ) within the individual beach transects (NWB04). "

APPENDIX E: Magnetic susceptibility data for used for mapping and statistics

LATITUDE	LONGITUDE	χ (2003) Susceptibility	χ (2004) Susceptibility	SIDE	BEACH	DISTANCE FROM SHORELINE	T RANSECT
375191	4643619	97.5	130	E	EB	0	1
375189.9	4643618.2	80	102.5	E	EB	1	1
375188.8	4643617.4	97	166	E	EB	2	1
375187.7	4643616.6	73	68	E	EB	3	1
375186.6	4643615.8	70	37	E	EB	4	1
375185.5	4643615	79	32	E	EB	5	1
375184.4	4643614.2	84.5	39.5	E	EB	6	1
375183.3	4643613.4	101.5	89	E	EB	7	1
375182.2	4643612.6	130	33.5	E	EB	8	1
375181.1	4643611.8	271	39.5	E	EB	9	1
375180	4643611	249	30.5	E	EB	10	1
375179.2	4643611.3	328	42.5	E	EB	11	1
375178.4	4643611.6	198	94.5	E	EB	12	1
375177.6	4643611.9	206.5	129	E	EB	13	1
375176.8	4643612.2	189	50.5	E	EB	14	1
375176	4643612.5	223.5	51.5	E	EB	15	1
375175.2	4643612.8	235.5	107	E	EB	16	1
375174.4	4643613.1	251.5	114	E	EB	17	1
375173.6	4643613.4	253	88	E	EB	18	1
375172.8	4643613.7	1263.5	362	E	EB	19	1
375172	4643614	1659	380	E	EB	20	1
375171.4	4643614.1	770.5	216	E	EB	21	1
375170.8	4643614.2	2284.5	160	E	EB	22	1
375170.2	4643614.3	1157	195	E	EB	23	1
375169.6	4643614.4	1140.5	399	E	EB	24	1
375166	4643615	1004.5	418.5	E	EB	25	1
375191	4643627	144	97.5	E	EB	0	2
375190.5	4643627	139.5	125	E	EB	1	2
375190	4643627	129	112	E	EB	2	2
375189.5	4643627	176.5	66.5	E	EB	3	2
375189	4643627	99	50	E	EB	4	2
375188.5	4643627	100.5	51	E	EB	5	2
375188	4643627	109.5	47	E	EB	6	2
375187.5	4643627	104	54.5	E	EB	7	2
375187	4643627	110.5	41.5	E	EB	8	2
375186.5	4643627	113	44.5	E	EB	9	2
375186	4643627	213	37	E	EB	10	2
375184.7	4643627	242	36.5	E	EB	11	2
375183.4	4643627	343	51.5	E	EB	12	2
375182.1	4643627	261.5	62	E	EB	13	2
375180.8	4643627	194.5	60	E	EB	14	2
375179.5	4643627	168.5	60	E	EB	15	2
375178.2	4643627	143.5	41	E	EB	16	2
375176.9	4643627	170.5	123.5	E	EB	17	2
375175.6	4643627	153	134.5	E	EB	18	2
375174.3	4643627	200	171.5	E	EB	19	2
375173	4643627	221	200.5	E	EB	20	2
375167	4643627	440.5	342	E	EB	21	2
375161	4643636	1421	315	E	EB	22	2
375159.25	4643633	2524.5	352	E	EB	23	2
375157.5	4643630	1445.5	331.5	E	EB	24	2
375155.75	4643627	1085.5	394	E	EB	25	2
375154	4643624	699	663.5	E	EB	26	2
375195	4643635	113.5	144	E	EB	0	3
375194.2	4643635.1	89	151	E	EB	1	3
375193.4	4643635.2	118.5	125	E	EB	2	3
375192.6	4643635.3	134	99.5	E	EB	3	3
375191.8	4643635.4	152	73	E	EB	4	3
375191	4643635.5	99	52	E	EB	5	3
375190.2	4643635.6	140	61	E	EB	6	3
375189.4	4643635.7	130	62	E	EB	7	3
375188.6	4643635.8	102.5	64	E	EB	8	3
375187.8	4643635.9	131	55	E	EB	9	3
375187	4643636	98.5	45	E	EB	10	3
375185.5	4643636.3	279	43	E	EB	11	3
375184	4643636.6	291.5	42.5	E	EB	12	3
375182.5	4643636.9	314.5	55	E	EB	13	3
375181	4643637.2	294	55	E	EB	14	3
375179.5	4643637.5	294.5	54	E	EB	15	3
375178	4643637.8	309	117	E	EB	16	3
375176.5	4643638.1	216.5	144	E	EB	17	3
375175	4643638.4	173	138	E	EB	18	3
375173.5	4643638.7	182.5	168	E	EB	19	3

375172	4643639	196	399.5	E	EB	20	3
375172	4643638.8	272	205	E	EB	21	3
375172	4643638.6	340	159	E	EB	22	3
375172	4643638.3	518.5	153	E	EB	23	3
375172	4643638.1	884.5	171.5	E	EB	24	3
375172	4643637.9	989.5	502.5	E	EB	25	3
375172	4643637.7	2057	517.5	E	EB	26	3
375172	4643637.4	1622.5	726	E	EB	27	3
375172	4643637.2	1350.5	573	E	EB	28	3
375172	4643637	820.5	481	E	EB	29	3
375199	4643641	118.5	123	E	EB	0	4
375198.1	4643641.4	191	141	E	EB	1	4
375197.2	4643641.8	178.5	68	E	EB	2	4
375196.3	4643642.2	296	55	E	EB	3	4
375195.4	4643642.6	107.5	46	E	EB	4	4
375194.5	4643643	110	46	E	EB	5	4
375193.6	4643643.4	82.5	66.5	E	EB	6	4
375192.7	4643643.8	102.5	56	E	EB	7	4
375191.8	4643644.2	126.5	46	E	EB	8	4
375190.9	4643644.6	260	47.5	E	EB	9	4
375190	4643645	147	49	E	EB	10	4
375188.7	4643645.4	231.5	38	E	EB	11	4
375187.4	4643645.8	526.5	46	E	EB	12	4
375186.1	4643646.2	373	7	E	EB	13	4
375184.8	4643646.6	295.5	60	E	EB	14	4
375183.5	4643647	307.5	67.5	E	EB	15	4
375182.2	4643647.4	301.5	119	E	EB	16	4
375180.9	4643647.8	325.5	172.5	E	EB	17	4
375179.6	4643648.2	415.5	214.5	E	EB	18	4
375178.3	4643648.6	321	264.5	E	EB	19	4
375177	4643649	306	286.5	E	EB	20	4
375175.7	4643649.4	410	346	E	EB	21	4
375174.4	4643649.8	525	180	E	EB	22	4
375173.1	4643650.2	669.5	174.5	E	EB	23	4
375171.8	4643650.6	1369.5	186	E	EB	24	4
375170.5	4643651	1957	335.5	E	EB	25	4
375169.2	4643651.4	3000.5	922	E	EB	26	4
375167.9	4643651.8	2581.5	1435.5	E	EB	27	4
375166.6	4643652.2	1553	1084.5	E	EB	28	4
375165.3	4643652.6	1165.5	1416	E	EB	29	4
375164	4643653	911	985.5	E	EB	30	4
375199	4643656	87	86.5	E	EB	0	5
375197.9	4643656	78.5	121	E	EB	1	5
375196.8	4643656	152.5	150.5	E	EB	2	5
375195.7	4643656	120	75	E	EB	3	5
375194.6	4643656	161	42	E	EB	4	5
375193.5	4643656	131.5	45.5	E	EB	5	5
375192.4	4643656	111.5	61	E	EB	6	5
375191.3	4643656	72	63.5	E	EB	7	5
375190.2	4643656	107.5	101	E	EB	8	5
375189.1	4643656	117	74	E	EB	9	5
375188	4643656	201	69	E	EB	10	5
375187	4643656.4	234	53	E	EB	11	5
375186	4643656.8	308.5	43	E	EB	12	5
375185	4643657.2	342.5	48.5	E	EB	13	5
375184	4643657.6	513	65.5	E	EB	14	5
375183	4643658	597	93.5	E	EB	15	5
375182	4643658.4	782.5	158.5	E	EB	16	5
375181	4643658.8	934	202.5	E	EB	17	5
375180	4643659.2	809.5	215.5	E	EB	18	5
375179	4643656	666.5	230	E	EB	19	5
375178	4643660	545.5	304	E	EB	20	5
375177.1	4643660	759	234.5	E	EB	21	5
375176.2	4643660	1259.5	222.5	E	EB	22	5
375175.3	4643660	1638.5	203	E	EB	23	5
375174.4	4643660	2550.5	173	E	EB	24	5
375173.5	4643660	1998	170.5	E	EB	25	5
375172.6	4643660	2050	343.5	E	EB	26	5
375171.7	4643660	1652.5	281.5	E	EB	27	5
375170.8	4643660	2618	792	E	EB	28	5
375169.9	4643660	1963.5	1188.5	E	EB	29	5
375169	4643660	2013	1272	E	EB	30	5
375208	4643711	115	137.5	E	EB	0	6
375206.9	4643710.8	224.5	161	E	EB	1	6
375205.8	4643710.6	78	107.5	E	EB	2	6
375204.7	4643710.4	149	133	E	EB	3	6
375203.6	4643710.2	89	170	E	EB	4	6
375202.5	4643710	144	76	E	EB	5	6

375201.4	4643709.8	72	81.5	E	EB	6	6
375200.3	4643709.6	74	116.5	E	EB	7	6
375199.2	4643709.4	94.5	198.5	E	EB	8	6
375198.1	4643711	94.5	185.5	E	EB	9	6
375197	4643709	106	85.5	E	EB	10	6
375195.6	4643708.4	176.5	68	E	EB	11	6
375194.2	4643707.8	68	71	E	EB	12	6
375192.8	4643707.2	160	60	E	EB	13	6
375191.4	4643706.6	141.5	96.5	E	EB	14	6
375190	4643706	140	158	E	EB	15	6
375188.6	4643705.4	158.5	337.5	E	EB	16	6
375187.2	4643704.8	215.5	530	E	EB	17	6
375185.8	4643704.2	440	637	E	EB	18	6
375184.4	4643709	260	764.5	E	EB	19	6
375183	4643703	394.5	619	E	EB	20	6
375183.1556	4643703.667	452.5	1100.5	E	EB	21	6
375183.3111	4643704.333	1158.5	696.5	E	EB	22	6
375183.4667	4643705	2222	958.5	E	EB	23	6
375183.6222	4643705.667	3973	1321.5	E	EB	24	6
375183.7778	4643706.333	3475.5	1727.5	E	EB	25	6
375183.9333	4643707	3365.5	663.5	E	EB	26	6
375184.0889	4643707.667	2789.5	902	E	EB	27	6
375184.8667	4643709	2397	2067.5	E	EB	28	6
375184.4	4643711	2239	1751	E	EB	29	6
375207	4643709	121.5	123.5	E	EB	0	7
375206	4643709	119	143.5	E	EB	1	7
375205	4643709	160.5	105.5	E	EB	2	7
375204	4643709	111	101	E	EB	3	7
375203	4643709	140.5	75.5	E	EB	4	7
375202	4643709	130	83	E	EB	5	7
375201	4643709	56	174.5	E	EB	6	7
375200	4643709	64.5	164	E	EB	7	7
375199	4643709	176	152.5	E	EB	8	7
375198	4643709	107.5	120	E	EB	9	7
375197	4643709	86	78	E	EB	10	7
375196	4643709	88.5	83.5	E	EB	11	7
375195	4643709	99	64	E	EB	12	7
375194	4643709	79	66.5	E	EB	13	7
375193	4643709	280	190	E	EB	14	7
375192	4643709	147	560	E	EB	15	7
375191	4643709	181.5	799	E	EB	16	7
375190	4643709	235	1382.5	E	EB	17	7
375189	4643709	582	1115	E	EB	18	7
375188	4643709	607.5	768.5	E	EB	19	7
375187	4643709	723.5	417	E	EB	20	7
375186	4643709	1646	2318.5	E	EB	21	7
375185	4643709	2123	2275.5	E	EB	22	7
375184	4643709	2777.5	1389	E	EB	23	7
375183	4643709	2663	1727	E	EB	24	7
375182	4643709	4271	1172	E	EB	25	7
375181	4643709	4255	1308	E	EB	26	7
375180	4643709	3584.5	1387	E	EB	27	7
375179	4643709	3354	1038.7	E	EB	28	7
375178	4643709	3332.5	691.5	E	EB	29	7
375177	4643709	3350.5	498	E	EB	30	7
375187	4643525	128	92	E	EB	0	8
375185.3	4643524.5	162.5	120	E	EB	1	8
375183.6	4643524	109	116	E	EB	2	8
375181.9	4643523.5	150	80	E	EB	3	8
375180.2	4643523	83	63.5	E	EB	4	8
375178.5	4643522.5	61.5	48	E	EB	5	8
375176.8	4643522	103.5	38	E	EB	6	8
375175.1	4643521.5	190	46.5	E	EB	7	8
375173.4	4643521	462.5	48	E	EB	8	8
375171.7	4643525	205	8.5	E	EB	9	8
375170	4643520	131.5	78	E	EB	10	8
375169.2222		131	144.5	E	EB	11	8
375168.4444		181.5	154	E	EB	12	8
375167.6667		132	120	E	EB	13	8
375166.8889		89	251	E	EB	14	8
375166.1111		86	807	E	EB	15	8
375165.3333		138.5	1698.5	E	EB	16	8
375164.5556		136.5	1372	E	EB	17	8
375163.7778		123	965.5	E	EB	18	8
375163	4643522	205	3756.5	E	EB	19	8
375165	4643523	1763.5	2534.5	E	EB	20	8
375167	4643524	2356	560	E	EB	21	8
375169	4643525	4459	302	E	EB	22	8

375171	4643526	8621.5	230	E	EB	23	8
3752219	4643957	90	126	E	EB	0	9
3752218.1	4643957.6	70.5	101.5	E	EB	1	9
3752217.2	4643958.2	92.5	162	E	EB	2	9
3752216.3	4643958.8	89.5	119	E	EB	3	9
3752215.4	4643959.4	83	236.5	E	EB	4	9
3752214.5	4643960	62.5	1507.5	E	EB	5	9
3752213.6	4643960.6	81.5	256.5	E	EB	6	9
3752212.7	4643961.2	146.5	509	E	EB	7	9
3752211.8	4643961.8	164	804.5	E	EB	8	9
3752210.9	4643957	234	519.5	E	EB	9	9
3752210	4643963	266	263.5	E	EB	10	9
3752208.556	4643963	166.5	223.5	E	EB	11	9
3752207.111	4643963	297	2002.5	E	EB	12	9
3752205.667	4643963	377	2891.5	E	EB	13	9
3752204.222	4643963	411	1120.5	E	EB	14	9
3752202.778	4643963	1236.5	3135.5	E	EB	15	9
3752201.333	4643963	3137.5	4480	E	EB	16	9
3752199.889	4643963	2508.5	2601	E	EB	17	9
3752198.444	4643963	2129.5	2382	E	EB	18	9
3752197	4643963	2693	1711.5	E	EB	19	9
375216	4643950	104.5	96	E	EB	0	10
375215.6	4643949.9	126	183	E	EB	1	10
375215.2	4643949.8	83	67	E	EB	2	10
375214.8	4643949.7	140.5	73	E	EB	3	10
375214.4	4643949.6	136	176.5	E	EB	4	10
375214	4643949.5	79	124.5	E	EB	5	10
375213.6	4643949.4	88.5	153	E	EB	6	10
375213.2	4643949.3	159.5	189.5	E	EB	7	10
375212.8	4643949.2	269.5	192	E	EB	8	10
375212.4	4643950	542.5	134.5	E	EB	9	10
375212	4643949	680.5	231.5	E	EB	10	10
375211.6	4643949.2	568	149	E	EB	11	10
375211.2	4643949.1	644.5	230	E	EB	12	10
375210.8	4643949	500	1050	E	EB	13	10
375210.4	4643948.9	434.5	1391.5	E	EB	14	10
375210	4643948.8	1517	2142	E	EB	15	10
375209.6	4643948.7	4331	1243.5	E	EB	16	10
375209.2	4643948.6	7194.5	3149	E	EB	17	10
375208.8	4643948.5	4919.5	4001	E	EB	18	10
375212	4643814	135.5	122	E	EB	0	11
375210.6	4643814	230	155.5	E	EB	1	11
375209.2	4643814	159	165	E	EB	2	11
375207.8	4643814	170	299.5	E	EB	3	11
375206.4	4643814	97.5	1027.5	E	EB	4	11
375205	4643814	160	521	E	EB	5	11
375203.6	4643814	165	927	E	EB	6	11
375202.2	4643814	156	3394.5	E	EB	7	11
375200.8	4643814	219.5	4106.5	E	EB	8	11
375199.4	4643814	187.5	1671.5	E	EB	9	11
375198	4643814	213.5	609	E	EB	10	11
375197.2	4643814.1	288	903	E	EB	11	11
375196.4	4643814.2	237	1386	E	EB	12	11
375195.6	4643814.3	737.5	769	E	EB	13	11
375194.8	4643814.4	487	692	E	EB	14	11
375194	4643814.5	715	1349	E	EB	15	11
375193.2	4643814.6	1093.5	2565	E	EB	16	11
375192.4	4643814.7	1312.5	2205	E	EB	17	11
375191.6	4643814.8	2813.5	1837.5	E	EB	18	11
375190.8	4643814	3606	4428.5	E	EB	19	11
375190	4643815	1864	4790	E	EB	20	11
375192	4643814.8	8887.5	2697.5	E	EB	21	11
375192.1333	4643814.9	6469.5	3347.5	E	EB	22	11
375192.7333	4643815	3735.5	2909	E	EB	23	11
375193.3333	4643815.1	3132.5	2475.5	E	EB	24	11
375193.9333	4643817	3735	1566.5	E	EB	25	11
375182	4643459	143	98	E	EB	0	12
375180.4	4643459.3	89	115.5	E	EB	1	12
375178.8	4643459.6	67	112.5	E	EB	2	12
375177.2	4643459.9	66	77.5	E	EB	3	12
375175.6	4643460.2	62	60	E	EB	4	12
375174	4643460.5	74.5	43.5	E	EB	5	12
375172.4	4643460.8	167.5	46	E	EB	6	12
375170.8	4643461.1	355.5	49	E	EB	7	12
375169.2	4643461.4	111.5	75.5	E	EB	8	12
375167.6	4643461.7	63.5	66.5	E	EB	9	12
375166	4643462	63	45.5	E	EB	10	12
375165.2	4643462.3	102	123	E	EB	11	12

375164.4	4643462.6	84.5	510	E	EB	12	12
375163.6	4643462.9	77	3108	E	EB	13	12
375162.8	4643463.2	86	4912	E	EB	14	12
375162	4643463.5	142	6329	E	EB	15	12
375161.2	4643463.8	257	6271	E	EB	16	12
375160.4	4643464.1	391.5	5004	E	EB	17	12
375159.6	4643464.4	732	5277	E	EB	18	12
375158.8	4643464.7	6547.5	3910.5	E	EB	19	12
375158	4643465	6865	4236	E	EB	20	12
375159.5	4643465.3	5980	3179.5	E	EB	21	12
375161	4643465.6	3841.5	2980.5	E	EB	22	12
375162	4643192	250	89	E	EB	0	13
375162.2	4643191.6	185	114.5	E	EB	1	13
375162.4	4643191.2	151	77	E	EB	2	13
375162.6	4643190.8	157.5	61	E	EB	3	13
375162.8	4643190.4	180	72	E	EB	4	13
375163	4643190	158.5	86	E	EB	5	13
375163.2	4643189.6	109	104	E	EB	6	13
375163.4	4643189.2	85.5	94	E	EB	7	13
375163.6	4643188.8	57	44.5	E	EB	8	13
375163.8	4643192	50	56	E	EB	9	13
375164	4643188	52	73	E	EB	10	13
375197.2	4643814.1	64	68.5	E	EB	11	13
375196.4	4643814.2	145	52	E	EB	12	13
375195.6	4643814.3	94.5	79.5	E	EB	13	13
375194.8	4643814.4	88	150.5	E	EB	14	13
375194	4643814.5	103	312	E	EB	15	13
375193.2	4643814.6	144	379.5	E	EB	16	13
375192.4	4643814.7	151	180.5	E	EB	17	13
375191.6	4643814.8	199	147	E	EB	18	13
375190.8	4643814	187	198	E	EB	19	13
375152	4643187	183	408	E	EB	20	13
375149.2	4643187	147.5	479	E	EB	21	13
375146.4	4643187	152.5	860	E	EB	22	13
375143.6	4643187	218.5	393.5	E	EB	23	13
375140.8	4643187	1142.5	1364	E	EB	24	13
375138	4643187	110.5	1754	E	EB	25	13
375135.2	4643187	173	1608.5	E	EB	26	13
375132.4	4643187	124.5	1854	E	EB	27	13
375129.6	4643187	115.5	1892	E	EB	28	13
375126.8	4643187	110.5	3505.5	E	EB	29	13
375124	4643187	115	3055.5	E	EB	30	13
375124.1667	4643187.75	110.5	2022.5	E	EB	31	13
375124.3333	4643188.5	88	2529	E	EB	32	13
375124.5	4643189.25	98	1857.8	E	EB	33	13
375124.6667	4643190	118	1538	E	EB	34	13
375124.8333	4643190.75	170	1318.5	E	EB	35	13
375125	4643191.5	684	1050.5	E	EB	36	13
375125.1667	4643192.25	607	542.5	E	EB	37	13
375125.3333	4643193	600	1214.5	E	EB	38	13
375125.5	4643193.75	642.5	1057	E	EB	39	13
375124.2	4643187.9	814	1237.5	E	EB	40	13
375124.4	4643188.8	520	1219	E	EB	41	13
375126	4643196	226	1280	E	EB	42	13
375124.3333	4643196.333	456.5	1167.5	E	EB	43	13
375124.3333	4643196.333	491.5	1198	E	EB	44	13
375121	4643197	309.5	787.5	E	EB	45	13
372470	4648014	70	35.5	W	SB	0	1
372470.9	4648014.4	73	39	W	SB	1	1
372471.8	4648014.8	62	32	W	SB	2	1
372472.7	4648015.2	43	36	W	SB	3	1
372473.6	4648015.6	40	31.5	W	SB	4	1
372474.5	4648016	33	36	W	SB	5	1
372475.4	4648016.4	20	31.5	W	SB	6	1
372476.3	4648016.8	14.5	23.5	W	SB	7	1
372477.2	4648017.2	15.5	23.5	W	SB	8	1
372478.1	4648017.6	16.5	52.5	W	SB	9	1
372479	4648018	19.5	83.5	W	SB	10	1
372480	4648018.25	17.5	91	W	SB	11	1
372481	4648018.5	14	94	W	SB	12	1
372482	4648018.75	16	65.5	W	SB	13	1
372483	4648019	114	124	W	SB	14	1
372466	4648021	65.5	60	W	SB	0	2
372466.9	4648021.3	66.5	63	W	SB	1	2
372467.8	4648021.6	60	34	W	SB	2	2
372468.7	4648021.9	47	35	W	SB	3	2
372469.6	4648022.2	72	33.5	W	SB	4	2
372470.5	4648022.5	48	49	W	SB	5	2

372471.4	4648022.8	45	46	W	SB	6	2
372472.3	4648023.1	37	25	W	SB	7	2
372473.2	4648023.4	33	29	W	SB	8	2
372474.1	4648023.7	43.5	41.5	W	SB	9	2
372475	4648024	48.5	97.5	W	SB	10	2
372475.8	4648024.6	56.5	51	W	SB	11	2
372476.6	4648025.2	46.5	91	W	SB	12	2
372477.4	4648025.8	79.5	83	W	SB	13	2
372478.2	4648026.4	69	112	W	SB	14	2
372479	4648027	234.5	82.5	W	SB	15	2
372462	4648025	63.5	112	W	SB	0	3
372462.9	4648026	54	82.5	W	SB	1	3
372463.8	4648027	50.5	122.5	W	SB	2	3
372464.7	4648028	75.5	192	W	SB	3	3
372465.6	4648029	36.5	51.5	W	SB	4	3
372466.5	4648030	21.5	37.5	W	SB	5	3
372467.4	4648031	18	39.5	W	SB	6	3
372468.3	4648032	24.5	34	W	SB	7	3
372469.2	4648033	29.5	27.5	W	SB	8	3
372470.1	4648034	52.5	120.5	W	SB	9	3
372471	4648035	151	149	W	SB	10	3
372471.5	4648035.167	119.5	81.5	W	SB	11	3
372472	4648035.333	59.5	42.5	W	SB	12	3
372472.5	4648035.5	89.5	79	W	SB	13	3
372473	4648035.667	243.5	44	W	SB	14	3
372474	4648036	204.5	56.5	W	SB	15	3
372474	4648036	149	72	W	SB	16	3
372461	4648040	69.5	55	W	SB	0	4
372461.2	4648040.5	54.5	58	W	SB	1	4
372461.4	4648041	53.5	42.5	W	SB	2	4
372461.6	4648041.5	73.5	44.5	W	SB	3	4
372461.8	4648042	77.5	41	W	SB	4	4
372462	4648042.5	44.5	25	W	SB	5	4
372462.2	4648043	46	39.5	W	SB	6	4
372462.4	4648043.5	29	35.5	W	SB	7	4
372462.6	4648044	28.5	34.5	W	SB	8	4
372462.8	4648044.5	45	49	W	SB	9	4
372463	4648045	50.5	58	W	SB	10	4
372463.2	4648045.5	38	78.5	W	SB	11	4
372463.4	4648046	52	58	W	SB	12	4
372452	4648045	66.5	48.5	W	SB	0	5
372457.5	4648048.5	62	32.5	W	SB	1	5
372463	4648052	55	46.5	W	SB	2	5
372462.375	4648052.375	61	45.5	W	SB	3	5
372461.75	4648052.75	85	19	W	SB	4	5
372461.125	4648053.125	36	29	W	SB	5	5
372460.5	4648053.5	53.5	49.5	W	SB	6	5
372459.875	4648053.875	40	34.5	W	SB	7	5
372459.25	4648054.25	45.5	29.5	W	SB	8	5
372458.625	4648054.625	61	33.5	W	SB	9	5
372458	4648055	76	42	W	SB	10	5
372458.75	4648052.5	98.5	68.5	W	SB	11	5
372459.5	4648050	210	104	W	SB	12	5
372460.25	4648047.5	167	179	W	SB	13	5
372461	4648045	53.5	88.5	W	SB	14	5
372446	4648056	62	69	W	SB	0	6
372446.9	4648056.3	79.5	47	W	SB	1	6
372447.8	4648056.6	49.5	38	W	SB	2	6
372448.7	4648056.9	50	60	W	SB	3	6
372449.6	4648057.2	80.5	25	W	SB	4	6
372450.5	4648057.5	107.5	22.5	W	SB	5	6
372451.4	4648057.8	80.5	56	W	SB	6	6
372452.3	4648058.1	86	42.5	W	SB	7	6
372453.2	4648058.4	54.5	20.5	W	SB	8	6
372454.1	4648058.7	51	45	W	SB	9	6
372455	4648059	53	74	W	SB	10	6
372455.6	4648059.6	40	106	W	SB	11	6
372456.2	4648060.2	60	112	W	SB	12	6
372456.8	4648060.8	91	65	W	SB	13	6
372457.4	4648061.4	54	72.5	W	SB	14	6
372458	4648062	33	54	W	SB	15	6
372404	4648132	50	77.5	W	SB	0	7
372405.2	4648132	66.5	52	W	SB	1	7
372406.4	4648132	53	85.5	W	SB	2	7
372407.6	4648132	58.5	64.5	W	SB	3	7
372408.8	4648132	32	371	W	SB	4	7
372410	4648132	25.5	254.5	W	SB	5	7
372411.2	4648132	18.5	157	W	SB	6	7

372412.4	4648132	20.5	151.5	W	SB	7	7
372413.6	4648132	26.5	164.5	W	SB	8	7
372414.8	4648132	45.5	170.5	W	SB	9	7
372416	4648132	51	133	W	SB	10	7
372417.2	4648132.7	33.5	119	W	SB	11	7
372418.4	4648133.4	32.5	103.5	W	SB	12	7
372419.6	4648134.1	56	56	W	SB	13	7
372420.8	4648134.8	71	62	W	SB	14	7
372422	4648135.5	125	52	W	SB	15	7
372423.2	4648136.2	70	51	W	SB	16	7
372424.4	4648136.9	70	44	W	SB	17	7
372425.6	4648137.6	86	59	W	SB	18	7
372426.8	4648138.3	97	81	W	SB	19	7
372428	4648139	122.5	46	W	SB	20	7
372429.2	4648139.7	135	48.5	W	SB	21	7
372430.4	4648140.4	95.5	80.5	W	SB	22	7
372328	4648274	64	48.5	W	SB	0	8
372329	4648274.4	76	45	W	SB	1	8
372330	4648274.8	48	51.5	W	SB	2	8
372331	4648275.2	31	26	W	SB	3	8
372332	4648275.6	27	32	W	SB	4	8
372333	4648276	16	26.5	W	SB	5	8
372334	4648276.4	14.5	41.5	W	SB	6	8
372335	4648276.8	10	17	W	SB	7	8
372336	4648277.2	16	16	W	SB	8	8
372337	4648277.6	28.5	43	W	SB	9	8
372338	4648278	55.5	221	W	SB	10	8
372323.5	4648300	57	165.5	W	SB	11	8
372309	4648322	144.5	116.5	W	SB	12	8
372294.5	4648344	161	180	W	SB	13	8
372280	4648366	130	213	W	SB	14	8
372251	4648410	120.5	130	W	SB	15	8
372251	4648410	50.5	48.5	W	SB	0	9
372252.1	4648409.9	46	37	W	SB	1	9
372253.2	4648409.8	137	41	W	SB	2	9
372254.3	4648409.7	76	42.5	W	SB	3	9
372255.4	4648409.6	62	64	W	SB	4	9
372256.5	4648409.5	66	56	W	SB	5	9
372257.6	4648409.4	65	91.5	W	SB	6	9
372258.7	4648409.3	30.5	105	W	SB	7	9
372259.8	4648409.2	36.5	89	W	SB	8	9
372260.9	4648409.1	27.5	95	W	SB	9	9
372262	4648409	153	83	W	SB	10	9
372260.9	4648410.1	53	67.5	W	SB	11	9
372259.8	4648411.2	103.5	95	W	SB	12	9
372258.7	4648412.3	188.5	138.5	W	SB	13	9
372257.6	4648413.4	195.5	160	W	SB	14	9
372256.5	4648414.5	179.5	102.5	W	SB	15	9
372255.4	4648415.6	160	118	W	SB	16	9
372254.3	4648416.7	160	92.5	W	SB	17	9
372253.2	4648417.8	145.5	63.5	W	SB	18	9
372252.1	4648418.9	233.5	76.5	W	SB	19	9
372251	4648420	139	62.5	W	SB	20	9
		165.5	28.5	W	SB	21	9
		175	135	W	SB	22	9
		163	140	W	SB	23	9
		88	105	W	SB	24	9
		101.5	52	W	SB	25	9
372274	4648424.286	74	60	W	SB	26	9
372545	4647869	50	44	W	SB	0	10
372545.7	4647868.7	54	33	W	SB	1	10
372546.4	4647868.4	67	36	W	SB	2	10
372547.1	4647868.1	26	19	W	SB	3	10
372547.8	4647867.8	29.5	130.5	W	SB	4	10
372548.5	4647867.5	64	56.5	W	SB	5	10
372549.2	4647867.2	103	38.5	W	SB	6	10
372549.9	4647866.9	63	63	W	SB	7	10
372550.6	4647866.6	36	58	W	SB	8	10
372551.3	4647866.3	48	52	W	SB	9	10
372552	4647866	89	78.5	W	SB	10	10
372552.3	4647867.4	137	168.5	W	SB	11	10
372552.6	4647868.8	109	158.5	W	SB	12	10
372552.9	4647870.2	126.5	133	W	SB	13	10
372553.2	4647871.6	74.5	132	W	SB	14	10
372553.5	4647873	58.5	155	W	SB	15	10
372553.8	4647874.4	69	152	W	SB	16	10
372554.1	4647875.8	68	136.5	W	SB	17	10
372554.4	4647877.2	121	61.5	W	SB	18	10

372554.7	4647878.6	123	82.5	W	SB	19	10
372555	4647880	139	87.5	W	SB	20	10
372555.3	4647881.4	190.5	80.5	W	SB	21	10
372555.6	4647882.8	177	80	W	SB	22	10
372545	4647883	155	40.5	W	SB	23	10
372555	4647850	43.5	39	W	SB	0	11
372556	4647850.5	68	41	W	SB	1	11
372557	4647851	60	18.5	W	SB	2	11
372558	4647851.5	41	24	W	SB	3	11
372559	4647852	52	36	W	SB	4	11
372560	4647852.5	72	15	W	SB	5	11
372561	4647853	96.5	37.5	W	SB	6	11
372562	4647853.5	50	55	W	SB	7	11
372563	4647854	70	53.5	W	SB	8	11
372564	4647854.5	57	69	W	SB	9	11
372565	4647855	79.5	86	W	SB	10	11
372565.7778	4647855.333	187.5	105	W	SB	11	11
372566.5556	4647855.667	145.5	86.5	W	SB	12	11
372567.3333	4647856	71.5	69.5	W	SB	13	11
372568.1111	4647856.333	45	54	W	SB	14	11
372568.8889	4647856.667	41.5	64	W	SB	15	11
372569.6667	4647857	47	29	W	SB	16	11
372570.4444	4647857.333	45	50	W	SB	17	11
372571.2222	4647857.667	42	61.5	W	SB	18	11
372572	4647858	68.5	43	W	SB	19	11
372865	4647232	27.5	61.5	W	NW	0	1
372866	4647232.9	19	32.5	W	NW	1	1
372867	4647233.8	19.5	39	W	NW	2	1
372868	4647234.7	26	48	W	NW	3	1
372869	4647235.6	27	51	W	NW	4	1
372870	4647236.5	23	68	W	NW	5	1
372871	4647237.4	35	79	W	NW	6	1
372872	4647238.3	22.5	57	W	NW	7	1
372873	4647239.2	17	52	W	NW	8	1
372874	4647240.1	23.5	44.5	W	NW	9	1
372875	4647241	72.5	38.5	W	NW	10	1
372876.4	4647241.2	47	22.5	W	NW	11	1
372877.8	4647241.4	72	37.5	W	NW	12	1
372879.2	4647241.6	67.5	45.5	W	NW	13	1
372880.6	4647241.8	67.5	35	W	NW	14	1
372882	4647242	69	49	W	NW	15	1
372883.4	4647242.2	62	50	W	NW	16	1
372884.8	4647242.4	74.5	56	W	NW	17	1
372886.2	4647242.6	70	55	W	NW	18	1
372887.6	4647242.8	63	46.5	W	NW	19	1
372889	4647243	66	56	W	NW	20	1
372890.4	4647243.2	82	58	W	NW	21	1
372854	4647243	52	52.2	W	NW	0	2
372855.6	4647243.4	40	51.5	W	NW	1	2
372857.2	4647243.8	37	32	W	NW	2	2
372858.8	4647244.2	37	31	W	NW	3	2
372860.4	4647244.6	47	47.5	W	NW	4	2
372862	4647245	47	219	W	NW	5	2
372863.6	4647245.4	36.5	76	W	NW	6	2
372865.2	4647245.8	30	68	W	NW	7	2
372866.8	4647246.2	46	57	W	NW	8	2
372868.4	4647246.6	50.5	38	W	NW	9	2
372870	4647247	40	47	W	NW	10	2
372870.7	4647247.7	29	41.5	W	NW	11	2
372871.4	4647248.4	45	43.5	W	NW	12	2
372872.1	4647249.1	69	45	W	NW	13	2
372872.8	4647249.8	48	27.5	W	NW	14	2
372873.5	4647250.5	68	35	W	NW	15	2
372874.2	4647251.2	75.5	49.5	W	NW	16	2
372874.9	4647251.9	77.5	35	W	NW	17	2
372875.6	4647252.6	63.5	42	W	NW	18	2
372876.3	4647253.3	61.5	36	W	NW	19	2
372877	4647254	72	33	W	NW	20	2
372877.7	4647254.7	57.5	68	W	NW	21	2
372853	4647254	44.5	70	W	NW	0	3
372853.9	4647254.4	45	44	W	NW	1	3
372854.8	4647254.8	34	38	W	NW	2	3
372855.7	4647255.2	35	42	W	NW	3	3
372856.6	4647255.6	51.5	61	W	NW	4	3
372857.5	4647256	60	58	W	NW	5	3
372858.4	4647256.4	47	46	W	NW	6	3
372859.3	4647256.8	53.5	80	W	NW	7	3
372860.2	4647257.2	52.5	71	W	NW	8	3

372861.1	4647257.6	49	60	W	NW	9	3
372862	4647258	44	46	W	NW	10	3
372862.3333	4647259	35	44	W	NW	11	3
372862.6667	4647260	62	71	W	NW	12	3
372863	4647261	44	51	W	NW	13	3
372853	4647263	62	47	W	NW	0	4
372853.6	4647263.5	26	58	W	NW	1	4
372854.2	4647264	24	28	W	NW	2	4
372854.8	4647264.5	26	35	W	NW	3	4
372855.4	4647265	39	70.5	W	NW	4	4
372856	4647265.5	57.5	53.5	W	NW	5	4
372856.6	4647266	61.5	53.5	W	NW	6	4
372857.2	4647266.5	49	43.5	W	NW	7	4
372857.8	4647267	52	57.5	W	NW	8	4
372858.4	4647267.5	58.5	47	W	NW	9	4
372859	4647268	54.5	51	W	NW	10	4
372663	4647656	71.5	81	W	NW	0	5
372664.1667	4647656.333	55	80.5	W	NW	1	5
372665.3333	4647656.667	36	35	W	NW	2	5
372666.5	4647657	33.5	48	W	NW	3	5
372667.6667	4647657.333	40.5	117.5	W	NW	4	5
372670	4647658	81.5	285.5	W	NW	5	5
372670	4647658	112	127	W	NW	6	5
372670.5	4647653.25	109.5	45	W	NW	7	5
372671	4647648.5	67.5	34	W	NW	8	5
372671.5	4647643.75	89.5	54.5	W	NW	9	5
372672	4647639	85.5	55	W	NW	10	5
372670.6	4647641.7	72	65.5	W	NW	11	5
372669.2	4647644.4	87.5	50	W	NW	12	5
372667.8	4647647.1	82.5	50.5	W	NW	13	5
372666.4	4647649.8	86.5	73	W	NW	14	5
372665	4647652.5	84.5	72	W	NW	15	5
372663.6	4647655.2	77.5	79	W	NW	16	5
372662.2	4647657.9	66.5	106.5	W	NW	17	5
372660.8	4647660.6	70.5	104	W	NW	18	5
372659.4	4647663.3	73.5	101	W	NW	19	5
372658	4647666	64	86.5	W	NW	20	5
372658	4647668.7	45.5	81.5	W	NW	21	5
372658	4647669	60	46.5	W	NW	0	6
372658.8	4647669.2	80	95	W	NW	1	6
372659.6	4647669.4	82	55	W	NW	2	6
372660.4	4647669.6	75.5	49	W	NW	3	6
372661.2	4647669.8	108.5	80	W	NW	4	6
372662	4647670	197	60	W	NW	5	6
372662.8	4647670.2	127.5	30	W	NW	6	6
372663.6	4647670.4	75.5	31.5	W	NW	7	6
372664.4	4647670.6	86.5	38	W	NW	8	6
372665.2	4647670.8	70	54	W	NW	9	6
372666	4647671	80	61	W	NW	10	6
372666.9	4647671.4	61	45.5	W	NW	11	6
372707.8	4647671.8	81.5	62	W	NW	12	6
372728.7	4647672.2	88.5	69	W	NW	13	6
372749.6	4647672.6	85	81	W	NW	14	6
372770.5	4647673	75	107.5	W	NW	15	6
372791.4	4647673.4	67.5	58.5	W	NW	16	6
372812.3	4647673.8	77.5	83.5	W	NW	17	6
372833.2	4647674.2	85.5	114	W	NW	18	6
372854.1	4647674.6	88	91.5	W	NW	19	6
372875	4647675	74	81.5	W	NW	20	6
372640	4647697	60.5	60	W	NW	0	7
372641.2	4647697.6	67.5	72.5	W	NW	1	7
372642.4	4647698.2	109	94	W	NW	2	7
372643.6	4647698.8	104	61.5	W	NW	3	7
372644.8	4647699.4	92.5	223	W	NW	4	7
372646	4647700	44	289.5	W	NW	5	7
372647.2	4647700.6	99	45	W	NW	6	7
372648.4	4647701.2	69.5	31.5	W	NW	7	7
372649.6	4647701.8	68.5	38	W	NW	8	7
372650.8	4647702.4	71	68.5	W	NW	9	7
372652	4647703	97.5	93	W	NW	10	7
372652.5556	4647703.667	96	59.5	W	NW	11	7
372653.1111	4647704.333	93	78	W	NW	12	7
372653.6667	4647705	101	89.5	W	NW	13	7
372654.2222	4647705.667	84.5	83	W	NW	14	7
372654.7778	4647706.333	99.5	82	W	NW	15	7
372655.3333	4647707	104	97.5	W	NW	16	7
372655.8889	4647707.667	81	108.5	W	NW	17	7
372656.4444	4647708.333	88	77.5	W	NW	18	7

372657	4647709	77.5	100	W	NW	19	7
372553	4647868	31.5	32.5	W	NW	0	8
372554	4647868.5	22.5	47	W	NW	1	8
372555	4647869	42.5	57	W	NW	2	8
372556	4647869.5	51.5	59	W	NW	3	8
372557	4647870	34	64	W	NW	4	8
372558	4647870.5	42	77.5	W	NW	5	8
372559	4647871	57	69	W	NW	6	8
372560	4647871.5	63	41.5	W	NW	7	8
372561	4647872	100.5	23	W	NW	8	8
372562	4647872.5	84.5	30	W	NW	9	8
372563	4647873	51.5	42	W	NW	10	8
372564	4647873.5	53.5	56	W	NW	11	8
373539	4645618	97	60.5	W	SH	0	1
373540.2	4645618	127	51.5	W	SH	1	1
373541.4	4645618	136	57.5	W	SH	2	1
373542.6	4645618	136	78	W	SH	3	1
373543.8	4645618	111	65.5	W	SH	4	1
373545	4645618	87	55	W	SH	5	1
373546.2	4645618	71	53	W	SH	6	1
373547.4	4645618	97	100.5	W	SH	7	1
373548.6	4645618	99	86	W	SH	8	1
373549.8	4645618	90	95.5	W	SH	9	1
373551	4645618	76.5	119	W	SH	10	1
373551.9	4645618.9	67.5	82	W	SH	11	1
373552.8	4645619.8	53	72	W	SH	12	1
373553.7	4645620.7	68	71	W	SH	13	1
373554.6	4645621.6	76.5	37	W	SH	14	1
373555.5	4645622.5	81.5	43	W	SH	15	1
373556.4	4645623.4	100	82	W	SH	16	1
373557.3	4645624.3	94.5	59	W	SH	17	1
373558.2	4645625.2	84	62	W	SH	18	1
373559.1	4645626.1	79	52.5	W	SH	19	1
373560	4645627	88	70	W	SH	20	1
373553	4645627	69	72	W	SH	21	1
373546	4645627	80.5	38	W	SH	22	1
373539	4645627	68.5	92	W	SH	23	1
373532	4645627	111	58.5	W	SH	0	2
373532.9	4645627.8	118.5	67.5	W	SH	1	2
373533.8	4645628.6	127	94	W	SH	2	2
373534.7	4645629.4	139.5	55.5	W	SH	3	2
373535.6	4645630.2	122.5	62	W	SH	4	2
373536.5	4645631	102.5	32.5	W	SH	5	2
373537.4	4645631.8	95.5	40	W	SH	6	2
373538.3	4645632.6	244.5	54	W	SH	7	2
373539.2	4645633.4	84	63	W	SH	8	2
373540.1	4645634.2	89	61.5	W	SH	9	2
373541	4645635	47	61.5	W	SH	10	2
373541.6	4645636	83	82.5	W	SH	11	2
373542.2	4645637	57.5	102	W	SH	12	2
373542.8	4645638	83	67	W	SH	13	2
373543.4	4645639	116	70	W	SH	14	2
373544	4645640	92	56.5	W	SH	15	2
373528	4645648	74.5	71	W	SH	0	3
373529.2	4645648	77	52.5	W	SH	1	3
373530.4	4645648	120.5	37	W	SH	2	3
373531.6	4645648	125.5	47	W	SH	3	3
373532.8	4645648	124	30	W	SH	4	3
373534	4645648	116	70	W	SH	5	3
373535.2	4645648	86.5	40.5	W	SH	6	3
373536.4	4645648	114.5	22	W	SH	7	3
373537.6	4645648	96	33	W	SH	8	3
373538.8	4645648	79	86	W	SH	9	3
373540	4645648	80	102	W	SH	10	3
373540.6667	4645649	62	66	W	SH	11	3
373541.3333	4645650	60.5	62	W	SH	12	3
373542	4645651	68.5	67	W	SH	13	3
373400	4645981	67.5	43	W	D	0	1
373401.4	4645981	78	56.5	W	D	1	1
373402.8	4645981	91.5	56	W	D	2	1
373404.2	4645981	130.5	50	W	D	3	1
373405.6	4645981	142	90	W	D	4	1
373407	4645981	90	30	W	D	5	1
373408.4	4645981	85	29.5	W	D	6	1
373409.8	4645981	70	28	W	D	7	1
373411.2	4645981	87	41	W	D	8	1
373412.6	4645981	108.5	101.5	W	D	9	1
373414	4645981	83.5	73	W	D	10	1

373415	4645981.6	62	54	W	D	11	1
373416	4645982.2	54.5	56.5	W	D	12	1
373417	4645982.8	71	69.5	W	D	13	1
373418	4645983.4	95	79.5	W	D	14	1
373419	4645984	88.5	73	W	D	15	1
373420	4645984.6	84	70.5	W	D	16	1
373421	4645985.2	79.5	68	W	D	17	1
373422	4645985.8	72	67.5	W	D	18	1
373423	4645986.4	71	65	W	D	19	1
373424	4645987	81	68	W	D	20	1
373421	4645987	81.5	43.5	W	D	21	1
373397	4645995	63.5	68.5	W	D	0	2
373398.1	4645995.5	57	68	W	D	1	2
373399.2	4645996	80	66.5	W	D	2	2
373400.3	4645996.5	131	48	W	D	3	2
373401.4	4645997	106.5	26	W	D	4	2
373402.5	4645997.5	91	29.5	W	D	5	2
373403.6	4645998	89	45	W	D	6	2
373404.7	4645998.5	117	73	W	D	7	2
373405.8	4645999	90	89.5	W	D	8	2
373406.9	4645999.5	77	79	W	D	9	2
373408	4646000	57.5	75	W	D	10	2
373380	4646035	90	58.5	W	D	0	3
373381.2222	4646035.333	97.5	33	W	D	1	3
373382.4444	4646035.667	94.5	216.5	W	D	2	3
373383.6667	4646036	71	48	W	D	3	3
373384.8889	4646036.333	61	58	W	D	4	3
373386.1111	4646036.667	58	30	W	D	5	3
373387.3333	4646037	74	25	W	D	6	3
373388.5556	4646037.333	83.5	38.5	W	D	7	3
373389.7778	4646037.667	91.5	41.5	W	D	8	3
373391	4646038	69.5	42.5	W	D	9	3
373783	4644933	56	65.5	W	BW	0	1
373784.1	4644933.4	70.5	55.5	W	BW	1	1
373785.2	4644933.8	86	75.5	W	BW	2	1
373786.3	4644934.2	103.5	94	W	BW	3	1
373787.4	4644934.6	160	106.5	W	BW	4	1
373788.5	4644935	107	64.5	W	BW	5	1
373789.6	4644935.4	100.5	64	W	BW	6	1
373790.7	4644935.8	108.5	66	W	BW	7	1
373791.8	4644936.2	97.5	50	W	BW	8	1
373792.9	4644936.6	95	67	W	BW	9	1
373794	4644937	108	51	W	BW	10	1
373795.1	4644937.5	52	67	W	BW	11	1
373796.2	4644938	73.5	58	W	BW	12	1
373797.3	4644952	94.5	69.5	W	BW	0	2
373796.2625	4644952.75	100	88	W	BW	1	2
373795.225	4644953.5	109	56	W	BW	2	2
373794.1875	4644954.25	94	103.5	W	BW	3	2
373793.15	4644955	80	96.5	W	BW	4	2
373792.1125	4644955.75	77.5	70	W	BW	5	2
373791.075	4644956.5	89	88.5	W	BW	6	2
373790.0375	4644957.25	88	84	W	BW	7	2
373789	4644958	62	147	W	BW	8	2
373771	4644977	63	59.5	W	BW	0	3
373772.2222	4644977.333	78	67.5	W	BW	1	3
373773.4444	4644977.667	91	57.5	W	BW	2	3
373774.6667	4644978	91.5	61.5	W	BW	3	3
373775.8889	4644978.333	77.5	82	W	BW	4	3
373777.1111	4644978.667	72	59	W	BW	5	3
373778.3333	4644979	62	66	W	BW	6	3
373779.5556	4644979.333	70.5	36.5	W	BW	7	3
373780.7778	4644979.667	70	60	W	BW	8	3
373782	4644980	60	52.5	W	BW	9	3
373989	4644304	87.5	48.5	W	WP	0	1
373990.5	4644304.8	43	35	W	WP	1	1
373992	4644305.6	62.5	38.5	W	WP	2	1
373993.5	4644306.4	91	33	W	WP	3	1
373995	4644307.2	82.5	37	W	WP	4	1
373996.5	4644308	68.5	39	W	WP	5	1
373998	4644308.8	64.5	28	W	WP	6	1
373999.5	4644309.6	47.5	42	W	WP	7	1
374001	4644310.4	28	47	W	WP	8	1
374002.5	4644311.2	26.5	46	W	WP	9	1
374004	4644312	26.5	40	W	WP	10	1
374004.5	4644312.333	26	40.5	W	WP	11	1
374005	4644312.667	45.5	30	W	WP	12	1
374005.5	4644313	53.5	38.5	W	WP	13	1

374006	4644313.333	63	69	W	WP	14	1
374006.5	4644313.667	60.5	41	W	WP	15	1
374007	4644314	89	45	W	WP	16	1
373994	4644298	83	63.5	W	WP	0	2
373995.3	4644298.5	66.5	63.5	W	WP	1	2
373996.6	4644299	77.5	50	W	WP	2	2
373997.9	4644299.5	105	36.5	W	WP	3	2
373999.2	4644300	74	33.5	W	WP	4	2
374000.5	4644300.5	50	58	W	WP	5	2
374001.8	4644301	51.5	131.5	W	WP	6	2
374003.1	4644301.5	33.5	25	W	WP	7	2
374004.4	4644302	28	27	W	WP	8	2
374005.7	4644302.5	25	33	W	WP	9	2
374007	4644303	41	31	W	WP	10	2
374004.6	4644300.4	35	33	W	WP	11	2
374002.2	4644297.8	36	33	W	WP	12	2
373999.8	4644295.2	49	51	W	WP	13	2
373997.4	4644292.6	62	60.5	W	WP	14	2
373995	4644290	91.5	64.5	W	WP	0	3
373995.9	4644290	99.5	55	W	WP	1	3
373996.8	4644290	99	83	W	WP	2	3
373997.7	4644290	104	43.5	W	WP	3	3
373998.6	4644290	42	65.5	W	WP	4	3
373999.5	4644290	34	48.5	W	WP	5	3
374000.4	4644290	38.5	60	W	WP	6	3
374001.3	4644290	32	30	W	WP	7	3
374002.2	4644290	22	52.5	W	WP	8	3
374003.1	4644290	28	51	W	WP	9	3
374004	4644290	29	25	W	WP	10	3
374005.6667	4644290.333	40.5	13	W	WP	11	3
374007.3333	4644290.667	29.5	70.5	W	WP	12	3
374009	4644291	38.5	19	W	WP	13	3
374001	4644280	95.5	51.5	W	WP	0	4
374001.8	4644280.3	92.5	54.5	W	WP	1	4
374002.6	4644280.6	89	60	W	WP	2	4
374003.4	4644280.9	87	59.5	W	WP	3	4
374004.2	4644281.2	48	64	W	WP	4	4
374005	4644281.5	32	33	W	WP	5	4
374005.8	4644281.8	64.5	42	W	WP	6	4
374006.6	4644282.1	52	39	W	WP	7	4
374007.4	4644282.4	49	40.5	W	WP	8	4
374008.2	4644282.7	31	40.5	W	WP	9	4
374009	4644283	25.5	37	W	WP	10	4
374009.8	4644283.3	30	28	W	WP	11	4
374010.6	4644283.6	40.5	24.5	W	WP	12	4
375648	4649294	43.5	21.5	E	NE	0	1
375647.5	4649294.5	62	22.5	E	NE	1	1
375647	4649295	400.5	25.5	E	NE	2	1
375646.5	4649295.5	1095	33.5	E	NE	3	1
375646	4649296	595.5	60.5	E	NE	4	1
375645.5	4649296.5	1783	48.5	E	NE	5	1
375645	4649297	246.5	28.5	E	NE	6	1
375644.5	4649297.5	190	36	E	NE	7	1
375644	4649298	92	36.5	E	NE	8	1
375642	4649288	45.5	39	E	NE	0	2
375641.25	4649288.625	67.5	29	E	NE	1	2
375640.5	4649289.25	525	64.5	E	NE	2	2
375639.75	4649289.875	752.5	44	E	NE	3	2
375639	4649290.5	526	44.5	E	NE	4	2
375638.25	4649291.125	737.5	48.5	E	NE	5	2
375637.5	4649291.75	241	50.5	E	NE	6	2
375636.75	4649292.375	144	60.5	E	NE	7	2
375636	4649293	118	249.5	E	NE	8	2
375635	4649281	51	96	E	NE	0	3
375635	4649282.5	74	42	E	NE	1	3
375635	4649284	856	95	E	NE	2	3
375634.3333	4649284.667	1264	56	E	NE	3	3
375633.6667	4649285.333	1394	59	E	NE	4	3
375633	4649286	4101.5	41	E	NE	5	3
375633.3333	4649287.667	184.5	43.5	E	NE	6	3
375633.6667	4649289.333	260	45.5	E	NE	7	3
375634	4649291	139	21	E	NE	8	3
375632	4649277	67	17.5	E	NE	0	4
375631	4649277.286	58	67	E	NE	1	4
375630	4649277.571	149.5	48	E	NE	2	4
375629	4649277.857	349	37	E	NE	3	4
375628	4649278.143	1446	59	E	NE	4	4
375627	4649278.429	1324	191	E	NE	5	4

375626	4649278.714	481	75.5	E	NE	6	4
375625	4649279	177.5	32	E	NE	7	4
375591	4649157	87.5	30	E	NE	0	5
375590	4649157.286	120	50	E	NE	1	5
375589	4649157.571	65.5	35	E	NE	2	5
375588	4649157.857	77.5	36.5	E	NE	3	5
375587	4649158.143	73.5	32.5	E	NE	4	5
375586	4649158.429	49.5	36.5	E	NE	5	5
375585	4649158.714	72	37	E	NE	6	5
375584	4649159	85	30	E	NE	7	5
375583	4649159.286	78	34	E	NE	8	5
375589	4649145	159	40	E	NE	0	6
375588.75	4649145.375	117.5	54	E	NE	1	6
375588.5	4649145.75	76	49.5	E	NE	2	6
375588.25	4649146.125	52	89.5	E	NE	3	6
375588	4649146.5	54	72	E	NE	4	6
375587.75	4649146.875	55	74	E	NE	5	6
375587.5	4649147.25	46	41	E	NE	6	6
375587.25	4649147.625	104	36	E	NE	7	6
375587	4649148	76	33	E	NE	8	6
375585	4649135	90	122	E	NE	0	7
375584.9	4649134.1	55.5	152.5	E	NE	1	7
375584.8	4649133.2	64	165	E	NE	2	7
375584.7	4649132.3	46.5	95.5	E	NE	3	7
375584.6	4649131.4	66	40	E	NE	4	7
375584.5	4649130.5	54	33.5	E	NE	5	7
375584.4	4649129.6	71	28	E	NE	6	7
375584.3	4649128.7	84	38.5	E	NE	7	7
375584.2	4649127.8	74	103	E	NE	8	7
375584.1	4649126.9	122.5	264	E	NE	9	7
375584	4649126	83.5	115.5	E	NE	0	8
375583.1	4649126.4	72.5	215	E	NE	1	8
375582.2	4649126.8	97.5	521.5	E	NE	2	8
375581.3	4649127.2	58	899.5	E	NE	3	8
375580.4	4649127.6	48	331.5	E	NE	4	8
375579.5	4649128	98	148.5	E	NE	5	8
375578.6	4649128.4	107	178	E	NE	6	8
375577.7	4649128.8	84	93	E	NE	7	8
375576.8	4649129.2	71.5	35	E	NE	8	8
375575.9	4649129.6	322.5	34	E	NE	9	8
375575	4649130	1369	119	E	NE	10	8
375574.325	4649124.65	1939	150.5	E	NE	11	8
375574	4649130.5	999	311.5	E	NE	12	8
375573.5	4649130.75	3659.5	250	E	NE	13	8
375573	4649131	1485	278.5	E	NE	14	8
375575	4649105	54	874	E	NE	0	9
375574.7	4649105.4	51	120.5	E	NE	1	9
375574.4	4649105.8	47	204	E	NE	2	9
375574.1	4649106.2	51	2589.5	E	NE	3	9
375573.8	4649106.6	46	4004.5	E	NE	4	9
375573.5	4649107	47	2823.5	E	NE	5	9
375573.2	4649107.4	40	806	E	NE	6	9
375572.9	4649107.8	62	153.5	E	NE	7	9
375572.6	4649108.2	71.5	58	E	NE	8	9
375572.3	4649108.6	71.5	53.5	E	NE	9	9
375572	4649109	99	90.5	E	NE	10	9
375571	4649109.8	969	54	E	NE	11	9
375570	4649110.6	3090.5	43.5	E	NE	12	9
375569	4649111.4	1213.5	29.5	E	NE	13	9
375568	4649112.2	1364.5	28.5	E	NE	14	9
375567	4649113	473.5	75	E	NE	15	9
375569	4649058	41	112.5	E	NE	0	10
375568.3	4649058.1	37.5	53	E	NE	1	10
375567.6	4649058.2	52.5	21	E	NE	2	10
375566.9	4649058.3	68.5	26	E	NE	3	10
375566.2	4649058.4	54.5	32.5	E	NE	4	10
375565.5	4649058.5	53	45	E	NE	5	10
375564.8	4649058.6	51	317.5	E	NE	6	10
375564.1	4649058.7	45.5	87	E	NE	7	10
375563.4	4649058.8	48	129.5	E	NE	8	10
375562.7	4649058.9	42	136.5	E	NE	9	10
375562	4649059	53.5	331	E	NE	10	10
375561	4649059	106	682	E	NE	11	10
375560	4649059	177	740.5	E	NE	12	10
375559	4649059	235.5	552	E	NE	13	10
375558	4649059	380	293.5	E	NE	14	10
375557	4649059	425.5	202.5	E	NE	15	10
375556	4649059	353.5	118	E	NE	16	10

375556	4648937	53.5	37	E	NE	0	11
375554.7	4648937.4	38	26.5	E	NE	1	11
375553.4	4648937.8	42	28	E	NE	2	11
375552.1	4648938.2	45	92	E	NE	3	11
375550.8	4648938.6	32	306.5	E	NE	4	11
375549.5	4648939	46	526	E	NE	5	11
375548.2	4648939.4	144	1205	E	NE	6	11
375546.9	4648939.8	78.5	291.5	E	NE	7	11
375545.6	4648940.2	80.5	143	E	NE	8	11
375544.3	4648940.6	51.5	74.5	E	NE	9	11
375543	4648941	54.5	58	E	NE	10	11
375542.5	4648941	49.5	56.5	E	NE	11	11
375542	4648941	44.5	84	E	NE	12	11
375551	4648889	46	37.5	E	NE	0	12
375550.2	4648888.9	49	28	E	NE	1	12
375549.4	4648888.8	70	29	E	NE	2	12
375548.6	4648888.7	153	31	E	NE	3	12
375547.8	4648888.6	229	27	E	NE	4	12
375547	4648888.5	662	30.5	E	NE	5	12
375546.2	4648888.4	189.5	29.5	E	NE	6	12
375545.4	4648888.3	262	44	E	NE	7	12
375544.6	4648888.2	607	22	E	NE	8	12
375543.8	4648888.1	232	55.5	E	NE	9	12
375543	4648888	119.5	49	E	NE	10	12
375551	4648759	83.5	51.5	E	NE	0	13
375550.6	4648758.8	85.5	31	E	NE	1	13
375550.2	4648758.6	60.5	27	E	NE	2	13
375549.8	4648758.4	66	29	E	NE	3	13
375549.4	4648758.2	57.5	26	E	NE	4	13
375549	4648758	88	23	E	NE	5	13
375548.6	4648757.8	718.5	26	E	NE	6	13
375548.2	4648757.6	327	28.5	E	NE	7	13
375547.8	4648757.4	506	24.5	E	NE	8	13
375547.4	4648757.2	170	36	E	NE	9	13
375547	4648757	88	37.5	E	NE	10	13
375546	4648757	70	63.5	E	NE	11	13
375545	4648757	93	68.5	E	NE	12	13
375544	4648757	94	258	E	NE	13	13
375550	4648750	90	46	E	NE	0	14
375549.3	4648749.9	106.5	37.5	E	NE	1	14
375548.6	4648749.8	102	28	E	NE	2	14
375547.9	4648749.7	39.5	25	E	NE	3	14
375547.2	4648749.6	40	26	E	NE	4	14
375546.5	4648749.5	59.5	29	E	NE	5	14
375545.8	4648749.4	1603.5	28	E	NE	6	14
375545.1	4648749.3	817.5	26	E	NE	7	14
375544.4	4648749.2	2002	35	E	NE	8	14
375543.7	4648749.1	912.5	33	E	NE	9	14
375543	4648749	407	64	E	NE	10	14
375542.2	4648748.8	90	48	E	NE	11	14
375541.4	4648748.6	74	129	E	NE	12	14
375540.6	4648748.4	70	212.5	E	NE	13	14
375539.8	4648748.2	69	475	E	NE	14	14
375539	4648748	52	41	E	NE	15	14
375554	4648739	61.5	39.5	E	NE	0	15
375553.2	4648738.3	88	29.5	E	NE	1	15
375552.4	4648737.6	58.5	22.5	E	NE	2	15
375551.6	4648736.9	141.5	29.5	E	NE	3	15
375550.8	4648736.2	238.5	29.5	E	NE	4	15
375550	4648735.5	679	29	E	NE	5	15
375549.2	4648734.8	736.5	29	E	NE	6	15
375548.4	4648734.1	611.5	31	E	NE	7	15
375547.6	4648733.4	284	34	E	NE	8	15
375546.8	4648732.7	156	35	E	NE	9	15
375546	4648732	200	41	E	NE	10	15
375545.725	4648732.275	104	42.5	E	NE	11	15
375543	4648735.5	193	87.5	E	NE	12	15
375541.5	4648737.25	145.5	114	E	NE	13	15
375540	4648739	129.5	213	E	NE	14	15
375553	4648734	66.5	46.5	E	NE	0	16
375552.1	4648733.9	57	34	E	NE	1	16
375551.2	4648733.8	89	31	E	NE	2	16
375550.3	4648733.7	119.5	26.5	E	NE	3	16
375549.4	4648733.6	561.5	26	E	NE	4	16
375548.5	4648733.5	654.5	28	E	NE	5	16
375547.6	4648733.4	405	23.5	E	NE	6	16
375546.7	4648733.3	1207	24.5	E	NE	7	16
375545.8	4648733.2	325	24	E	NE	8	16

375544.9	4648733.1	511	21	E	NE	9	16
375544	4648733	162	28.5	E	NE	10	16
375544.95	4648731.725	179	36.5	E	NE	11	16
375541.5	4648734	125	58	E	NE	12	16
375540.25	4648734.5	107	62.5	E	NE	13	16
375539	4648735	94.5	77	E	NE	14	16
375555	4648727	63.5	41	E	NE	0	17
375554.2	4648727.1	45.5	27.5	E	NE	1	17
375553.4	4648727.2	137.5	31.5	E	NE	2	17
375552.6	4648727.3	241	19.5	E	NE	3	17
375551.8	4648727.4	942	28.5	E	NE	4	17
375551	4648727.5	490.5	30.5	E	NE	5	17
375550.2	4648727.6	714.5	23.5	E	NE	6	17
375549.4	4648727.7	534	23	E	NE	7	17
375548.6	4648727.8	412.5	25.5	E	NE	8	17
375547.8	4648727.9	320	30.5	E	NE	9	17
375547	4648728	274	52.5	E	NE	10	17
375547.825	4648723.35	222	40	E	NE	11	17
375543	4648728.5	189	42	E	NE	12	17
375541	4648728.75	156	57.5	E	NE	13	17
375539	4648729	85	53	E	NE	14	17
375562	4648704	100	37	E	NE	0	18
375560.7	4648704.6	43.5	29.5	E	NE	1	18
375559.4	4648705.2	42	26	E	NE	2	18
375558.1	4648705.8	117.5	23	E	NE	3	18
375556.8	4648706.4	241.5	28	E	NE	4	18
375555.5	4648707	197.5	39	E	NE	5	18
375554.2	4648707.6	755	35	E	NE	6	18
375552.9	4648708.2	961.5	30.5	E	NE	7	18
375551.6	4648708.8	618.5	28	E	NE	8	18
375550.3	4648709.4	696.5	43.5	E	NE	9	18
375549	4648710	671	36.5	E	NE	10	18
375548	4648710.2	660	36	E	NE	11	18
375547	4648710.4	151	34	E	NE	12	18
375546	4648710.6	252.5	34.5	E	NE	13	18
375545	4648710.8	237	75	E	NE	14	18
375544	4648711	167.5	39.5	E	NE	15	18
375556	4648704	75.5	22.5	E	NE	0	19
375555.4	4648703.9	134	23.5	E	NE	1	19
375554.8	4648703.8	53	27	E	NE	2	19
375554.2	4648703.7	48	23.5	E	NE	3	19
375553.6	4648703.6	56.5	28	E	NE	4	19
375553	4648703.5	88	37.5	E	NE	5	19
375552.4	4648703.4	137.5	30	E	NE	6	19
375551.8	4648703.3	222.5	26.5	E	NE	7	19
375551.2	4648703.2	185.5	29	E	NE	8	19
375550.6	4648703.1	212.5	26	E	NE	9	19
375550	4648703	335.5	26	E	NE	10	19
375548.5714	4648703.143	1527.5	29	E	NE	11	19
375547.1429	4648703.286	435	28.5	E	NE	12	19
375545.7143	4648703.429	199.5	22.5	E	NE	13	19
375544.2857	4648703.571	258	132.5	E	NE	14	19
375542.8571	4648703.714	187	166.5	E	NE	15	19
375541.4286	4648703.857	201	67.5	E	NE	16	19
375540	4648704	148	85	E	NE	17	19
375559	4648695	45	35	E	NE	0	20
375558.7	4648695	60	34	E	NE	1	20
375558.4	4648695	72	21	E	NE	2	20
375558.1	4648695	49	26	E	NE	3	20
375557.8	4648695	45	28	E	NE	4	20
375557.5	4648695	47.5	36	E	NE	5	20
375557.2	4648695	79.5	45	E	NE	6	20
375556.9	4648695	117.5	37	E	NE	7	20
375556.6	4648695	99.5	3022	E	NE	8	20
375556.3	4648695	159.5	25.5	E	NE	9	20
375556	4648695	189	28.5	E	NE	10	20
375553.6667	4648694.833	436.5	36.5	E	NE	11	20
375551.3333	4648694.667	321	22.5	E	NE	12	20
375549	4648694.5	300	38.5	E	NE	13	20
375546.6667	4648694.333	149.5	117.5	E	NE	14	20
375544.3333	4648694.167	242.5	86.5	E	NE	15	20
375542	4648694	148	75.5	E	NE	16	20
375437	4647096	101	39	E	ME	0	1
375434.5	4647095.8	73.5	33	E	ME	1	1
375432	4647095.6	50	29.5	E	ME	2	1
375429.5	4647095.4	534.5	26	E	ME	3	1
375427	4647095.2	3024.5	57	E	ME	4	1
375424.5	4647095	4331.5	206	E	ME	5	1

375422	4647094.8	7552	357.5	E	ME	6	1
375419.5	4647094.6	2288.5	459	E	ME	7	1
375417	4647094.4	2135.5	314	E	ME	8	1
375414.5	4647094.2	1687	645	E	ME	9	1
375412	4647094	1834.5	2276	E	ME	10	1
375412	4647095	5072.5	2401	E	ME	11	1
375412	4647096	2957	2412	E	ME	12	1
375412	4647097	7807.5	4650	E	ME	13	1
375409	4647096	5244	3401.5	E	ME	14	1
375420	4647068	115.5	60	E	ME	0	2
375419.2	4647068	91	63	E	ME	1	2
375418.4	4647068	150.5	62	E	ME	2	2
375417.6	4647068	57	158	E	ME	3	2
375416.8	4647068	148.5	557.5	E	ME	4	2
375416	4647068	659.5	552	E	ME	5	2
375415.2	4647068	2494	509	E	ME	6	2
375414.4	4647068	5345.5	273.5	E	ME	7	2
375413.6	4647068	3301.5	895.5	E	ME	8	2
375412.8	4647068	2735	1143.5	E	ME	9	2
375412	4647068	1651	4509.5	E	ME	10	2
375413	4647069	4654.5	5006	E	ME	11	2
375424	4647049	90.5	32.5	E	ME	0	3
375422.5	4647049.3	108	20	E	ME	1	3
375421	4647049.6	446.5	39	E	ME	2	3
375419.5	4647049.9	144	69.5	E	ME	3	3
375418	4647050.2	1263	436.5	E	ME	4	3
375416.5	4647050.5	2132.5	301.5	E	ME	5	3
375415	4647050.8	4075.5	840	E	ME	6	3
375413.5	4647051.1	7105.5	690	E	ME	7	3
375412	4647051.4	8881.5	1017	E	ME	8	3
375410.5	4647051.7	3717.5	1974	E	ME	9	3
375409	4647052	9162	1952	E	ME	10	3
375408	4647052	8239.5	1325	E	ME	11	3
375407	4647052	7372	1061.5	E	ME	12	3
375406	4647052	8027	780	E	ME	13	3
375405	4647052	4519	796	E	ME	14	3
375404	4647052	5606.5	911.5	E	ME	15	3
375403	4647052	2759	816.5	E	ME	16	3
375402	4647052	2853.5	859.5	E	ME	17	3
375401	4647052	3347.5	1168.5	E	ME	18	3
375400	4647052	4318	2536	E	ME	19	3
375399	4647052	1485.5	1394	E	ME	20	3
375398.1	4647052.1	8684	2501	E	ME	21	3
375397.2	4647052.2	2960	6163	E	ME	22	3
375396.3	4647052.3	8684	5390	E	ME	23	3
375395.4	4647052.4	2960	6565	E	ME	24	3
375394.5	4647052.5	901.5	6573	E	ME	25	3
375393.6	4647052.6	7916.5	5278	E	ME	26	3
375392.7	4647052.7	3785.5	4749.5	E	ME	27	3
375391.8	4647052.8	3334.5	4045	E	ME	28	3
375390.9	4647052.9	3334.5	4880	E	ME	29	3
375390	4647053	2500	4926	E	ME	30	3
375389.1	4647053.2	2125	4936.5	E	ME	31	3
375388.2	4647053.4	3834.5	3924	E	ME	32	3
375387.3	4647053.6	4281.5	3854.5	E	ME	33	3
375386.4	4647053.8	2391	5216.5	E	ME	34	3
375385.5	4647054	6063	3006.5	E	ME	35	3
375384.6	4647054.2	975.5	2794	E	ME	36	3
375383.7	4647054.4	2875	1922	E	ME	37	3
375382.8	4647054.6	2195	2336.5	E	ME	38	3
375381.9	4647054.8	2232.5	1916.5	E	ME	39	3
375381	4647055	3050	2635	E	ME	40	3
375381	4647054	2114.5	1556	E	ME	41	3
375416	4647030	113	53	E	ME	0	4
375415.1	4647030	1626.5	56	E	ME	1	4
375414.2	4647030	457.5	80	E	ME	2	4
375413.3	4647030	477.5	44	E	ME	3	4
375412.4	4647030	1077.5	115	E	ME	4	4
375411.5	4647030	1672.5	120.5	E	ME	5	4
375410.6	4647030	2185.5	240.5	E	ME	6	4
375409.7	4647030	2623.5	285.5	E	ME	7	4
375408.8	4647030	2923.5	532	E	ME	8	4
375407.9	4647030	4468.5	549.5	E	ME	9	4
375407	4647030	4919	336.5	E	ME	10	4
375406	4647030	6300	591	E	ME	11	4
375405	4647030	1863.5	335.5	E	ME	12	4
375404	4647030	1891.5	474	E	ME	13	4
375403	4647030	1475.5	545	E	ME	14	4

375402	4647030	2607	401	E	ME	15	4
375401	4647030	3257	265.5	E	ME	16	4
375400	4647030	2669	381	E	ME	17	4
375399	4647030	2164	279.5	E	ME	18	4
375398	4647030	2064.5	234	E	ME	19	4
375397	4647030	1314	326	E	ME	20	4
375395.9	4647030.2	1888.5	205	E	ME	21	4
375394.8	4647030.4	1057.5	323.5	E	ME	22	4
375393.7	4647030.6	1041	332.5	E	ME	23	4
375392.6	4647030.8	805	406.5	E	ME	24	4
375391.5	4647031	1648.5	487	E	ME	25	4
375390.4	4647031.2	666.5	433	E	ME	26	4
375389.3	4647031.4	454	657	E	ME	27	4
375388.2	4647031.6	565	801.5	E	ME	28	4
375387.1	4647031.8	666.5	495	E	ME	29	4
375386	4647032	726.5	544	E	ME	30	4
375385	4647032.2	751.5	539	E	ME	31	4
375384	4647032.4	763.5	804.5	E	ME	32	4
375383	4647032.6	725	24	E	ME	33	4
375382	4647032.8	544.5	20.5	E	ME	34	4
375381	4647033	661	36.5	E	ME	35	4
375416	4647005	66.5	29	E	ME	0	5
375415	4647004.9	99.5	26	E	ME	1	5
375414	4647004.8	76	42	E	ME	2	5
375413	4647004.7	239	232	E	ME	3	5
375412	4647004.6	1580	85	E	ME	4	5
375411	4647004.5	3089.5	71	E	ME	5	5
375410	4647004.4	6963	199	E	ME	6	5
375409	4647004.3	1237	336	E	ME	7	5
375408	4647004.2	2577	373.5	E	ME	8	5
375407	4647004.1	2918.5	559.5	E	ME	9	5
375406	4647004	963.5	4011	E	ME	10	5
375404.8	4647004.1	1064.5	349	E	ME	11	5
375403.6	4647004.2	2160.5	253	E	ME	12	5
375402.4	4647004.3	1844.5	292	E	ME	13	5
375401.2	4647004.4	2593.5	291	E	ME	14	5
375400	4647004.5	1673	209	E	ME	15	5
375398.8	4647004.6	944	233.5	E	ME	16	5
375397.6	4647004.7	762.5	158	E	ME	17	5
375396.4	4647004.8	715	98	E	ME	18	5
375395.2	4647004.9	633	165.5	E	ME	19	5
375394	4647005	605.5	214	E	ME	20	5
375393.1	4647005.2	639	154	E	ME	21	5
375392.2	4647005.4	612.5	259	E	ME	22	5
375391.3	4647005.6	397	233	E	ME	23	5
375390.4	4647005.8	382	290	E	ME	24	5
375389.5	4647006	291.5	196	E	ME	25	5
375388.6	4647006.2	320.5	520.5	E	ME	26	5
375387.7	4647006.4	323.5	520	E	ME	27	5
375386.8	4647006.6	333.5	566.5	E	ME	28	5
375385.9	4647006.8	305	652	E	ME	29	5
375385	4647007	449.5	717	E	ME	30	5
375383.8571	4647007	556.5	4097	E	ME	31	5
375382.7143	4647007	465	711	E	ME	32	5
375381.5714	4647007	503.5	794	E	ME	33	5
375380.4286	4647007	354.5	852	E	ME	34	5
375379.2857	4647007	168	170.5	E	ME	35	5
375378.1429	4647007	203.5	189.5	E	ME	36	5
375377	4647007	362.5	366	E	ME	37	5
375414	4646982	68	49	E	ME	0	6
375413	4646982.2	112.5	79	E	ME	1	6
375412	4646982.4	101.5	29	E	ME	2	6
375411	4646982.6	145	37	E	ME	3	6
375410	4646982.8	604	63.5	E	ME	4	6
375409	4646983	2569.5	71	E	ME	5	6
375408	4646983.2	365	140	E	ME	6	6
375407	4646983.4	7500	539	E	ME	7	6
375406	4646983.6	2209	364	E	ME	8	6
375405	4646983.8	5279	291.5	E	ME	9	6
375404	4646984	1139.5	383	E	ME	10	6
375403	4646984	3868.5	313	E	ME	11	6
375402	4646984	4827	203	E	ME	12	6
375401	4646984	3839	268	E	ME	13	6
375400	4646984	3513	205	E	ME	14	6
375399	4646984	3522.5	124.5	E	ME	15	6
375398	4646984	2678	1137	E	ME	16	6
375397	4646984	2614	620	E	ME	17	6
375413	4646961	171.5	30	E	ME	0	7

375411.8	4646960.8	330	26	E	ME	1	7
375410.6	4646960.6	156.5	28	E	ME	2	7
375409.4	4646960.4	94	88	E	ME	3	7
375408.2	4646960.2	185	71	E	ME	4	7
375407	4646960	1482	135.5	E	ME	5	7
375405.8	4646959.8	891	106	E	ME	6	7
375404.6	4646959.6	2008.5	161	E	ME	7	7
375403.4	4646959.4	1636	460	E	ME	8	7
375402.2	4646959.2	1811.5	313	E	ME	9	7
375401	4646959	2129.5	134	E	ME	10	7
375400.2857	4646959.429	447	202.5	E	ME	11	7
375399.5714	4646959.857	637.5	158.5	E	ME	12	7
375398.8571	4646960.286	1973.5	198.5	E	ME	13	7
375398.1429	4646960.714	1544.5	234	E	ME	14	7
375397.4286	4646961.143	2801.5	139	E	ME	15	7
375396.7143	4646961.571	2065.5	246	E	ME	16	7
375396	4646962	1325	268.5	E	ME	17	7
375400	4646934	854	126.5	E	ME	0	8
375400	4646936	2259	73.5	E	ME	1	8
375399	4646936	178.5	94	E	ME	2	8
375398	4646936	346.5	51.5	E	ME	3	8
375397	4646936	899.5	47	E	ME	4	8
375396	4646936	599	59	E	ME	5	8
375395	4646936	1556.5	90	E	ME	6	8
375394	4646936	8529.5	261	E	ME	7	8
375393	4646936	1353	263.5	E	ME	8	8
375392	4646936	1480	269.5	E	ME	9	8
375401	4646936	1603.5	341	E	ME	10	8
375400	4646936	1166.5	290	E	ME	11	8
375399	4646936	1200.5	5434.5	E	ME	12	8
375398	4646936	1406.5	3551.5	E	ME	13	8
375397	4646936	1027	1171.5	E	ME	14	8
375396	4646936	1105.5	1036	E	ME	15	8
375395	4646936	1276	540	E	ME	16	8
375394	4646936	869	415.5	E	ME	17	8
375393	4646936	487	328.5	E	ME	18	8
375392	4646936	693	268	E	ME	19	8
375391	4646936	409.5	256	E	ME	20	8
375390.3333	4646936.667	528.5	249	E	ME	21	8
375389.6667	4646937.333	326	433	E	ME	22	8
375389	4646938	214	340	E	ME	23	8
374175	4643688	92.5	63.5	W	WB	0	1
374176	4643688.8	76.5	61	W	WB	1	1
374177	4643689.6	72	59	W	WB	2	1
374178	4643690.4	97.5	57	W	WB	3	1
374179	4643691.2	97	85	W	WB	4	1
374180	4643692	85.5	91	W	WB	5	1
374181	4643692.8	65	69	W	WB	6	1
374182	4643693.6	44.5	70	W	WB	7	1
374183	4643694.4	37	53.5	W	WB	8	1
374184	4643695.2	51	62	W	WB	9	1
374185	4643696	62.5	51	W	WB	10	1
374186.6	4643697	68	41	W	WB	11	1
374188.2	4643698	73.5	70.5	W	WB	12	1
374189.8	4643699	82.5	27	W	WB	13	1
374191.4	4643700	109	67	W	WB	14	1
374193	4643701	90	63	W	WB	15	1
374178	4643688	80	59.5	W	WB	0	2
374179	4643687.9	64	23	W	WB	1	2
374180	4643687.8	70	53	W	WB	2	2
374181	4643687.7	71	97.5	W	WB	3	2
374182	4643687.6	91.5	80	W	WB	4	2
374183	4643687.5	57.5	77.5	W	WB	5	2
374184	4643687.4	45	52	W	WB	6	2
374185	4643687.3	39.5	46	W	WB	7	2
374186	4643687.2	64	37	W	WB	8	2
374187	4643687.1	73	53	W	WB	9	2
374188	4643687	61	30	W	WB	10	2
374189.2	4643687.4	62	39.5	W	WB	11	2
374190.4	4643687.8	59.5	49	W	WB	12	2
374191.6	4643688.2	80	89	W	WB	13	2
374192.8	4643688.6	93	84	W	WB	14	2
374194	4643689	74	65	W	WB	15	2
374183	4643675	61	52	W	WB	0	3
374183.9	4643674.9	54	72	W	WB	1	3
374184.8	4643674.8	82.5	81.5	W	WB	2	3
374185.7	4643674.7	74	68	W	WB	3	3
374186.6	4643674.6	63	53.5	W	WB	4	3

374187.5	4643674.5	65	53	W	WB	5	3
374188.4	4643674.4	67.5	103	W	WB	6	3
374189.3	4643674.3	72	52	W	WB	7	3
374190.2	4643674.2	82	77	W	WB	8	3
374191.1	4643674.1	49.5	77.5	W	WB	9	3
374192	4643674	52	52	W	WB	10	3
374192.8	4643674.8	62	48	W	WB	11	3
374193.6	4643675.6	71	57	W	WB	12	3
374194.4	4643676.4	77.5	60	W	WB	13	3
374195.2	4643677.2	86	56	W	WB	14	3
374196	4643678	102	54	W	WB	15	3
374132	4643664	107	54	W	WB	0	4
374138.2	4643664.2	58	69	W	WB	1	4
374144.4	4643664.4	67.5	57	W	WB	2	4
374150.6	4643664.6	86.5	68	W	WB	3	4
374156.8	4643664.8	85	57	W	WB	4	4
374163	4643665	61.5	52	W	WB	5	4
374169.2	4643665.2	56.5	54	W	WB	6	4
374175.4	4643665.4	58	30	W	WB	7	4
374181.6	4643665.6	92	38.5	W	WB	8	4
374187.8	4643665.8	66	51.5	W	WB	9	4
374194	4643666	54.5	38.5	W	WB	10	4
374195	4643665.8	67	52	W	WB	11	4
374196	4643665.6	66	58	W	WB	12	4
374197	4643665.4	80	58	W	WB	13	4
374198	4643665.2	100.5	40	W	WB	14	4
374199	4643665	141	51	W	WB	15	4
374226	4643506	132	81.5	W	WB	0	5
374227	4643506.2	62	70.5	W	WB	1	5
374228	4643506.4	81.5	102	W	WB	2	5
374229	4643506.6	95.5	86.5	W	WB	3	5
374230	4643506.8	113.5	62	W	WB	4	5
374231	4643507	84.5	69	W	WB	5	5
374232	4643507.2	45.5	44	W	WB	6	5
374233	4643507.4	69.5	50	W	WB	7	5
374234	4643507.6	80.5	38	W	WB	8	5
374235	4643507.8	80.5	48.5	W	WB	9	5
374236	4643508	70	41.5	W	WB	10	5
374239	4643507	65.5	31	W	WB	11	5
374240	4643507.2	70	49	W	WB	12	5
374241	4643507.4	79	39	W	WB	13	5
374242	4643507.6	75.5	54	W	WB	14	5
374243	4643507.8	95	54	W	WB	15	5
374244	4643508	109.5	55	W	WB	16	5
374245	4643433	88.5	59	W	WB	0	6
374246.3	4643433	75.5	84	W	WB	1	6
374247.6	4643433	81.5	105	W	WB	2	6
374248.9	4643433	95.5	70	W	WB	3	6
374250.2	4643433	91.5	85	W	WB	4	6
374251.5	4643433	79	98	W	WB	5	6
374252.8	4643433	63	79	W	WB	6	6
374254.1	4643433	64	62	W	WB	7	6
374255.4	4643433	66	41.5	W	WB	8	6
374256.7	4643433	60	42	W	WB	9	6
374258	4643433	59	33	W	WB	10	6
374257.1333	4643433	67.5	51	W	WB	11	6
374260	4643433.667	81.5	93	W	WB	12	6
374261	4643434	116	103	W	WB	13	6
374262	4643434.333	102.5	98	W	WB	14	6
374263	4643434.667	98.5	75	W	WB	15	6
374264	4643435	113	64	W	WB	16	6
374254	4643410	104.5	80	W	WB	0	7
374255	4643410.3	73.5	104	W	WB	1	7
374256	4643410.6	73.5	79	W	WB	2	7
374257	4643410.9	78	94.5	W	WB	3	7
374258	4643411.2	59.5	84	W	WB	4	7
374259	4643411.5	59	96	W	WB	5	7
374260	4643411.8	42	70	W	WB	6	7
374261	4643412.1	50	64	W	WB	7	7
374262	4643412.4	57.5	79.5	W	WB	8	7
374263	4643412.7	50	63	W	WB	9	7
374264	4643413	52	62	W	WB	10	7
374264.6667	4643401.05	73.5	41.5	W	WB	11	7
374265.3333	4643389.1	72.5	45	W	WB	12	7
374266	4643377.15	93	46.5	W	WB	13	7
374266.6667	4643365.2	81.5	55	W	WB	14	7
374267.3333	4643353.25	91.5	93	W	WB	15	7
374268	4643414	101	108.5	W	WB	16	7

374285	4643293	100.5	80	W	WB	0	8
374285.9	4643293.5	86	97	W	WB	1	8
374286.8	4643294	63	91	W	WB	2	8
374287.7	4643294.5	84	114	W	WB	3	8
374288.6	4643295	61.5	83	W	WB	4	8
374289.5	4643295.5	54.5	96	W	WB	5	8
374290.4	4643296	63.5	78.5	W	WB	6	8
374291.3	4643296.5	52	72	W	WB	7	8
374292.2	4643297	66	51.5	W	WB	8	8
374293.1	4643297.5	75	55	W	WB	9	8
374294	4643298	67.5	42.5	W	WB	10	8
374294.875	4643298.125	66	53.5	W	WB	11	8
374295.75	4643298.25	68.5	56.5	W	WB	12	8
374296.625	4643298.375	68	58	W	WB	13	8
374297.5	4643298.5	64.5	61	W	WB	14	8
374298.375	4643298.625	83	71	W	WB	15	8
374299.25	4643298.75	87.5	62	W	WB	16	8
374300.125	4643298.875	96	72	W	WB	17	8
374301	4643299	104.5	62	W	WB	18	8
374319	4643169	109	70	W	WB	0	9
374319.8	4643169.3	52	62	W	WB	1	9
374320.6	4643169.6	97	82	W	WB	2	9
374321.4	4643169.9	87.5	91	W	WB	3	9
374322.2	4643170.2	74.5	110	W	WB	4	9
374323	4643170.5	69.5	93	W	WB	5	9
374323.8	4643170.8	90.5	74	W	WB	6	9
374324.6	4643171.1	96	78	W	WB	7	9
374325.4	4643171.4	91.5	52.5	W	WB	8	9
374326.2	4643171.7	107	87	W	WB	9	9
374327	4643172	123.5	46	W	WB	10	9
374327	4643171	98.5	57.5	W	WB	11	9
374327	4643170	83	48	W	WB	12	9
374327	4643169	113	83.5	W	WB	13	9
374327	4643168	84.5	70	W	WB	14	9
374327	4643167	105	48	W	WB	15	9
374327	4643166	94.5	83.5	W	WB	16	9

APPENDIX F: East beach random data used for mapping

Longitude	Latitude	Susceptibility (χ)
375127	4643060	65
375123	4643061	932
375117	4643061	813
375107	4643063	224
375100	4643064	193
375096	4643064	166
375107	4643075	175
375115	4643073	314
375120	4643072	517
375125	4643072	322
375129	4643073	61
375130	4643087	309
375124	4643089	751
375117	4643094	470
375108	4643098	550
375098	4643100	240
375104	4643119	297
375121	4643112	431
375127	4643111	994
375133	4643111	46
375130	4643117	1186
375124	4643115	1920
375115	4643123	357
375109	4643133	370
375103	4643134	379
375108	4643147	701
375126	4643149	974
375136	4643147	826
375144	4643145	341
375147	4643158	341
375139	4643162	152
375129	4643161	343
375118	4643164	791
375108	4643168	512
375112	4643185	671
375108	4643191	590
375128	4643178	1957
375141	4643183	1717
375148	4643185	63
375145	4643191	59
375142	4643196	3189
375131	4643198	382
375126	4643204	1600
375118	4643204	958
375113	4643210	755
375124	4643223	1265
375140	4643233	145
375145	4643230	1188
375156	4643241	98
375148	4643257	883
375135	4643272	1387
375130	4643282	635

375140	4643295	4497
375151	4643303	252
375161	4643308	101
375150	4643319	994
375145	4643315	3966
375143	4643329	3553
375152	4643337	4925
375160	4643339	98
375167	4643349	77
375163	4643355	109
375153	4643363	9978
375157	4643379	449
375164	4643388	121
375159	4643392	1312
375168	4643400	110
375170	4643405	110
375164	4643410	84
375157	4643416	9961
375161	4643438	8184
375161	4643447	5203
375170	4643446	68
375175	4643452	39
375176	4643459	106
375169	4643461	86
375164	4643465	7239
375162	4643483	3706
375169	4643505	3549
375176	4643508	42
375180	4643510	60
375171	4643526	36
375165	4643543	1630
375176	4643547	40
375183	4643554	92
375173	4643567	24
375168	4643585	2337
375178	4643590	28
375186	4643591	80
375171	4643601	229
375196	4643654	96
375188	4643656	65
375179	4643656	67
375169	4643655	1049
375165	4643659	540
375179	4643667	199
375190	4643674	291
375200	4643681	119
375193	4643688	100
375187	4643695	153
375181	4643701	607
375190	4643708	313
375195	4643713	397
375202	4643720	113
375197	4643725	37
375195	4643727	913
375192	4643730	784
375187	4643737	2032

375181	4643742	1449
375188	4643745	812
375194	4643749	2015
375204	4643756	76
375199	4643760	125
375191	4643762	2704
375189	4643764	864
375181	4643764	937
375191	4643773	1980
375193	4643779	9103
375193	4643780	9827
375192	4643784	8046
375188	4643785	735
375203	4643786	502
375199	4643795	126
375115	4643800	945
375188	4643806	3041
375196	4643811	4333
375194	4643818	8889
375188	4643823	2426
375193	4643829	3737
375197	4643833	9300
375202	4643832	78
375208	4643833	119
375207	4643844	106
375202	4643848	177
375197	4643852	5179
375194	4643860	2407
375201	4643869	2737
375208	4643873	316
375215	4643877	182
375208	4643887	325
375200	4643890	5295
375196	4643894	2043
375210	4643912	1773
375217	4643921	76
375213	4643926	221
375211	4643927	2507
375203	4643934	6602
375209	4643946	8501
375201	4643945	3138
375216	4643953	115

APPENDIX G: Rondeau field magnetic susceptibility data points

S/N	LATITUDE	LONGITUDE	SUSCEP(χ)	Distance from shoreline	TRANS
1	430695	4685613	18	0	1
2	430694.0	4685613.18	12.5	1	1
3	430693.1	4685613.36	15	2	1
4	430692.2	4685613.54	27	3	1
5	430691.3	4685613.72	20	4	1
6	430690.4	4685613.90	11	5	1
7	430689.5	4685614.09	10	6	1
8	430688.6	4685614.27	10	7	1
9	430687.7	4685614.45	9.5	8	1
10	430686.8	4685614.63	9.5	9	1
11	430685	4685615	9.5	10	1
12	430684	4685614.72	15	11	1
13	430683	4685614.45	14.5	12	1
14	430682	4685614.18	14	13	1
15	430681	4685613.90	14.5	14	1
16	430680	4685613.63	15	15	1
17	430679	4685613.36	12	16	1
18	430678	4685613.09	12	17	1
19	430677	4685612.81	10	18	1
20	430676	4685612.54	11	19	1
21	430674	4685612	10	20	1
22	430696	4685592	35.5	0	2
23	430695	4685591.81	30	1	2
24	430694	4685591.63	24	2	2
25	430693	4685591.45	8	3	2
26	430692	4685591.27	9.5	4	2
27	430691	4685591.09	10	5	2
28	430690	4685590.90	7	6	2
29	430689	4685590.72	8.5	7	2
30	430688	4685590.54	7.5	8	2
31	430687	4685590.36	7	9	2
32	430685	4685590	6	10	2
33	430683.9	4685590	6	11	2
34	430682.8	4685590	6	12	2
35	430681.7	4685590	9	13	2
36	430680.6	4685590	9	14	2
37	430679.5	4685590	9.5	15	2
38	430678.4	4685590	11	16	2
39	430677.3	4685590	11	17	2
40	430676.2	4685590	11	18	2
41	430675.1	4685590	11	19	2
42	430673	4685590	10.5	20	2
43	430714	4681345	59.5	0	3
44	430713.3	4681344.90	63	1	3
45	430712.7	4681344.81	37	2	3
46	430712.0	4681344.72	62	3	3
47	430711.4	4681344.63	168	4	3
48	430710.8	4681344.54	106.5	5	3
49	430710.1	4681344.45	119.5	6	3
50	430709.5	4681344.36	83.5	7	3
51	430708.9	4681344.27	70	8	3
52	430708.2	4681344.18	65	9	3

53	430707	4681344	59.5	10	3
54	430706.1	4681343.90	40	11	3
55	430705.3	4681343.81	60.5	12	3
56	430704.5	4681343.72	173	13	3
57	430703.7	4681343.63	249	14	3
58	430702.9	4681343.54	359.5	15	3
59	430702.0	4681343.45	364	16	3
60	430701.2	4681343.36	375.5	17	3
61	430700.4	4681343.27	260.5	18	3
62	430699.6	4681343.18	261	19	3
63	430698	4681343	478	20	3
64	430697.0	4681343.45	624	21	3
65	430696.1	4681343.90	598.5	22	3
66	430695.2	4681344.36	469.5	23	3
67	430694.3	4681344.81	380	24	3
68	430693.4	4681345.27	577.5	25	3
69	430692.5	4681345.72	679	26	3
70	430691.6	4681346.18	511.5	27	3
71	430690.7	4681346.63	482	28	3
72	430689.8	4681347.09	499.5	29	3
73	430688	4681348	623	30	3
74	430687	4681347.90	330	31	3
75	430686	4681347.81	592.5	32	3
76	430685	4681347.72	694	33	3
77	430684	4681347.63	690	34	3
78	430683	4681347.54	558.5	35	3
79	430682	4681347.45	427.5	36	3
80	430681	4681347.36	470.5	37	3
81	430680	4681347.27	354	38	3
82	430679	4681347.18	354	39	3
83	430677	4681347	733.5	40	3
84	430676.1	4681347.09	762	41	3
85	430675.3	4681347.18	737	42	3
86	430674.5	4681347.27	844	43	3
87	430673.7	4681347.36	626	44	3
88	430672.9	4681347.45	586	45	3
89	430672.0	4681347.54	687.5	46	3
90	430671.2	4681347.63	551.5	47	3
91	430670.4	4681347.72	587	48	3
92	430669.6	4681347.81	502	49	3
93	430668	4681348	261.5	50	3
94	430715	4681274	97.5	0	4
95	430714.3	4681274	78.5	1	4
96	430713.7	4681274	55.5	2	4
97	430713.0	4681274	74	3	4
98	430712.4	4681274	95	4	4
99	430711.8	4681274	99	5	4
100	430711.1	4681274	70.5	6	4
101	430710.5	4681274	96.5	7	4
102	430709.9	4681274	117	8	4
103	430709.2	4681274	60	9	4
104	430708	4681274	46.5	10	4
105	430707	4681273.90	59	11	4
106	430706	4681273.81	72.5	12	4
107	430705	4681273.72	165	13	4
108	430704	4681273.63	201.5	14	4

109	430703	4681273.54	217.5	15	4
110	430702	4681273.45	181	16	4
111	430701	4681273.36	358	17	4
112	430700	4681273.27	232	18	4
113	430699	4681273.18	272	19	4
114	430697	4681273	328.5	20	4
115	430696	4681273	207	21	4
116	430695	4681273	198	22	4
117	430694	4681273	207	23	4
118	430693	4681273	146	24	4
119	430692	4681273	220	25	4
120	430691	4681273	250	26	4
121	430690	4681273	302.5	27	4
122	430689	4681273	204	28	4
123	430688	4681273	231	29	4
124	430686	4681273	233	30	4
125	430685.1	4681272.81	196	31	4
126	430684.3	4681272.63	322	32	4
127	430683.5	4681272.45	521	33	4
128	430682.7	4681272.27	687	34	4
129	430681.9	4681272.09	491.5	35	4
130	430681.0	4681271.90	376.5	36	4
131	430680.2	4681271.72	374	37	4
132	430679.4	4681271.54	379	38	4
133	430678.6	4681271.36	197.5	39	4
134	430677	4681271	110	40	4

VITA AUCTORIS

Name: Blessing Adaku Igbokwe

Place of Birth: Lokoja, Nigeria

Education: University Secondary School, Ilorin
1985-1991

University of Lagos, Nigeria

1995- 1999 B.Sc. Ed (Geography)

University of Windsor, Windsor, Canada

2003-2004 M.Sc.